Selected Applications of Reinforcement Learning in Electricity Markets: Strategic Bidding and Bidding Objective Identification

by

Reza Khalilisenobari

A Dissertation Presented in Partial Fulfillment
of the Requirements for the Degree
Doctor of Philosophy

Approved October 2023 by the
Graduate Supervisory Committee:

Meng Wu, Chair
Vijay Vittal
Anamitra Pal
Mojdeh Khorsand

ARIZONA STATE UNIVERSITY

December 2023

ABSTRACT

Renewable energy and carbon reduction policies are creating new challenges for electricity markets. To achieve carbon-free goals, large-scale battery energy storage systems (BESSs) are necessary to ensure grid reliability and flexibility. The impact of BESSs on market and grid operation, as well as the optimal portfolio across the energy and ancillary services markets, must be analyzed to guide their operation. At the same time, the expansion of renewable and storage resources and the adoption of carbon reduction policies have introduced new complexities to the bidding behavior of market participants, which cannot be easily described by cost-based bidding objectives. In response to these challenges, this dissertation aims to achieve two research objectives: (I) enable BESS participation in energy and ancillary services markets under uncertainties, considering the battery's degradation cost; (II) identify robust bidding objectives for electricity market participants based on their historical bidding data.

Three optimization frameworks are proposed in Part I to model a BESS as a price-maker in energy markets, evaluating its impact on market outcomes. The preliminary framework models automatic generation control signals, while the detailed framework proposes a participation factor for dispatching AGC signals and accounts for battery degradation costs. The stochastic framework models spinning reserve deployment with uncertainty and propose an optimization-based approximation method based on reinforcement learning. Case studies on proposed frameworks validate operational models for Battery Energy Storage Systems (BESS) and markets, showing the accuracy and efficiency of the approximation approach. Key findings include that accurate degradation cost modeling is essential, and participation in ancillary services markets is more profitable.

Part II proposes a data-driven approach using Adversarial Inverse Reinforcement

Learning to identify robust bidding objectives for electricity market participants. It introduces a tailored reinforcement learning model for bidding objective identification without data discretization, and a special policy structure compliant with multi-segment bidding rules. Two approaches are suggested for electricity market environment modeling in RL/IRL problems, ensuring the robustness of the identified bidding objective. Three case studies validated the accuracy and robustness of the proposed bidding objective identification method in various application scenarios.

TABLE OF CONTENTS

LIST OF TABLES

LIST OF FIGURES

Part I

PARTICIPATION OF BATTERY ENERGY STORAGE SYSTEMS IN ENERGY AND ANCILLARY SERVICES MARKETS

NOMENCLATURE

Acronyms

AGC	Automatic Generation Control.
BESS	Battery Energy Storage System.
CAISO	California Independent System Operator.
DER	Distributed Energy Resource.
EPEC	Equilibrium Problem with Equilibrium Constraints.
FERC	Federal Energy Regulatory Commission.
ISO	Independent System Operator.
KKT	Karush-Kuhn-Tucker.
LLP	Lower-Level Problem.
LMP	Locational Marginal Price.
MILP	Mixed Integer Linear Problem.
MPEC	Mathematical Problems with Equilibrium Constraints.
PJM	Pennsylvania, Jersey, Maryland Power Pool.
PSH	Pumped-Storage Hydropower.
RTO	Regional Transmission Organization.
SOC	State of Charge.
U.S.	United States.
ULP	Upper-Level Problem.

Sets and Indices

$\mathcal{B}$	Set of battery storage buses, indexed by i.
$\mathcal{G}$	Set of generator buses, indexed by j.
$\mathcal{K}$	Set of battery degradation cost curve's segments, indexed by k.
$\mathcal{L}$	Set of transmission lines, indexed by (n, w).
$\mathcal{N}$	Set of all buses, indexed by n and w.
$\mathcal{S}$	Set of scenarios, indexed by s.

$\mathcal{T}$	Set of market-clearing intervals, indexed by t.
$\mathcal{Z}$	Set of AGC signals sub-intervals, indexed by z.
B	Superscript for battery energy storage units.
Ch	Superscript for each degradation segment's charge power.
D	Superscript for BESS demanding energy.
DE	Superscript for demand in energy market.
Dis	Superscript for each degradation segment's discharge power.
E	Superscript for energy market.
G	Superscript for generators.
RgC	Superscript for regulation capacity market.
RgM	Superscript for regulation mileage market.
Rs	Superscript for reserve market.
RsD	Superscript for reserve deployment.
S	Superscript for BESS supplying energy.
SE	Superscript for supply in energy market.
TCh	Superscript for total charging power in each sub-interval.
$TDis$	Superscript for total discharging power in each sub-interval.

Parameters and Constants

α	Generator's price offer.
$\bar{t}$	The last interval.
$\bar{z}$	The last sub-interval.
Δt	Market clearing interval time spans.
Δz	Sub-interval time spans.
η	Battery unit's charge/discharge efficiency.
Φ	Cycle depth stress function of battery.
AGC	Automatic generation control signal set points.
C	Degradation cost function of battery.

C^{Deg}	Slope of each degradation cost segment.
e^{Max}	Capacity limit of each degradation segment.
f	Reserve deployment factor.
H	Susceptance of transmission line.
m	Regulation mileage multiplier.
P^{Load}	System load.
P^{Max}	Generator's maximum output power limit.
P^{Min}	Generator's minimum output power limit.
P^{Rate}	Battery unit's charge/discharge limit.
$P^{Rg,Ramp}$	Generator's regulation provision ramp limit.
$P^{Rs,Ramp}$	Generator's reserve provision ramp limit.
$prob(S)$	Scenario's probability.
R	System ancillary services' requirements.
SOC^{Init}	Battery unit's initial state of charge.
SOC^{Max}	Battery unit's maximum state of charge.
SOC^{Min}	Battery unit's minimum state of charge.
TL	Transmission line's thermal limit.

Variables

β	Battery unit's price offer.
δ	battery charge/discharge cycle depth.
π	Markets' clearing prices.
θ	Buses' voltage angles.
e	Degradation segment stored energy.
O	Battery unit's quantity offer.
P	Power.
PF	Regulation market participation factor.
u	Energy market supply/demand indicator.
v	Sub-interval charge/discharge indicator.

Chapter 1

INTRODUCTION

The concept of energy storage is not new. Batteries and pumped-storage hydropower (PSH) units have been operating in the United States (U.S.) for more than a century. However, the application of electrochemical energy storage technologies in the grid have been always suppressed by cheaper sources of electricity generation like conventional generators. Recently, the increase of renewable resources along with the production cost reduction of the batteries lead to the development and expansion of new energy storage systems, especially battery energy storage ones [26]. This expansion necessitates doing studies on a wide range of topics from batteries manufacturing to the operation of BESSs and their effects on other aspects of the grid. This part of the dissertation falls in the research direction mentioned above and focuses on the optimal operation of large-scale BESSs and their impact on the electricity markets and gird.

In order to provide the background of this topic and explain the motivation behind this research, the first section gives a brief overview of the energy storage technologies and application in the grid, while the second section focuses on the BESSs's characteristics, applications and expansion. The motivation of this work is described in the third section. Finally, the last section gives an overview of the contents in this part of the dissertation.

1.1 Energy Storage Technologies and Applications

The electricity grid can benefit from the existence of energy storage systems in various aspects. Some of these aspects are: gird modernization; improving system

resiliency, reliability and sustainability; providing flexibility for having diverse and secure generation mix; enhancing the economic competitiveness for remote communities; facilitating micro-grids formation; and stabilizing the grid by offering various range of energy management services and leveling the load [74]. The storage systems can have applications in multiple levels of the power system, as shown in figure 1.1, from the residential and behind the meter storage units and electric vehicles to utility-scale storage units in the generation level.

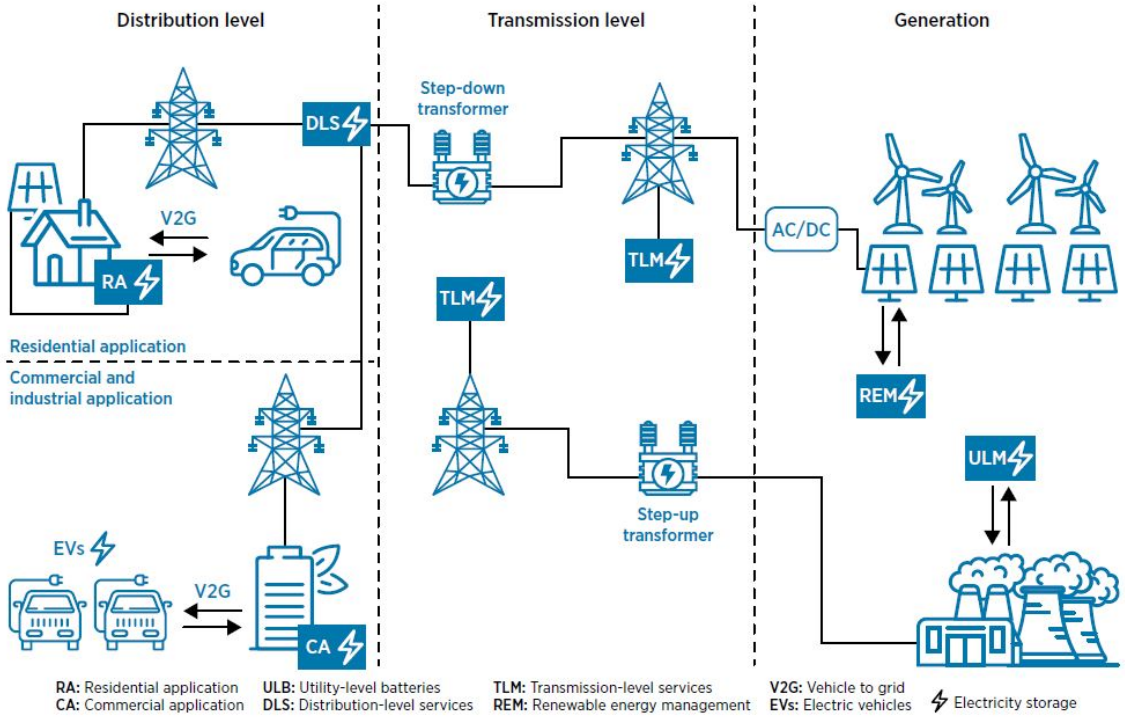

Figure 1.1: Potential Locations and Applications of Electricity Storage in the Power System [44].

Various types of technologies have been developed for storing energy, including thermal, mechanical, gravitational, and electrochemical technologies. Names of these technologies define the scientific concept behind each of them for saving energy; hence no further descriptions are brought here to avoid prolongation and more explanations can be found in [43]. Just to clarify, mechanical energy storage term covers a wide

range of technologies like PSH and compressed air, and gravitational technologies also fit in this group. However, the gravitational term mostly refers to the artificial structures that are used for storing energy rather than using geological formations like PSH. The application of energy storing technologies in the grid depends on the duration of energy provision.

Figure 1.2 shows the operational durations of several energy storage technologies and their related application in the grid. In this figure, the ramping application refers to the action of rapidly changing output to align supply and demand; smoothing is the process of flattening the output curve of intermittent sources like wind and solar, and peaking is the ability for supplying extra energy in the peak hours.

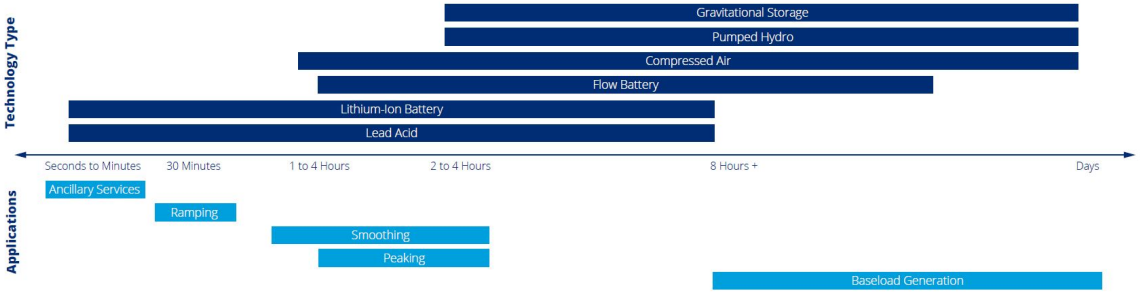

Figure 1.2: Energy Storage Technologies' Applications [69].

The PSH accounts for the most significant share of the energy storage capacity across the U.S., where 95 % of utility-scale energy storage plants are PSH [26]. The PSH projects are dependent on the availability of specific geological formations and can cause environmental impacts. Also, these projects have long construction times [69]. As a result, this type of energy storage is not currently expanding in the grid.

Recent developments in the electrochemical technologies improved the energy density, and operational duration of the batteries, which enables them to provide various services as it is shown in Figure 1.2. On the other hand, these developments reduced the battery production cost [74]. As a result, almost all of the storage capacity expansion to the U.S. grid since 2003 are BESSs [7]. For this reason, our research work,

similar to most of the other works in this area, focuses on the BESSs specifically large-scale ones.

1.2 Battery Energy Storage Systems

Among various electrochemical technologies, lithium-ion batteries, lead-acid batteries, and flow batteries are the popular ones for the power system applications [26]. Lithium-ion batteries are currently the most advanced batteries for various fields as well as electricity grid applications, and their price has declined by 72.9% since 2013. Thus, lithium-ion batteries account for 90% of the deployed BESS these days [69]. This section briefly summarizes the characteristics of BESSs and explains their applications in the grid. Subsequently, it deals with the expansion trend of the BESSs in the gird.

Some of the characteristics of the BESSs which stimulate their applications in the power grid are categorized as follows [5].

- BESSs can change their output in a short time and have fast responses. This is the most important characteristic of BESSs. This feature makes BESSs distinct from most of the other power gird assets and enables them to provide a wide range of services.

- BESSs are very efficient and they return almost all of the stored energy in them. Lithium-ion batteries as an example have round-trip efficiency of 90-95 %, which is higher than any other technologies.

- BESSs are flexible and can match the supply and demand on the timescales from milliseconds to hours, covering most of the standard needs of the grid.

- BESSs can both dispatch and store energy. Although it looks trivial and all of the energy storage technologies are able to be reversible, this feature, besides

other characteristics of BESSs, makes them beneficial for the system and also gives them some advantages over other units.

- BESSs have become large enough to be used for grid services. Also, they are currently cheaper than most of the other new competitive technologies. All of these enhancements are the result of the recent investments in battery technology.

Based on the mentioned characteristics, BESSs have a broad range of applications in the power system. These applications are named and shortly explained below. Note that due to the current development in this technology, BESSs may also be used in other areas in the future [7, 8].

- **Frequency Regulation:** Managing the momentary balance between supply and demand to maintain the system's frequency within the permitted range.
- **Spinning Reserve:** Providing synchronized capacity for the grid to recover from any significant deviations in the system's generation due to unexpected events.
- **Energy Arbitrage:** This is also referred to as energy time-shift and happens when BESS charges with inexpensive energy in off-peak hours and discharges in the hours with higher energy price.
- **Electric Service Resiliency:** Supplying a backup power that can be used after a system outage or blackout for energizing transmission lines, starting up generators ,or providing a reference frequency.
- **Renewable Firming:** Co-locating BESS with intermittent generation sources like wind and solar to maintain a constant output power over a period of time and have more predictable generation.

- **Peak Shaving:** Reducing or deferring electricity demands during peak hours to lower the need for building new generating units.
- **Demand Side Services/Management:** Providing customer-related services such as demand change management, renewable power consumption maximization, power quality, and reliability.
- **Voltage and Reactive Power Services:** Serving as source or sink of reactive power for maintaining the local voltage.
- **Micro-Grids:** Using BESSs besides dispatchable or non-dispatchable generators for building a local set of loads and generations that can be islanded from the gird.
- **Transmission/Distribution System Deferral:** Lowering or differing the congestions of transmission or distribution lines by use of BESSs to avoid or reduce the requirement of new line construction.

It is worth mentioning that optimizing BESSs for doing multiple of the above-mentioned applications can result in better operation of them, and the system also can benefit more from them. This idea is known as value stacking [8].

As a result of this vast range of applications and the reduction in the manufacturing costs of the batteries, BESSs have become valuable assets in the power system. Hence, more BESSs are being integrated more into the system.

A considerable portion of the BESSs' expansion is behind the meter installation of the small-scale batteries. Using BESSs in commercial, industrial or residential locations can reduce their electricity consumption from the grid and lower their utility bills. Additionally, BESSs are also used in these locations for increasing resilience and enhancing the performance of the distributed energy resources (DER) [8]. In 2016,

two-thirds of small-scale battery storage capacity was installed in the commercial sector [7].

Large-scale or utility-scale BESSs, which are grid-connected units with an output power of 1 MW or more, are also expanding in recent years based on their advantages for the gird, and existing policy drivers. Large-scale BESSs can benefit utilities by improving their grid reliability, doing transmission/distribution deferrals, and enhancing renewable resources integration and generation management [8].

Policy drivers have an indisputable role in the expansion of the utility-scale BESS into the U.S. grid. At the federal level, there exist several investment tax credits for the co-ops that are installing BESSs. At the state policy level, an increasing number of states are supporting the expansion of BESSs by adding energy storage targets to their renewable portfolio standards [8]. The most consequential policy drivers are FERC's orders. Among them, order 841 is the most important one which requires independent system operators (ISOs) and regional transmission organizations (RTOs) to remove barriers to the participation of BESSs into the wholesale markets [29]. FERC order 755 also incentives expansion of BESSs by promoting fast response units[28].

As a result of all of the characteristics mentioned above, applications of BESSs, and existing incentives, the U.S.power system is experiencing a growing integration of BESSs. It is expected that the total capacity of installed BESSs in the U.S. could reach 15000 MW by 2030 [4]. More importantly, installed capacity of the utility-scale BESSs in the U.S. reaches 2500 MW by 2023 [10].

This growth necessitates the U.S. power industry to evaluate and address potential challenges caused by BESSs integration. Thus, in the past years, various research works have been done on this issue, and also there is a large number of ongoing investigations on this topic. This research work also deals with this subject. The

next section explains the motivation of the present dissertation and also describes the research problem that we deal with in this work.

1.3 Motivation

The previous section entirely described that integration of BESSs into the power grid can have lots of benefits and enhances the grid operation in many aspects, but it does not happen easily. Not only it is needed to study how the system can benefit the most from BESSs expansion but also it is necessary to investigate how using BESSs for a particular application may affect other aspects of the system or may affect other assets in the grid.

As a result, a wide range of research studies should be done in response to the expansion of BESSs. Several of the most important ones are power system stability analysis in the presence of BESSs; coordination of renewable resources with BESSs; control and operation of BESSs; electrical vehicles operation and their coordination with BESSs; generation/transmission expansion planning with BESSs; Impact of BESSs on the grid and market operations; and optimal scheduling of merchant BESSs. This dissertation mainly focuses on the last two topics.

On the one side, large-scale BESSs are expanding rapidly and FERC order 841 enables them to participate independently in the wholesale markets. On the other side, the specific technical characteristics of BESSs give them flexibility in the operation and distinguish them from other participants in the market. Hence, the operation of independent large-scale BESSs in the market can be different from other generating units, and it may affect the markets' outcome and also grid operations. This issue is investigated in this dissertation to understand the interaction between BESSs and markets better.

The concept of value stacking is much more important for large-scale BESSs as

they have more capacity, and it is easier to use them in multiple applications. Additionally, based on the portfolio concept, the operation of a large-scale BESS in various markets may increase its profit and decrease its investment risk. Thus, this work tries to find the most profitable operation scheduling for a large-scale BESS in the energy and ancillary services markets.

In order to move toward the above-mentioned research directions, this dissertation proposes various optimization frameworks for the participation of a price-maker large-scale BESSs in real-time energy, spinning reserve, and pay as performance frequency regulation market. Subsequently, several case studies based on real-world data are done using the proposed models. The next section provides an overview of the structure of this part of the dissertation.

1.4 Summery of Content

The rest of this part of the dissertation is organized as follows. Chapter 2 does a comprehensive literature review on this topic. This chapter divides the literature into two different groups based on the approach that they use for modeling the BESSs in the markets. These two approaches model the BESS as a price-taker or price-maker participant in various markets. Besides reviewing the research works, this chapter explains the concept behind each of the modeling approaches and their pros and cons.

Chapter 3 deals with the methodology and formulation of the proposed optimization frameworks for the participation of a price-maker BESS in energy and ancillary services markets. In this chapter, before the explanation of each model, a general overview of the concept of each of the modeled markets is provided. Subsequently, each of the three optimization frameworks is formulated in detail. The difference between the first two optimization frameworks is in the extent of their accuracy for

modeling BESS's operation and market structures, while the third framework introduces uncertainty to the bidding problem.

Chapter 4 provides various case studies on the three models to validate their performance and compare them. Additionally, the intended research goal is pursued by these case studies. For each of the deterministic models, four different case studies are done, where each case represents a particular market participation policy for the BESS. In addition to those eight case studies, the effects of several controversial BESS parameters on the result are also analyzed in this chapter. Finally, the accuracy of the approximation method for a stochastic framework is evaluated, and the BESS participation problem is solved while errors are imposed into the optimization parameters.

Finally, chapter 5 summarizes the main outcomes of this research work and also depicts the path for the continuation of this work in the future.

Chapter 2

LITERATURE REVIEW

In general, a large portion of the literature on the topic of BESSs in the grid deal with the sizing, placement, and scheduling of these systems for maximizing the system reliability and operation efficiency [86]. Note that the intended system can be the whole gird with various types of generations and loads or a generation fleet with several DERs [59, 84, 53, 16, 60, 49]. The focus of these works is not necessarily the profitability of the BESS and does not consider BESS as an independently-operated unit. As these works do not directly deal with the concept of the electricity market and the market participation of BESSs, they are not in-line with the topic of this dissertation.

The literature that models the operation of the BESSs in the markets and grid can be divided into two main categories based on their approach for BESSs' modeling in the system. The first group models BESS as a price-taker in various markets. It means that BESS cannot affect the markets' outcome and the grid and markets' structures are not modeled in these works. In the second group of research works, BESS is modeled as a price-maker or strategic participant in the markets due to its size and specific operational capabilities. Hence, the profit maximization problem is a bi-level optimization that not only finds the optimal scheduling pattern for BESSs but also models the grid and markets' structure in the problem.

The following sections are dedicated to each of the categories as mentioned earlier. In each section, first, the structure of the modeling approach is explained. Subsequently, some of the recent most important published works in that group are reviewed. Finally, each section concludes with the pros and cons of the modeling

approach.

2.1 Price-taker Model

In the price-taker model, as it is shown in Figure 2.1, a single-level optimization problem is solved for finding the optimal scheduling pattern for the BESS. In the objective function, the BESS owner who can have several units across the grid, maximizes its revenue from each of the markets, while it may or may not consider operational costs (degradation costs) for the batteries. Note that the horizon of this optimization can change from hours to days or more. The constraints of the problem are mostly operational limitations of the battery units like output power limits and state of charge (SOC) limits. However, any other constraints may also be added to this problem for specific operation modeling or degradation cost modeling.

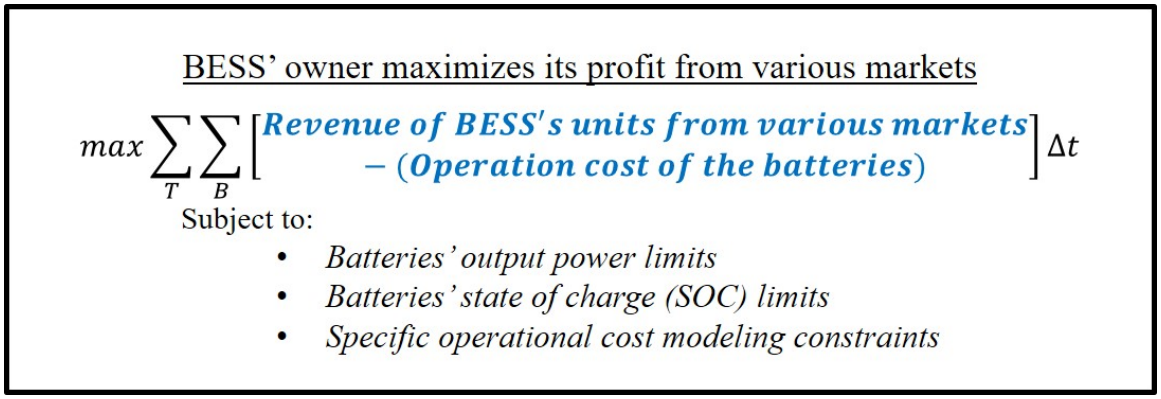

Figure 2.1: Problem Structure in the Price-taker Modeling Approach.

Scheduled power of the BESS's unit in each market for each time step are the variables of this optimization framework. The revenue of the BESS from each market is the multiplication of the scheduled power and the market prices. These market prices are parameters of this optimization model and are not affected by the BESS's operation.

It is worth mentioning that most of the research works in this area co-optimize the

operation of BESS along with other generation resources like renewable resources or DERs. It is also possible that BESS owner has electric vehicles charging fleets or performs demand response aggregation and maximize the profit of its assets altogether. In these cases, the objective function maximizes the revenue from BESS units and all of the other resources. Additional constraints may also be added regarding the operation of any other assets, and collaboration between batteries and those units. Several of the most important published papers in this area are reviewed below.

An optimization framework for coordinating the participation of a price-taker BESS in day-ahead and real-time energy markets is proposed in [55]. This work considers three different bidding options for BESS. In the first one, BESS submit self-scheduling bids, which means that BESS wants to participate in the market regardless of the market price. In the second and third options, BESS bids have both of the price offers and quantity offers. In the second one, day-ahead and real-time market prices are independent, but in the third option, these prices statistically depend on each other. Based on the proposed framework, several case studies are presented using real market data to assess the impact of location, season, battery efficiency, lifetime, charge and discharge rates, and using second-life/used batteries.

Reference[40] solves the profit maximization problem for a BESS participating in the day-ahead energy, reserve, and pay as performance frequency regulation markets. It also considers a battery life cycling model in the optimization problem. This work is close to our work as it is considering energy and ancillary services markets and also the life loss of the batteries is incorporated in the decision-making process. However, in contrast to our models, BESS is a price-taker in this paper. Their result shows that consideration of performance-based regulation market and degradation in the model changes the operation strategy of the BESS.

Charging/discharging schedules based on the battery's aging cost is achieved

through an online optimal control algorithm for providing peak shaving and frequency regulation services with a BESS [68]. The BESS owner of this work is a large commercial load that is using batteries for its electricity consumption in the peak hours while participating in the regulation market. The results show that the joint optimization significantly affect the total profit.

Uncertainty in the market prices for a price-taker BESS profit maximization problem is handled by a robust optimization approach in [47]. The uncertainties are modeled when the BESS is participating in the day-ahead energy, reserve and frequency regulation markets. The proposed model in previous work is further developed by adding the aging cost to it in [46]. The aging cost is considered by dividing the problem into the short-time and long-time problems, where the short-time problem imposes operational limits on the long-time one based on the aging cost. Subsequently, benders decomposition is used for solving the whole optimization consists of short- and long-time problems.

A piecewise function for battery degradation cost approximation is proposed in [82] and used for maximizing BESS's revenue from energy and reserve markets. The proposed degradation cost model provides a mathematical representation for the rainflow algorithm to be used in the problem. Using the rainflow algorithm for calculating batteries' cycle life loss is one of the accurate methods in this field. The authors of this paper also prove that if the number of the segments in the piecewise approximated function goes to the infinity their model will be exact.

The proposed cost approximation model of [82] is further developed in [75] for the optimal participation of an electric vehicle and battery storage aggregator in the frequency regulation market. This work also considers uncertainties in the parameters by the use of stochastic optimization. We have also used this degradation cost model in our proposed framework for the participation of a price-maker BESS in the energy

and ancillary services markets.

In the price-taker approach, it is possible to focus on the battery modeling's details and its control procedure for the optimal scheduling of merchant BESS. However, this approach cannot capture the possible effects that the BESS operation may have on the markets. Hence, it is not possible to investigate the effect of BESS on the market/grid operation using this approach. Additionally, the lack of grid operational limits like transmission line flow limits or not considering the maximum system requirement for each ancillary services may result in overestimating the potential profit of the BESS [24, 15].

2.2 Price-maker Model

This paper falls into the second category of existing literature, where the BESS is modeled as a price-maker or strategic participant in the markets due to its size and specific operational capabilities. Hence, the profit maximization problem is a bi-level optimization that not only solves the bidding strategy problem but also provides a framework for analyzing the impact of BESS on the markets.

As illustrated in Figure 2.2, the bi-level optimization problem consists of the upper-level problem (ULP) and the lower-level problem (LLP). The ULP is exactly the optimization problem of the price-taker (Figure 2.1) model. In this model market clearing prices for each of the services are not constant, and they are determined in the LLP along with the scheduled power.

The LLP is a simulation of the ISO's joint market-clearing process. It is an optimal power flow problem that is solved by ISOs for maximizing social welfare or minimizing total system cost. The objective function of the LLP is the total cost of supplying demands in the gird and also maintaining reliability services. Constraints of this problem are four groups in general: operational limits of the units that are

participating in various markets; specific requirements of some markets like pay as performance frequency regulation market; ancillary services requirements of the system; and physical constraints of the gird such as power balance of each node and transmission line flows.

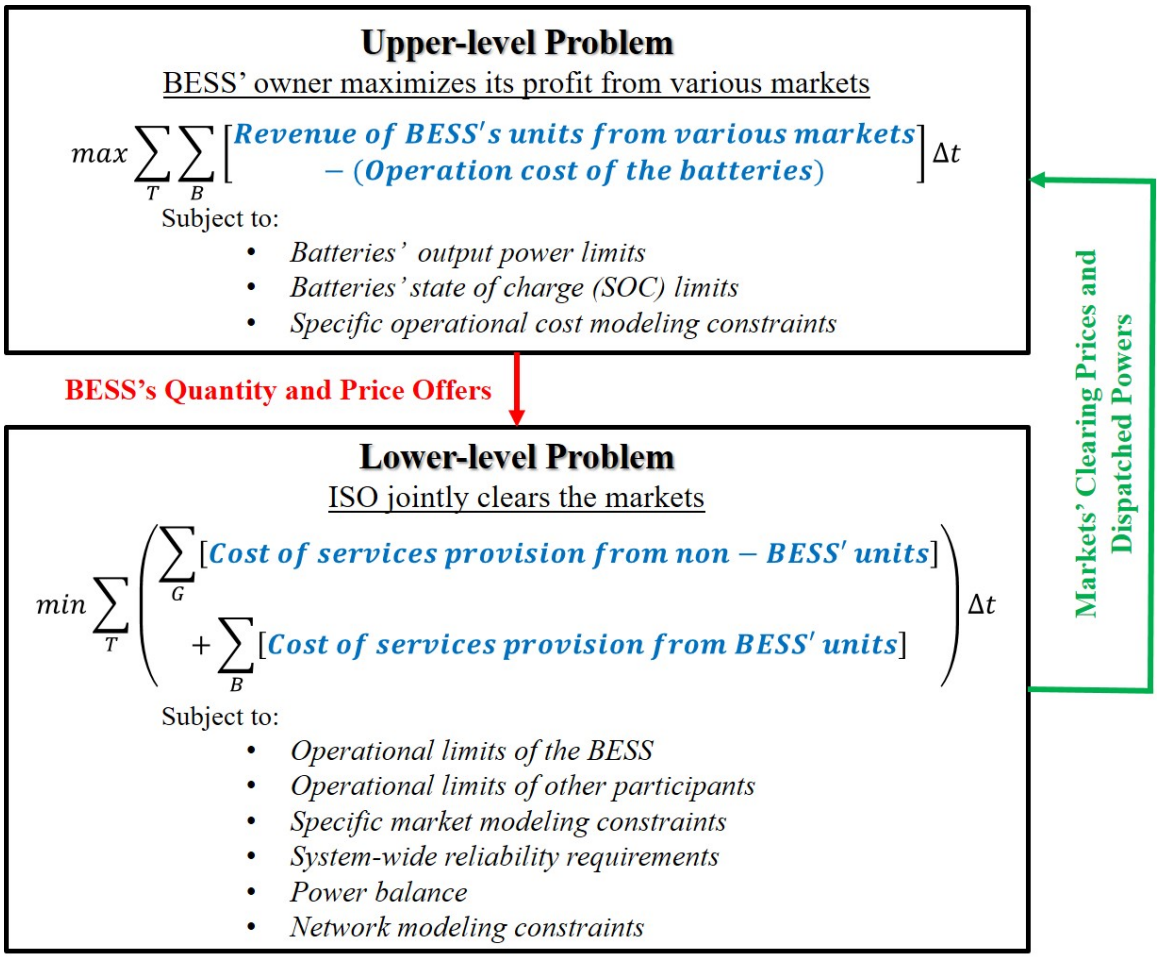

Figure 2.2: Problem Structure in the Price-maker Modeling Approach.

BESS's quantity and price offers are variables for the ULP and serve as input parameters to the LLP. On the other hand, market clearing prices and the scheduled power of the BESS's units result from the LLP. Thus, these two problems (ULP and LLP) are coupled together. In contrast to the price-taker approach, market clearing prices are not constant in this method, and decision variables of the BESS in the

ULP can affect the prices in LLP, hence it is called a price-maker participant. Note that modeling a participant as a price-maker allows the market participant to serve as a marginal unit in the markets. Some of the research works that model BESS as a price-maker are reviewed in the remainder of this section.

With a general perspective, [24] proposes a price-maker model for the participation of grid-scale energy storage in the day-ahead energy market with a high penetration of wind resources. Comparing price-taker and price-maker models is one of the main purposes of this work, and it shows that the price-taker model overestimates the energy storage revenue. Ancillary services markets are among the main revenue sources for energy storage systems. Thus, neglecting these markets in this paper may cause inaccurate conclusions.

Reference [88] constructs a Nash-Cournot equilibrium model for strategic interaction between various generation resources and an energy storage fleet. This paper models the participation of energy storage in the energy, reserve, and frequency regulation markets. Authors use the concept of potential functions for converting the bi-level model to a single-level optimization. Case study results based on the proposed model show that the addition of energy storage to the system increases the penetration of renewable resources and reduces the prices. The model proposed in this work deals with general energy storage instead of BESSs, hence it does not consider degradation cost and specific operational limits of this type of energy storage.

The performance of various market mechanisms in the existence of a utility-scale BESS is evaluated in [41]. The authors of this work conduct a comparative analysis on three market mechanisms that have appeared in the literature: the centralized mechanism, the semi-centralized mechanism, and the deregulated mechanism. In the first mechanism, BESS is operated by ISO, while in second and third mechanisms, BESS is modeled as a price-maker participant with various levels of freedom on its

output control. Their work establishes the equivalence between semi-centralized and deregulated mechanisms. This paper also proposes some modifications to the semi-centralized mechanism to compensate for its malfunction in particular cases.

The coordination problem of a price-maker BESS in the day-ahead energy market is addressed in [54]. Although this work does not model ancillary services markets that are usually more appealing for a BESS, it performs a comprehensive analysis of the markets' outcome and BESS's profit in different conditions. The case studies of this work are more focused on the transmission line congestions and show that even the existence of a price-maker BESS can benefit the system in these conditions. However, degradation cost is not considered in their model, and the addition of it can change the results.

The participation of a price-maker BESS in the day-ahead energy and reserve markets, along with the real-time balancing market, is discussed in [66]. This work considers uncertainties by doing stochastic optimization in the real-time balancing market. Modeling day-ahead reserve and real-time balancing markets in this paper makes its analysis more accurate and closer to the real opportunities that price-maker BESS can have. However, this paper does not model the frequency regulation market, and this exclusion may lead to inaccurate assessment of BESSs' stacked services and total profit. Additionally, this paper considers a linear cost for BESS's degradation, which is not an accurate model for batteries.

A BESS is modeled as price-taker in the energy market and price-maker in ancillary services markets in [15], where uncertainties in parameters are also considered. Instead of solving a bi-level optimization, this paper captures the effect of BESS on the ancillary services markets by predicting price quota curves for the reserve and regulation market. The use of price quota curves in this paper is similar to the concept of potential functions proposed in [88]. Although the proposed model in

this work is comprehensive and covers various details of the BESS and markets operations, the used price-maker modeling approach may not capture the correlation between markets, and adequately represent the BESS's effect on the markets' outcomes. Furthermore, the lack of battery degradation cost modeling is a hedge for having a realistic study on BESS's performance.

The common shortcoming for all pieces of literature that are modeling BESS as a price-maker is the lack of degradation costs for batteries. Consideration of an accurate degradation cost model for batteries is challenging and adds to the complexity of the model. Additionally, degradation cost modeling for a unit that is participating in the frequency regulation market requires exact AGC signals modeling, which also adds to the size and complexity of the optimization specially in the price-maker approach. These challenges are addressed in this dissertation by proposing two independent optimization frameworks for the participation of a large-scale price-maker BESS in real-time energy, reserve and pay as performance frequency regulation markets.The preliminary model of this work is published in [48].

Chapter 3

METHODOLOGY AND FORMULATION

As it was explained in chapter one, the current expansion of the large-scale BESSs throughout the grid necessitates researchers to not only study BESS's impact on the market and grid operations but also analyze the optimal allocation of merchant BESSs across various markets. Chapter two described that it is possible to move along both of these research directions by modeling BESS as a price-maker in various markets. The literature review also shows some of the shortcomings of existing works in this area. In this chapter, three separate optimization frameworks are proposed for the participation of a utility-scale price-maker BESS in the real-time energy and ancillary services markets. These frameworks try to fill the gap of the existing models, hence it is possible to study the issues mentioned above more accurately.

The general structure of all proposed bi-level optimization frameworks is similar. In their ULP, BESS maximizes its profit from real-time energy and ancillary services markets. The LLP problem of these models simulates the ISO's joint market-clearing process. In one of the models, batteries' degradation cost is neglected, and instead of an exact deployment modeling of AGC signals from BESS, a novel approach is used for handling AGC dispatches. This optimization framework is called the preliminary model as it is less sophisticated than the other one. The detailed model is developed upon this preliminary model. The detailed model uses an accurate degradation cost model for batteries, and AGC signals are dispatched to BESS based on the market outcomes. Note that improvement from the preliminary model to the detailed one increases the optimization problem size and complexity. Finally, the stochastic framework introduces uncertainties to the participation problem.

In the rest of this chapter, Section 3.1 explains the structure of the markets that are modeled in this work. The preliminary formulation for the optimal participation of price-maker BESS in the real-time energy and ancillary services markets is proposed in Section 3.2. Section 3.3 explains the development of the preliminary model to the detailed version. Section 3.4 describes the stochastic framework. Section 3.5 demonstrates the procedure for solving the proposed bi-level optimizations. Finally, Section 3.6 proposes an approximation approach for solving the stochastic model.

3.1 Market Structures

In this work, the optimal participation of a price-maker BESS in real-time energy, spinning reserve, and pay as performance frequency regulation markets are modeled. A general description of these markets' structures is brought in this section to ease the description of the proposed formulations.

3.1.1 Energy Market

The real-time energy market is modeled using a simplified approach. This model allows BESSs to submit supply or demand bids in order to gain profit from energy arbitraging between different time intervals or various markets. It means that in each market interval, BESS can either buy electricity and charges itself from the grid (demand bid) or sell energy and discharges (supply bid). BESS's bids consist of two components: quantity offers and price offers. Quantity offer shows the maximum amount of power that BESS is willing to sell or buy in a specific market interval. The price offer is the minimum/maximum price at which BESS wants to sell/buy power. The supply and demand bids are variables for the ULP.

Other market participants (such as conventional generators) submit supply bids to the real-time energy market to fulfill system net demand in each time interval. Price-

responsive loads are not modeled in this work, and there is no demand bid submitted by non-BESS participants in the real-time energy market. It is also assumed that conventional generators' bids are equal to their marginal costs, and BESS is able to perfectly predict their bids. Thus, other market participant bids are parameters for the LLP. For each market clearing interval, the LLP optimizes the real-time energy market and determines the share of the BESS and conventional generators in this market based on their bids.

3.1.2 Spinning Reserve

The modeled real-time spinning reserve market in this work is an upward-only market. The units that participate in this market do not operate at their maximum capacity, so they are able to increase their output power in case of a power shortage in the system. The reserve market clearing price compensates reserve market participants (including BESSs) for each MW of their reserved capacities.

Similar to the energy market, BESS bids for the reserve market consist of quantity and price offers in each market interval. They are respectively BESS's maximum amount of selling power at this market and minimum price that it requires for providing reserve. Bids of BESS in the reserve market are variable to the ULP, other market participants' bids are known to the BESS and are parameters for the LLP.

The joint market clearing procedure that is modeled in the LLP determines system-wide reserve market prices and scheduled reserves for each participating unit. Although it is not usual to consider a downward reserve market, it is similar to the upward reserve and can be handled by the proposed framework through minor adjustments. Deployment of spinning reserve products is only modeled in the stochastic framework since the reserve deployment is called in contingency situations.

3.1.3 Frequency Regulation Market

The modeled real-time frequency regulation market in this work is a pay as performance market, which is implemented by ISOs due to FERC order 755 [28]. The pay as performance regulation market consists of two different payment components for regulation capacity and regulation mileage. The regulation capacity payment is paid to the regulating units for reserving each MW of their generation capacity to provide regulation services. The regulation mileage payment is paid for each MW of deployed regulation service (for both up-regulation and down-regulation). The amount of deployed regulation service is the share of the regulation unit in following AGC signals that are continuously sent to the regulation market participants (every four seconds). The payment components of the regulation market are affected by the units' accuracy in following AGC signals. It means that the regulation market revenue of a unit decreases as the difference between its output and instructed AGC setpoint increases. Additionally, in the pay as performance market structure, the historical performance of the units in following AGC signals also affects the units' share in the market.

Figure 3.1 shows the concepts of regulation mileage and accuracy. In this figure, the blue curve is the instructed AGC signal to a unit, and the red curve is the output of the unit which is not exactly the same as the blue due to generator dynamics.

The modeled pay as performance frequency regulation market of this work is similar to the California ISO (CAISO) regulation market [1], and it is formulated based on the proposed model in [65]. Market participants submit quantity and price offers for regulation capacity provision, which are respectively the maximum amount of power that they want to sell in the regulation capacity market and the minimum price that they require for providing regulation capacity service. For the regulation

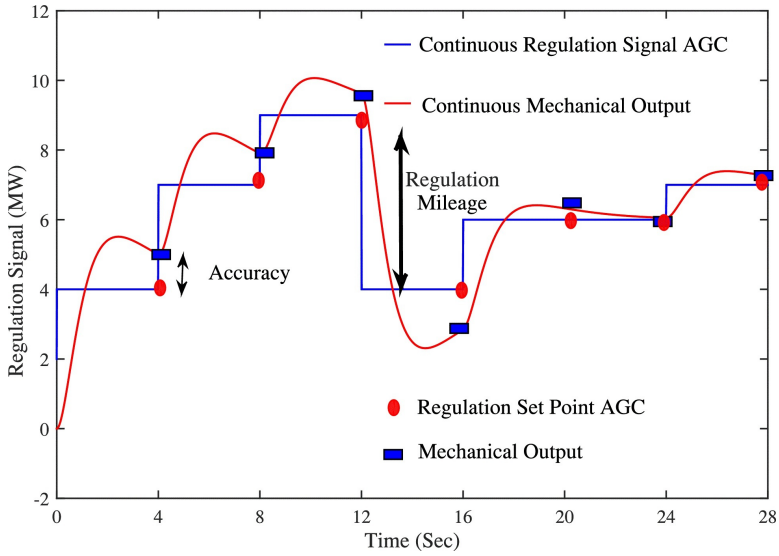

Figure 3.1: An Example of Regulation Mileage and Accuracy [65].

mileage, participants only submit price offers to the market, while their scheduled regulation mileage in the market is lower-bounded by their scheduled regulation capacity and upper-bounded by a factor (> 1) of their regulation capacity. This factor is determined by ISO based on the units' historical performance.

Similar to the energy and reserve markets, BESS's bids in the regulation market are variable to the ULP, and other market participants' bids are parameters to the LLP as it is assumed that BESS can predict their bids. Based on these bids, the LLP problem optimizes the regulation market along with reserve and energy to find the scheduled power of each unit and system-wide regulation capacity and mileage prices. In reality, ISOs try to dispatch AGC signals according to the market outcomes. Thus, it is not trivial to model AGC signal deployments from BESS in a bi-level optimization framework. The way of handling AGC signal deployment from BESS is one of the main differences between the two optimization models that are presented in this work and will be further discussed in the model formulation sections.

This section provided a general structural overview of the real-time energy, spinning reserve, and pay as performance frequency regulation markets. Two different

optimization models for optimal participation of a price-maker BESS in the above-mentioned markets are presented in the remainder of this chapter.

3.2 Preliminary Optimization Framework for the Participation of a BESS in Energy and Ancillary Services Markets

An optimization framework for the participation of a large-scale price-maker BESS in real-time energy and ancillary services markets is proposed in this section. The model is called the preliminary one as it is fundamental for the other framework that is discussed in the next section. Although in comparison to the other model, this preliminary model neglects degradation cost and has fewer details; it still captures all of the operational principles of BESS participation in several markets. The main features of the proposed preliminary optimization framework are as follows.

- The bidding and operation problem for a price-maker BESS in energy, spinning reserve, and pay as performance frequency regulation markets is formulated as a bi-level optimization problem while considering operational details of BESS and structural elements of each market.

- BESSs' fast ramping capability and accurate regulation signal tracking ability enable them to not only gain more profit from the pay as performance frequency regulation market but also become price makers and impact the market outcomes. Thus, it is crucial to consider the participation of a price-maker BESS in the pay as performance regulation market.

- In this model, deployment of AGC signals in a bi-level problem and coordination between energy, reserve, and regulation markets are handled through a particular choice of market clearing intervals.

- BESSs are technically capable of multiple-service provision. Thus, simultaneously participating in several markets may increase their profit and also benefit the power system more, compared to operating in a single market. Consideration of the spinning reserve markets besides energy and regulation markets in this model enables us to understand better the BESS operation and its effects on the grid.

In the rest of this section, the formulation of the ULP and LLP of the preliminary optimization framework is proposed along with a complete explanation of them.

3.2.1 Upper-level Problem Formulation

In the ULP, the BESS owner that has several units across the grid maximizes its revenue from participating in real-time energy, spinning reserve and pay as performance frequency regulation markets. The ULP is formulated as follows. These equations are indexed with PU, which represents ULP of the preliminary model.

$$\text{Max} \sum_{t\in\mathcal{T}} \sum_{i\in\mathcal{B}} \left[\pi^{E}_{i,t}(P^{B,S}_{i,t} - P^{B,D}_{i,t}) + \pi^{Rs}_{t} P^{B,Rs}_{i,t} + \pi^{RgC}_{t} P^{B,RgC}_{i,t} + \pi^{RgM}_{t} P^{B,RgM}_{i,t}\right]\Delta t \tag{PU.1}$$

Subject to:

$$0 \le O^{S}_{i,t} \le u_{i,t} P^{Rate}_{i} \qquad \forall i \in \mathcal{B}, \forall t \in \mathcal{T} \text{ (PU.2)}$$

$$0 \le O^{D}_{i,t} \le (1 - u_{i,t}) P^{Rate}_{i} \qquad \forall i \in \mathcal{B}, \forall t \in \mathcal{T} \text{ (PU.3)}$$

$$0 \le O^{Rs}_{i,t} \le P^{Rate}_{i} \qquad \forall i \in \mathcal{B}, \forall t \in \mathcal{T} \text{ (PU.4)}$$

$$0 \le O^{RgC}_{i,t} \le P^{Rate}_{i} \qquad \forall i \in \mathcal{B}, \forall t \in \mathcal{T} \text{ (PU.5)}$$

$$-P^{Rate}_{i} + P^{B,RgC}_{i,t} \le P^{B,S}_{i,t} - P^{B,D}_{i,t} \le P^{Rate}_{i} - P^{B,RgC}_{i,t} - P^{B,Rs}_{i,t} \qquad \forall i \in \mathcal{B}, \forall t \in \mathcal{T} \text{ (PU.6)}$$

$$SOC_{i,t} = SOC_{i,t-1} + (P^{B,D}_{i,t} - P^{B,S}_{i,t})\Delta t \qquad \forall i \in \mathcal{B}, \forall t \in \mathcal{T} \text{ (PU.7)}$$

$$SOC_i^{Min} + (P_{i,t}^{B,Rs} + P_{i,t}^{B,RgC})\Delta t \leq SOC_{i,t} \leq SOC_i^{Max} - P_{i,t}^{B,RgC}\Delta t \quad \forall i \in \mathcal{B}, \forall t \in \mathcal{T} \text{ (PU.8)}$$

$$SOC_{i,t} = SOC_i^{Init} \quad \forall i \in \mathcal{B}, t = 0, t = \bar{t} \text{ (PU.9)}$$

$$u_{i,t} \in \{0, 1\} \quad \forall i \in \mathcal{B}, \forall t \in \mathcal{T} \text{ (PU.10)}$$

The first term in the objective function (PU.1) is BESS's revenue for its units' power exchange in the real-time energy market. Each unit can have either supply or demand bids in each market interval, which is imposed by the use of binary variables $u_{i,t}$ in constraints (PU.2) and (PU.3). These two constraints also limit the quantity offers of BESS's units for supply or demand to be within its charge/discharge limit.

The revenue of reserve service provision is considered in the second term of the objective function, and (PU.4) bounds the units' reserve quantity offers to their operating limits. The third and fourth terms of objective function respectively represent regulation capacity and regulation mileage payments to the BESS. Constraint (PU.5) serves the same role as previous constraints for regulation capacity quantity offers.

In order to model AGC signal deployment, it is assumed that the AGC signals have similar features as the RegD signals in the regulation market of PJM Interconnection. In this way, the average of the AGC signal is zero in each 15-minute time interval [80]. Using this AGC signal model and choosing 15-minute market clearing intervals, battery units' SOC at the beginning and end of each interval remains unchanged if they only participate in the regulation market. Thus, it is not required to model AGC signal deployments in the formulation, and it is enough to calculate mileage payment based on the scheduled power to each unit. Additionally, it is considered that the BESS's units can perfectly follow AGC signals, which is a realistic assumption due to the technical capabilities of the power electronic units at the output of battery units. As a result, regulation market payments of BESS are not affected by any accuracy

factor.

It is worth mentioning that consideration of 15-minute market intervals in addition to facilitating regulation market modeling is closer to the ISOs' practical operation routine. Hence, this assumption makes the model more realistic.

The fact that the cumulation of scheduled power for each BESS unit in various markets must not violate the unit's charge/discharge rate is described in (PU.6). Note that the up-ward only reserve provision and both direction regulation provision is considered in this constraint. Constraint (PU.7) updates BESS's units' SOC at each interval based on the previous interval SOC and share of each unit in the energy market. Note that ignoring reserve deployment and having AGC signals with zero average lead to just having energy market scheduled power in (PU.7). Constraint (PU.8) imposes the SOC limits of battery units while enough capacity is maintained for up-ward reserve provision and both direction regulation provision. Finally, Constraint (PU.9) not only specifies the initial SOC of the units but also ensures that SOC at the end of the day equals the initial SOC. Having similar SOC at the beginning and end of the day links operating periods to each other and help to generalize simulation results of a single day to a longer time horizon.

3.2.2 Lower-level Problem Formulation

The LLP describes the joint market-clearing process for ISO's real-time energy, spinning reserve, and pay as performance frequency regulation markets. The equations that are indexed by PL represent the LLP of the preliminary model.

The objective function (PL.1) determines the total operating cost of the system, considering energy and ancillary services provision. The constraints (PL.2) through (PL.4) describe that for each generating unit, its total power delivery at each time interval lies within its maximum and minimum generation limits, and its reserve and

regulation capacity provision at each time interval does not exceed the corresponding ramp rates. Similarly, constraints (PL.6) to (PL.9) describe that the corresponding power quantity offers limit the scheduled power of BESS's units in different markets.

$$\text{Min} \sum_{t\in\mathcal{T}} \Big[\sum_{j\in\mathcal{G}} \big(\alpha^{E}_{j,t} P^{G,E}_{j,t} + \alpha^{Rs}_{j,t} P^{G,Rs}_{j,t} + \alpha^{RgC}_{j,t} P^{G,RgC}_{j,t} + \alpha^{RgM}_{j,t} P^{G,RgM}_{j,t}\big) + \sum_{i\in\mathcal{B}} \big(\beta^{S}_{i,t} P^{B,S}_{i,t} - \beta^{D}_{i,t} P^{B,D}_{i,t} + \beta^{Rs}_{i,t} P^{B,Rs}_{i,t} + \beta^{RgC}_{i,t} P^{B,RgC}_{i,t} + \beta^{RgM}_{i,t} P^{B,RgM}_{i,t}\big) \Big] \Delta t \tag{PL.1}$$

Subject to:

$$P^{Min}_{j} + P^{G,RgC}_{j,t} \le P^{G,E}_{j,t} \le P^{Max}_{j} - P^{G,Rs}_{j,t} - P^{G,RgC}_{j,t} \qquad \forall j \in \mathcal{G}, \forall t \in \mathcal{T} \text{ (PL.2)}$$

$$0 \le P^{G,Rs}_{j,t} \le P^{Rs,ramp}_{j} \qquad \forall j \in \mathcal{G}, \forall t \in \mathcal{T} \text{ (PL.3)}$$

$$0 \le P^{G,RgC}_{j,t} \le P^{Rg,ramp}_{j} \qquad \forall j \in \mathcal{G}, \forall t \in \mathcal{T} \text{ (PL.4)}$$

$$P^{G,RgC}_{j,t} \le P^{G,RgM}_{j,t} \le m_{j,t} P^{G,RgC}_{j,t} \qquad \forall j \in \mathcal{G}, \forall t \in \mathcal{T} \text{ (PL.5)}$$

$$0 \le P^{B,S}_{i,t} \le O^{S}_{i,t} \qquad \forall i \in \mathcal{B}, \forall t \in \mathcal{T} \text{ (PL.6)}$$

$$0 \le P^{B,D}_{i,t} \le O^{D}_{i,t} \qquad \forall i \in \mathcal{B}, \forall t \in \mathcal{T} \text{ (PL.7)}$$

$$0 \le P^{B,Rs}_{i,t} \le O^{Rs}_{i,t} \qquad \forall i \in \mathcal{B}, \forall t \in \mathcal{T} \text{ (PL.8)}$$

$$0 \le P^{B,RgC}_{i,t} \le O^{RgC}_{i,t} \qquad \forall i \in \mathcal{B}, \forall t \in \mathcal{T} \text{ (PL.9)}$$

$$P^{B,RgC}_{i,t} \le P^{B,RgM}_{i,t} \le m_{i,t} P^{B,RgC}_{i,t} \qquad \forall i \in \mathcal{B}, \forall t \in \mathcal{T} \text{ (PL.10)}$$

$$\sum_{j\in\mathcal{G}} P^{G,Rs}_{j,t} + \sum_{i\in\mathcal{B}} P^{B,Rs}_{i,t} \ge R^{Rs}_{t} : [\pi^{Rs}_{t}] \qquad \forall t \in \mathcal{T} \text{ (PL.11)}$$

$$\sum_{j\in\mathcal{G}} P^{G,RgC}_{j,t} + \sum_{i\in\mathcal{B}} P^{B,RgC}_{i,t} \ge R^{RgC}_{t} : [\pi^{RgC}_{t}] \qquad \forall t \in \mathcal{T} \text{ (PL.12)}$$

$$\sum_{j\in\mathcal{G}} P^{G,RgM}_{j,t} + \sum_{i\in\mathcal{B}} P^{B,RgM}_{i,t} \ge R^{RgM}_{t} : [\pi^{RgM}_{t}] \qquad \forall t \in \mathcal{T} \text{ (PL.13)}$$

$$\sum_{j\in\mathcal{G}|j=n} P^{G,E}_{j,t} + \sum_{i\in\mathcal{B}|i=n} P^{B,E}_{i,t} = P^{Load}_{n,t} + \sum_{w\in\mathcal{N}} H_{nw}(\theta_{n,t} - \theta_{w,t}) : [\pi^{E}_{n,t}]$$

$$\forall n \in \mathcal{N}, \forall t \in \mathcal{T} \text{ (PL.14)}$$

$$-TL_{nw} \leq H_{nw}(\theta_{n,t} - \theta_{w,t}) \leq TL_{nw} \qquad \forall (n,w) \in \mathcal{L}, \forall t \in \mathcal{T} \text{ (PL.15)}$$

Constraints (PL.5) and (PL.10) are imposed for each regulation market participant (including the BESS's units and generating units) due to the pay as performance market model. The regulation mileage multiplier (m) in these constraints are parameters that ISO assigns to each unit based on its historical performance in following AGC signals.

According to the constraints (PL.11) through (PL.13), system requirements for reserve, regulation capacity, and regulation mileage are satisfied when the markets are cleared at each time interval. The dual variables of these constraints (indicated in front of each constraint) are market clearing prices for each of these services and are used in the ULP. The power balance in each node is satisfied by (PL.14), and its dual variable is the locational marginal price (LMP) of that bus. Finally, the thermal limits of transmission lines are considered by the last constraint (PL.15).

In Chapter 4, several simulations are done on the proposed model to analyze the optimal allocation of BESS's capacity across various markets and the effect of BESS's operation on the markets. Furthermore, case studies will evaluate the performance of the proposed model and also compare it with the detailed framework.

The preliminary optimization framework is further developed in the next section to add a degradation cost model for the batteries and a more accurate AGC signal dispatch model. The resulting model is called the detailed optimization framework.

3.3 Detailed Optimization Framework for the Participation of a BESS in Energy and Ancillary Services Markets

The preliminary model that was proposed in the previous section has various operational details of the BESS and markets, and it is possible to study multiple topics with this model. However, similar to most of the literature in this area, the preliminary framework suffers from not having an accurate model for battery degradation cost. Additionally, the lack of the AGC signal dispatch model not only can weaken the frequency regulation market model but also cause problems in degradation cost modeling. Therefore, this section extend the preliminary model to address these shortcomings. General features of the detailed optimization framework which is proposed in this section are summarized as follows.

- The strategic bidding problem for a price-maker BESS in real-time energy, spinning reserve, and pay as performance frequency regulation markets is formulated as a bi-level optimization problem while considering operational details of BESS and structural elements of each market.

- BESSs' fast ramping capability and accurate regulation signal tracking ability enable them to not only gain more profit from the pay as performance frequency regulation market but also become price makers and impact the market outcomes. Thus, it is crucial to consider the participation of price-maker BESS in the pay as performance regulation market.

- Frequency regulation market is BESSs' main source of profit, and it is important to study the effect of following AGC signals on BESS's operation and costs, which is not considered in the previous model. An AGC signal dispatch model is proposed here to deploy AGC signals in the bi-level framework based on

market outcomes.

- BESSs are technically capable of multiple-service provision. Thus, simultaneously participating in several markets may increase their profit and also benefit the power system more, compared to operating in a single market. Consideration of the spinning reserve markets besides energy and regulation markets in this model enables us to better understand the BESS operation and its effects on the grid.

- Despite BESS's technical capabilities, their high manufacturing cost is a huge hedge against their expansion, hence lack of cost consideration in the analysis may lead to misleading results. A realistic and accurate cost function is deployed in this model to have a proper analysis.

The formulation of the detailed optimization framework for the participation of the BESS in real-time energy and ancillary services markets is brought in the following subsections along with the description of the changes from the previous model and additions.

3.3.1 Upper-level Problem Formulation

The ULP maximizes BESS revenue from the real-time energy, spinning reserve, and pay as performance frequency regulation markets. The problem is formulated below and indexed with DU as it is the ULP of the detailed model. After pinpointing the changes in the ULP formulation from the preliminary one, the AGC signal dispatching approach and battery degradation cost model are described in detail.

Similar to the preliminary model, the first four terms of the objective function represent the revenue of BESS from various markets, but the energy market bids and accordingly scheduled power are handled differently in this model. BESS submits

one bid for the energy market in each interval, while its quantity offer can have negative or positive values to respectively represent demanding (charging) or supplying (discharging) energy. As a result, Constraint (DU.2) replaces (PU.2) and (PU.3) of the previous framework. Constraints (DU.3) through (DU.5) are similar to (PU.4) through (PU.6) with the corresponding changes for energy market scheduled power in (DU.5). The addition of AGC deployment and cost models are explained in the following subsections with their resulting modifications to the ULP formulation.

$$\text{Max} \sum_{t\in\mathcal{T}}\sum_{i\in\mathcal{B}} \Big\{ \Big[\pi^{E}_{i,t}P^{B,E}_{i,t} + \pi^{Rs}_{t}P^{B,Rs}_{i,t} + \pi^{RgC}_{t}P^{B,RgC}_{i,t} + \pi^{RgM}_{t}P^{B,RgM}_{i,t}\Big]\Delta t - \sum_{z\in\mathcal{Z}}\sum_{k\in\mathcal{K}} C^{Deg}_{i,k}P^{Dis}_{i,t,z,k}\Delta z\Big\} \tag{DU.1}$$

Subject to:

$$-P^{Rate}_{i} \le O^{E}_{i,t} \le P^{Rate}_{i} \qquad \forall i\in\mathcal{B},\forall t\in\mathcal{T} \text{ (DU.2)}$$

$$0 \le O^{Rs}_{i,t} \le P^{Rate}_{i} \qquad \forall i\in\mathcal{B},\forall t\in\mathcal{T} \text{ (DU.3)}$$

$$0 \le O^{RgC}_{i,t} \le P^{Rate}_{i} \qquad \forall i\in\mathcal{B},\forall t\in\mathcal{T} \text{ (DU.4)}$$

$$-P^{Rate}_{i} + P^{B,RgC}_{i,t} \le P^{B,E}_{i,t} \le P^{Rate}_{i} - P^{B,RgC}_{i,t} - P^{B,Rs}_{i,t} \qquad \forall i\in\mathcal{B},\forall t\in\mathcal{T} \text{ (DU.5)}$$

$$PF_{i,t} = \frac{P^{B,RgM}_{i,t}}{R^{RgM}_{t}} \qquad \forall i\in\mathcal{B},\forall t\in\mathcal{T} \text{ (DU.6)}$$

$$\sum_{i\in\mathcal{B}} PF_{i,t} \le 1 \qquad \forall t\in\mathcal{T} \text{ (DU.7)}$$

$$P^{B,E}_{i,t} + PF_{i,t}AGC_{t,z} = P^{TDis}_{i,t,z} - P^{TCh}_{i,t,z} \qquad \forall i\in\mathcal{B},\forall t\in\mathcal{T},\forall z\in\mathcal{Z} \text{ (DU.8)}$$

$$0 \le P^{TDis}_{i,t,z} \le v_{i,t,z}P^{Rate}_{i} \qquad \forall i\in\mathcal{B},\forall t\in\mathcal{T},\forall z\in\mathcal{Z} \text{ (DU.9)}$$

$$0 \le P^{TCh}_{i,t,z} \le (1-v_{i,t,z})P^{Rate}_{i} \qquad \forall i\in\mathcal{B},\forall t\in\mathcal{T},\forall z\in\mathcal{Z} \text{ (DU.10)}$$

$$P^{TDis}_{i,t,z}(\frac{1}{\eta_i}) = \sum_{k\in\mathcal{K}} P^{Dis}_{i,t,z,k} \qquad \forall i\in\mathcal{B},\forall t\in\mathcal{T},\forall z\in\mathcal{Z} \text{ (DU.11)}$$

$$P^{TCh}_{i,t,z}\eta_i = \sum_{k\in\mathcal{K}} P^{Ch}_{i,t,z,k} \qquad \forall i\in\mathcal{B},\forall t\in\mathcal{T},\forall z\in\mathcal{Z} \text{ (DU.12)}$$

$$P^{Ch}_{i,t,z,k}, P^{Dis}_{i,t,z,k} \geq 0 \qquad \forall i\in\mathcal{B},\forall t\in\mathcal{T},\forall z\in\mathcal{Z},\forall k\in\mathcal{K} \text{ (DU.13)}$$

$$e_{i,t,z,k} - e_{i,t,z-1,k} = (P^{Ch}_{i,t,z,k} - P^{Dis}_{i,t,z,k})\Delta z \qquad \forall i\in\mathcal{B},\forall t\in\mathcal{T},\forall z\neq 1\in\mathcal{Z},\forall k\in\mathcal{K} \text{ (DU.14)}$$

$$e_{i,t,z,k} - e_{i,t-1,\bar{z},k} = (P^{Ch}_{i,t,z,k} - P^{Dis}_{i,t,z,k})\Delta z \qquad \forall i\in\mathcal{B},\forall t\in\mathcal{T},\tau=1,\forall k\in\mathcal{K} \text{ (DU.15)}$$

$$0 \leq e_{i,t,z,k} \leq e^{Max}_{i,k} \qquad \forall i\in\mathcal{B},\forall t\in\mathcal{T},\forall z\in\mathcal{Z},\forall k\in\mathcal{K} \text{ (DU.16)}$$

$$SOC^{Min}_i + (P^{B,Rs}_{i,t}\Delta t) \leq \sum_{k\in\mathcal{K}} e_{i,t,z,k} \leq SOC^{Max}_i \qquad \forall i\in\mathcal{B},\forall t\in\mathcal{T},\forall z\in\mathcal{Z} \text{ (DU.17)}$$

$$\sum_{k\in\mathcal{K}} e_{i,t,z,k} = SOC^{Init}_i \qquad \forall i\in\mathcal{B}, t=0\,\&\,z=\bar{z}, t=\bar{t}\,\&\,z=\bar{z} \text{ (DU.18)}$$

$$v_{i,t,z}\in\{0,1\} \qquad \forall i\in\mathcal{B},\forall t\in\mathcal{T},\forall z\in\mathcal{Z} \text{ (DU.19)}$$

AGC Signal Dispatch Model

In reality, ISOs try to dispatch AGC signals based on the frequency regulation market outcomes, they may use various definitions of participation factors for doing it. However, they do not just rely on the participation factors and modifications may happen during post-optimization corrective actions [65]. In this work, a participation factor is defined for assigning a portion of the system's AGC signal to the BESS based on its share in the regulation mileage market.

Constraint (DU.6) defines the participation factor (PF), which is the ratio of the unit's scheduled regulation mileage power to the system total regulation mileage requirement in each interval. Constraint (DU.7) completes the PF definition by limiting the total share of BESS in each interval to one.

As mentioned, mileage payment is paid for the deployment of regulation service in each interval. So, based on the defined PF, Equation (3.1) calculates the mileage

payment for a unit $\hat{i}$ in an interval $\hat{t}$, and $\hat{z}$ is the index for AGC signal dispatching sub-intervals in that period. Note that the regulation mileage payment must also be affected by the units' accuracy in following AGC signals, but it is assumed that the BESS can perfectly follow AGC signals.

$$\pi_{\hat{t}}^{RgM} PF_{\hat{i},\hat{t}} \sum_{\hat{z}} |AGC_{\hat{t},\hat{z}} - AGC_{\hat{t},\hat{z}-1}| \tag{3.1}$$

The system regulation mileage requirement for the $\hat{t}$ interval is the summation of the absolute value differences between every two consecutive AGC setpoints (see Figure 3.1), and it can be written as (3.2).

$$R_{\hat{t}}^{RgM} = \sum_{\hat{z}} |AGC_{\hat{t},\hat{z}} - AGC_{\hat{t},\hat{z}-1}| \tag{3.2}$$

Therefore, Equation (3.3) shows that regulation mileage payment of each unit is equal to the fourth term of the objective function (DU.1) if one substitutes the (3.2) and (DU.6) in (3.1).

$$\pi_{\hat{t}}^{RgM} \frac{P_{\hat{i},\hat{t}}^{B,RgM}}{\sum_{\hat{z}} |AGC_{\hat{t},\hat{z}} - AGC_{\hat{t},\hat{z}-1}|} \sum_{\hat{z}} |AGC_{\hat{t},\hat{z}} - AGC_{\hat{t},\hat{z}-1}| = \pi_{\hat{t}}^{RgM} P_{\hat{i},\hat{t}}^{B,RgM} \tag{3.3}$$

Using the defined PF, constraints (DU.8) through (DU.10) determine whether each BESS's unit is charging or discharging in each sub-interval by accumulating its energy market share with the dispatched AGC signal to it. Resulting charge or discharge values are used for updating batteries' SOC in each sub-interval and calculating batteries' degradation cost.

The only concern about dispatching AGC signals using defined PF is the possibility that dispatched AGC signal to a unit in a sub-interval be greater than its scheduled regulation capacity in that interval. This issue is resolved by properly choosing the regulation market multipliers of the LLP. As was mentioned, the scheduled power of each unit for the regulation mileage market is upper bounded by a

factor (m) of the scheduled power for the regulation capacity market (see constraints (DL.5) and (DL.9) or (PL.5) and (PL.10)). As these multipliers and AGC signals are both parameters for the LLP, it is possible to choose these multipliers in a way that inequality condition (3.4) always holds. Note that mileage multipliers are also greater than one.

$$m_{n,t} < \frac{R_t^{RgM}}{Max_z(|AGC_{t,z} - AGC_{t,z-1}|)} \qquad \forall n \in \mathcal{B} \cup \mathcal{G}, \forall t \in \mathcal{T} \quad (3.4)$$

Based on (3.4) and regulation mileage constraints in LLP (constraints (DL.5) and (DL.9) or (PL.5) and (PL.10)), the following equation holds.

$$P_{n,t}^{RgM} \leq \frac{R_t^{RgM}}{Max_z(|AGC_{t,z} - AGC_{t,z-1}|)} P_{n,t}^{RgC} \qquad \forall n \in \mathcal{B} \cup \mathcal{G}, \forall t \in \mathcal{T} \quad (3.5)$$

By dividing both sides of (3.5) over R_t^{RgM} and multiplying by $Max_z(|AGC_{t,z} - AGC_{t,z-1}|)$, the following inequality condition results, which shows that the dispatched AGC signal to each unit using the defined PF will not be more than the unit's scheduled regulation capacity power.

$$PF_{n,t} Max_z(|AGC_{t,z} - AGC_{t,z-1}|) \leq P_{n,t}^{RgC} \qquad \forall n \in \mathcal{B} \cup \mathcal{G}, \forall t \in \mathcal{T} \quad (3.6)$$

Finally, it is worth mentioning that by defining PF, it is no longer needed to have 15-minutes market clearing intervals. Hence, it is possible to unconditionally choose the market clearing intervals' duration and also AGC signal dispatching periods' duration in this optimization model.

Battery Degradation Cost Model

Active materials of electrochemical batteries fade through the charging and discharging cycles, and chemists describe these processes using partial differential equations [27]. Although these models are very accurate, it is not possible to incorporate them

into the dispatch calculations [50]. Another way of modeling batteries degradation is defining stress functions for each of the factors that contribute to the capacity loss of the batteries [62]. These stress factors can be divided into two groups for a grid-connected battery.

The first group of these factors consists of the temperature and humidity of the batteries along with their state of life and calendar time. These are non-operational factors, hence it is not needed to model them in the dispatch scheduling model [45]. The most critical operational factors for lithium-ion batteries are charge/discharge cycle depth, current rate, overcharge/discharge, and average SOC [77]. Among these factors, the charge/discharge cycle depth is the most important one and has a more significant impact on battery degradation [64]. The second important factor is over-charge/discharge, which is avoided by adding SOC limits on BESS's units' operations. Furthermore, The effect of the current rate and average SOC factors are negligible in the grid-connected batters [56, 25]. Therefore, a degradation cost model that is based on the depth of charge/discharge cycles is used in this work.

The rainflow counting algorithm is used extensively in materials stress analysis to count cycles and quantify their cumulative impact, and this algorithm has been also used for batteries' degradation calculation [81]. For example, in the given SOC profile of Figure 3.2, there exist two full charge/discharge cycles of depth 10% and a full cycle of 40% based on rainflow algorithm. The life loss from each full charge/discharge cycle of depth δ is given by a cycle depth stress function $\Phi(\delta)$. Cycle depth stress functions are derived for each type of battery using experimental tests. As a result, the capacity loss of the battery whose SOC profile is shown in Figure 3.2 is equal to $2\Phi(0.1) + \Phi(0.4)$.

It is possible to convert the calculated capacity loss with the rainflow algorithm to a cost by multiplying it with battery replacement price. However, the problem is

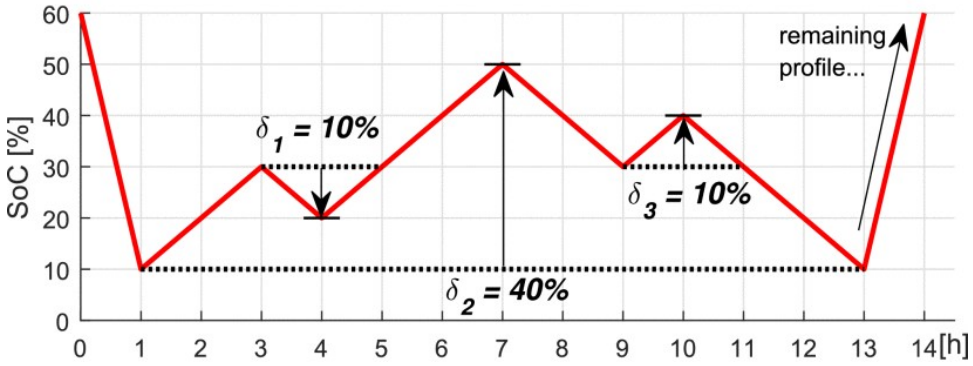

Figure 3.2: An Example of SOC Profile and Cycle Depth [82].

that the rainflow algorithm does not have an analytical mathematical expression and cannot be integrated directly within an optimization problem [18]. Thus, the used degradation cost model in this formulation works based on a linear approximation of rainflow algorithm and is proposed in [82].

In the degradation cost model, 0 to 100% of the battery capacity is uniformly divided into several segments that are represented by the $\mathcal{K}$ set. The energy capacity limit of each segment (e^{Max}) is a portion of the battery capacity, and also, a piecewise linear approximation of the degradation cost is assigned to each segment (C^{Deg}). For the $\hat{i}$-th unit of BESS the piecewise linear upper-approximation of its degradation cost function is calculated as follows.

$$C_{\hat{i}}^{Deg}(\delta) = \begin{cases} C_{\hat{i},1}^{Deg} & \text{if } \delta \in [0, \frac{1}{K}) \\ \vdots & \\ C_{\hat{i},k}^{Deg} & \text{if } \delta \in [\frac{k-1}{K}, \frac{k}{K}) \\ \vdots & \\ C_{\hat{i},K}^{Deg} & \text{if } \delta \in [\frac{K-1}{K}, 1] \end{cases} \tag{3.7}$$

Where

$$C_{\hat{i},k}^{Deg} = C_{\hat{i}}^{Rep} K [\Phi_{\hat{i}}(\frac{k}{K}) - \Phi_{\hat{i}}(\frac{k-1}{K})] \tag{3.8}$$

Here, K is the total number of segments, $C_{\hat{i}}^{Rep}$ is the $\hat{i}$-th unit's battery replacement cost ($/MWh), and $\Phi_{\hat{i}}$ is the cycle depth stress function of the $\hat{i}$-th unit. Figure 3.3 illustrates an example of cycle depth stress function and its piecewise linearization with different number of segments.

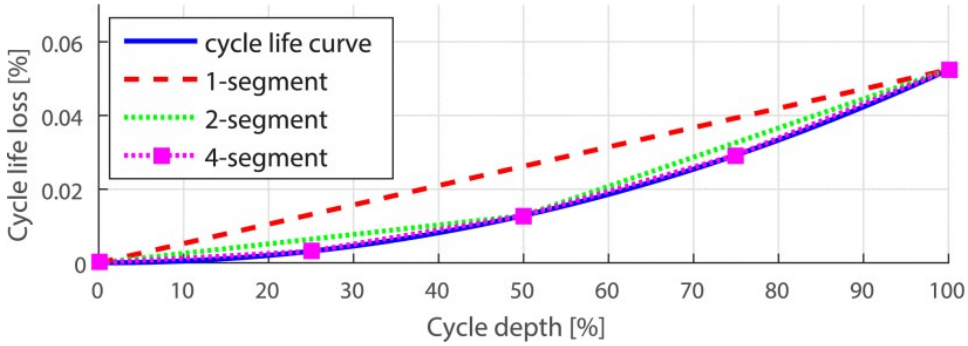

Figure 3.3: Upper-approximation to the Cycle Depth Aging Stress Function [82].

In the degradation cost model, battery cycle aging is only associated with the discharge stage of each charge/discharge cycle as each discharge stage will have a corresponding charging stage throughout the day. Therefore, the last term of the objective function (DU.1) uses the discharge powers in each sub-interval and the above-mentioned cost function approximation to calculate the degradation cost of the batteries.

Constraint (DU.11) to (DU.13) assign the charge and discharge power to the respective degradation segments, while the battery's charge/discharge efficiency is considered. Subsequently, Constraints (DU.14) and (DU.15) evaluate the stored energy in each segment, and (DU.16) enforce the segment energy limits. Note that (DU.15) relates the first sub-interval of each market-clearing interval to the last sub-interval of the previous market-clearing interval, while (DU.14) deals with consecutive sub-intervals in a market-clearing interval.

Due to the last term in the objective function and constraints (DU.11) through (DU.16), in each sub-interval, if the battery unit is charging, it charges the segments

with the lowest cost that have not reached their maximum energy limit yet. If it is discharging, energy discharges from the segments with the lowest cost that have been charged previously. According to our formulation, degradation cost is calculated in each sub-interval; hence, it includes the degradation cost resulted from following AGC signals. More details on the degradation cost approximation model can be found in [82, 75].

Finally, Constraint (DU.17) imposes the SOC limits of battery units while enough capacity is maintained for up-ward reserve provision. Constraint (DU.18) specifies the initial SOC of the units and also ensures that SOC at the end of the day equals the initial SOC.

3.3.2 Lower-level Problem Formulation

All of the developments from the preliminary framework to the detailed model happens in the ULP. Hence, The LLP of the detailed model remains almost the same as the LLP of the preliminary one. The formulation of the LLP that models ISO's market clearing process is as follows. The equations are indexed with (DL) to show that they are LLP of the detailed optimization framework.

$$\text{Min} \sum_{t\in\mathcal{T}} \Big[\sum_{j\in\mathcal{G}} \big(\alpha^{E}_{j,t} P^{G,E}_{j,t} + \alpha^{Rs}_{j,t} P^{G,Rs}_{j,t} + \alpha^{RgC}_{j,t} P^{G,RgC}_{j,t} + \alpha^{RgM}_{j,t} P^{G,RgM}_{j,t}\big) + \sum_{i\in\mathcal{B}} \big(\beta^{E}_{i,t} P^{B,E}_{i,t} + \beta^{Rs}_{i,t} P^{B,Rs}_{i,t} + \beta^{RgC}_{i,t} P^{B,RgC}_{i,t} + \beta^{RgM}_{i,t} P^{B,RgM}_{i,t}\big) \Big] \Delta t \qquad \text{(DL.1)}$$

Subject to:

$$P^{Min}_{j} + P^{G,RgC}_{j,t} \le P^{G,E}_{j,t} \le P^{Max}_{j} - P^{G,Rs}_{j,t} - P^{G,RgC}_{j,t} \qquad \forall j \in \mathcal{G}, \forall t \in \mathcal{T} \text{ (DL.2)}$$

$$0 \le P^{G,Rs}_{j,t} \le P^{Rs,ramp}_{j} \qquad \forall j \in \mathcal{G}, \forall t \in \mathcal{T} \text{ (DL.3)}$$

$$0 \le P^{G,RgC}_{j,t} \le P^{Rg,ramp}_{j} \qquad \forall j \in \mathcal{G}, \forall t \in \mathcal{T} \text{ (DL.4)}$$

$$P^{G,RgC}_{j,t} \le P^{G,RgM}_{j,t} \le m_{j,t} P^{G,RgC}_{j,t} \qquad \forall j \in \mathcal{G}, \forall t \in \mathcal{T} \text{ (DL.5)}$$

$$-O^{E}_{i,t} \leq P^{B,E}_{i,t} \leq O^{E}_{i,t} \qquad \forall i \in \mathcal{B}, \forall t \in \mathcal{T} \text{ (DL.6)}$$

$$0 \leq P^{B,Rs}_{i,t} \leq O^{Rs}_{i,t} \qquad \forall i \in \mathcal{B}, \forall t \in \mathcal{T} \text{ (DL.7)}$$

$$0 \leq P^{B,RgC}_{i,t} \leq O^{RgC}_{i,t} \qquad \forall i \in \mathcal{B}, \forall t \in \mathcal{T} \text{ (DL.8)}$$

$$P^{B,RgC}_{i,t} \leq P^{B,RgM}_{i,t} \leq m_{i,t} P^{B,RgC}_{i,t} \qquad \forall i \in \mathcal{B}, \forall t \in \mathcal{T} \text{ (DL.9)}$$

$$\sum_{j \in \mathcal{G}} P^{G,Rs}_{j,t} + \sum_{i \in \mathcal{B}} P^{B,Rs}_{i,t} \geq R^{Rs}_{t} : \pi^{Rs}_{t} \qquad \forall t \in \mathcal{T} \text{ (DL.10)}$$

$$\sum_{j \in \mathcal{G}} P^{G,RgC}_{j,t} + \sum_{i \in \mathcal{B}} P^{B,RgC}_{i,t} \geq R^{RgC}_{t} : \pi^{RgC}_{t} \qquad \forall t \in \mathcal{T} \text{ (DL.11)}$$

$$\sum_{j \in \mathcal{G}} P^{G,RgM}_{j,t} + \sum_{i \in \mathcal{B}} P^{B,RgM}_{i,t} \geq R^{RgM}_{t} : \pi^{RgM}_{t} \qquad \forall t \in \mathcal{T} \text{ (DL.12)}$$

$$\sum_{j \in \mathcal{G} | j=n} P^{G,E}_{j,t} + \sum_{i \in \mathcal{B} | i=n} P^{B,E}_{i,t} = P^{Load}_{n,t} + \sum_{w \in \mathcal{N}} H_{nw}(\theta_{n,t} - \theta_{w,t}) : \pi^{E}_{n,t}$$

$$\forall n \in \mathcal{N}, \forall t \in \mathcal{T} \text{ (DL.13)}$$

$$-TL_{nw} \leq H_{nw}(\theta_{n,t} - \theta_{w,t}) \leq TL_{nw} \qquad \forall (n,w) \in \mathcal{L}, \forall t \in \mathcal{T} \text{ (DL.14)}$$

The objective function (DL.1) of the problem is the total system costs for satisfying demands and ancillary services provision. Similar to the previous model, constraints describe operational limits of generators (DL.2 through DL.4); limits of BESS's scheduled power due to its quantity offers (DL.6 through DL.8); limitations related to regulation mileage market model (DL.5 and DL.9); the satisfaction of system ancillary services requirements (DL.10 through DL.12); the power balance in each node (DL.13); and transmission line thermal limits (DL.14). The only difference between LLP of this model and the previous one is that Constraint (DL.6) replaces Constraints (PL.6) and (PL.7) as BESS's units share in the energy market is represented with one variable.

After describing the solving procedure of both proposed frameworks in the next section, chapter four presents the case study simulation results of these models.

3.4 Stochastic Optimization Framework for the participation of a BESS in Energy and Ancillary Services Market under Uncertainties

Although the proposed framework in the previous section meticulously models the operation parameters of the BESS and markets, it does not consider uncertainties in forecasted data e.g., load, and errors in the predicted variables e.g., other market participants offer. On the one hand, modeling BESS participation in energy and ancillary services markets needs to forecast a large amount of system operation data including load, each service requirement, and each service deployment value. On the other hand, price-maker modeling is based on having full knowledge of other participants' operation parameters and offers besides the grid model's data. Hence, a lack of uncertainty modeling in the optimization parameters may cause inaccuracies in the results. Additionally, stochastic optimization enables us to model reserve services deployment that was not modeled in the previous frameworks. As a result, this section proposes a stochastic optimization framework for the participation of a BESS in energy and ancillary services markets to introduce uncertainties to the detailed framework proposed previously.

3.4.1 Upper-level Problem Formulation

Similar to the previous frameworks, ULP maximizes BESS revenue from the real-time energy, spinning reserve, and pay as performance frequency regulation markets. The main difference in this framework ULP is that it maximizes the revenue for all uncertain scenarios. In other words, ULP determines a set of quantity and price offers for all scenarios that maximize the weighted average of BESS revenue in all possible scenarios. As the ULP of this framework is very similar to the detailed one (DU.1 - DU.19), only the changed or added equations are described here. Note that equations

in this section are labeled with SU to represent the ULP of the stochastic model.

$$\text{Max} \sum_{s\in\mathcal{S}} prob(s) \sum_{t\in\mathcal{T}} \sum_{i\in\mathcal{B}} \Big\{ \Big[\pi^{E}_{s,i,t}(P^{B,E}_{s,i,t} + P^{B,RsD}_{s,i,t}) + \pi^{Rs}_{t} P^{B,Rs}_{s,i,t} + \pi^{RgC}_{s,t} P^{B,RgC}_{s,i,t} + \pi^{RgM}_{s,t} P^{B,RgM}_{s,i,t} \Big] \Delta t - \sum_{z\in\mathcal{Z}} \sum_{k\in\mathcal{K}} C^{Deg}_{i,k} P^{Dis}_{s,i,t,z,k} \Delta z \Big\} \quad \text{(SU.1)}$$

Subject to:

$$0 \le O^{SE}_{i,t} \le u_{i,t} P^{Rate}_{i} \qquad \forall i \in \mathcal{B}, \forall t \in \mathcal{T} \text{ (SU.2)}$$

$$0 \le O^{DE}_{i,t} \le (1 - u_{i,t}) P^{Rate}_{i} \qquad \forall i \in \mathcal{B}, \forall t \in \mathcal{T} \text{ (SU.3)}$$

$$\beta^{E}_{i,t} \ge (1 - u_{i,t}) M \qquad \forall i \in \mathcal{B}, \forall t \in \mathcal{T} \text{ (SU.4)}$$

$$0 \le O^{Rs}_{i,t} \le P^{Rate}_{i} \qquad \forall i \in \mathcal{B}, \forall t \in \mathcal{T} \text{ (SU.5)}$$

$$0 \le O^{RgC}_{i,t} \le P^{Rate}_{i} \qquad \forall i \in \mathcal{B}, \forall t \in \mathcal{T} \text{ (SU.6)}$$

$$-P^{Rate}_{i} + P^{B,RgC}_{s,i,t} \le P^{B,E}_{s,i,t} \le P^{Rate}_{i} - P^{B,RgC}_{s,i,t} - P^{B,Rs}_{s,i,t} \qquad \forall s \in \mathcal{S}, \forall i \in \mathcal{B}, \forall t \in \mathcal{T} \text{ (SU.7)}$$

$$PF_{s,i,t} = \frac{P^{B,RgM}_{s,i,t}}{R^{RgM}_{s,t}} \qquad \forall s \in \mathcal{S}, \forall i \in \mathcal{B}, \forall t \in \mathcal{T} \text{ (SU.8)}$$

$$\sum_{i\in\mathcal{B}} PF_{s,i,t} \le 1 \qquad \forall s \in \mathcal{S}, \forall t \in \mathcal{T} \text{ (SU.9)}$$

$$P^{B,E}_{s,i,t} + PF_{s,i,t} AGC_{s,t,z} + P^{B,RsD}_{s,i,t} = P^{TDis}_{s,i,t,z} - P^{TCh}_{s,i,t,z} \qquad \forall s \in \mathcal{S}, \forall i \in \mathcal{B}, \forall t \in \mathcal{T}, \forall z \in \mathcal{Z} \text{ (SU.10)}$$

$$0 \le P^{TDis}_{s,i,t,z} \le v_{s,i,t,z} P^{Rate}_{i} \qquad \forall s \in \mathcal{S}, \forall i \in \mathcal{B}, \forall t \in \mathcal{T}, \forall z \in \mathcal{Z} \text{ (SU.11)}$$

$$0 \le P^{TCh}_{s,i,t,z} \le (1 - v_{s,i,t,z}) P^{Rate}_{i} \qquad \forall s \in \mathcal{S}, \forall i \in \mathcal{B}, \forall t \in \mathcal{T}, \forall z \in \mathcal{Z} \text{ (SU.12)}$$

$$P^{TDis}_{s,i,t,z}(\frac{1}{\eta_i}) = \sum_{k\in\mathcal{K}} P^{Dis}_{s,i,t,z,k} \qquad \forall s \in \mathcal{S}, \forall i \in \mathcal{B}, \forall t \in \mathcal{T}, \forall z \in \mathcal{Z} \text{ (SU.13)}$$

$$P^{TCh}_{s,i,t,z} \eta_i = \sum_{k\in\mathcal{K}} P^{Ch}_{s,i,t,z,k} \qquad \forall s \in \mathcal{S}, \forall i \in \mathcal{B}, \forall t \in \mathcal{T}, \forall z \in \mathcal{Z} \text{ (SU.14)}$$

$$P^{Ch}_{s,i,t,z,k}, P^{Dis}_{s,i,t,z,k} \ge 0 \qquad \forall s \in \mathcal{S}, \forall i \in \mathcal{B}, \forall t \in \mathcal{T}, \forall z \in \mathcal{Z}, \forall k \in \mathcal{K} \text{ (SU.15)}$$

$$e_{s,i,t,z,k} - e_{s,i,t,z-1,k} = (P^{Ch}_{s,i,t,z,k} - P^{Dis}_{s,i,t,z,k})\Delta z$$
$$\forall s \in \mathcal{S}, \forall i \in \mathcal{B}, \forall t \in \mathcal{T}, \forall z \neq 1 \in \mathcal{Z}, \forall k \in \mathcal{K} \quad \text{(SU.16)}$$

$$e_{s,i,t,z,k} - e_{s,i,t-1,\bar{z},k} = (P^{Ch}_{s,i,t,z,k} - P^{Dis}_{s,i,t,z,k})\Delta z$$
$$\forall s \in \mathcal{S}, \forall i \in \mathcal{B}, \forall t \in \mathcal{T}, \tau = 1, \forall k \in \mathcal{K} \quad \text{(SU.17)}$$

$$0 \leq e_{s,i,t,z,k} \leq e^{Max}_{i,k} \qquad \forall s \in \mathcal{S}, \forall i \in \mathcal{B}, \forall t \in \mathcal{T}, \forall z \in \mathcal{Z}, \forall k \in \mathcal{K} \quad \text{(SU.18)}$$

$$SOC^{Min}_i + (P^{B,Rs}_{s,i,t}\Delta t) \leq \sum_{k \in \mathcal{K}} e_{s,i,t,z,k} \leq SOC^{Max}_i$$
$$\forall s \in \mathcal{S}, \forall i \in \mathcal{B}, \forall t \in \mathcal{T}, \forall z \in \mathcal{Z} \quad \text{(SU.19)}$$

$$\sum_{k \in \mathcal{K}} e_{s,i,t,z,k} \geq SOC^{Init}_i \qquad \forall s \in \mathcal{S}, \forall i \in \mathcal{B}, t = 0 \,\&\, z = \bar{z}, t = \bar{t} \,\&\, z = \bar{z} \quad \text{(SU.20)}$$

$$v_{s,i,t,z} \in \{0, 1\} \qquad \forall s \in \mathcal{S}, \forall i \in \mathcal{B}, \forall t \in \mathcal{T}, \forall z \in \mathcal{Z} \quad \text{(SU.21)}$$

$$LLP_s \qquad \forall s \in \mathcal{S} \quad \text{(SU.22)}$$

In this framework, the s subscript is added to represent the value of each variable for each scenario. The only variables that are the same for all scenarios are BESS's quantity O and price β offer meaning that this framework solution provides BESS with offers that maximize its overall profit. Hence, the objective function (SU.1) is the weighted average of BESS's revenue from various markets based on each scenario probability $prob(s)$. In this framework, a new revenue stream is added for BESS for the deployment of spinning reserve services. In reality, if a unit provides spinning reserve services, it will be compensated based on the real-time energy market price in after-market settlement. Hence, in the second expression of (SU.1), the share of BESS for spinning reserve provision in each scenario is multiplied by the energy price in that scenario. Also, Constraint (SU.10) considers the effect of spinning reserve deployment on the charge/discharge power of BESS in each hour.

Constraints (SU.2) and (SU.3) have replaced Constraint (DU.2) to ensure that BESS for each hour over different scenarios, BESS submits either a supply or a

demand bid. Additionally, Constraint (SU.4) forces the price of BESS's demand bid to be a high value making it a price-maker once buying energy. It is added to have a consistent model with other demands as flexible demands have not been modeled and all demands are price-taker. Constraint (SU.20) enforces BESS's SOC at the last interval to be greater than or equal to the initial SOC, which, similar to Constraint (DU.18), makes it possible to expand a short-time simulation result to a longer period. However, equality has changed to inequality in Constraint (SU.20) in comparison to Constraint (DU.18) as satisfying such equality constraint over several scenarios may have a considerable impact on the problem complexity and solution time. Finally, The last change in the ULP of this framework is Constraint (SU.22), which is only added to emphasize that uncertainties are added to the parameters in the LLP and for each scenario a different LLP is modeled. This Constraint could also be written in the previous frameworks as it is inherent in bi-level optimization modeling that ULP maximizes its objective subject to its own constraint and LLP. As described in Section 3.5, the LLP will be replaced with its KKT conditions to have a single-level optimization.

3.4.2 Lower-level Problem Formulation

The LLP of this framework similar to previous ones represents the ISO market clearing procedure. However, due to stochastic modeling in this framework, uncertainties are imposed on the parameters of the LLP, and there is a separate LLP for each scenario.

$\forall s \in \mathcal{S}$:

$$\text{Min} \sum_{t \in \mathcal{T}} \Big[\sum_{j \in \mathcal{G}} \big(\alpha^{E}_{s,j,t} (P^{G,E}_{s,j,t} + P^{G,RsD}_{s,j,t}) + \alpha^{Rs}_{s,j,t} P^{G,Rs}_{s,j,t} + \alpha^{RgC}_{s,j,t} P^{G,RgC}_{s,j,t} + \alpha^{RgM}_{s,j,t} P^{G,RgM}_{s,j,t} \big) +$$

$$\sum_{i\in\mathcal{B}}\left(\beta^{E}_{i,t}(P^{B,E}_{s,i,t}+P^{B,RsD}_{s,i,t})+\beta^{Rs}_{i,t}P^{B,Rs}_{s,i,t}+\beta^{RgC}_{i,t}P^{B,RgC}_{s,i,t}+\beta^{RgM}_{i,t}P^{B,RgM}_{s,i,t}\right)\Big]\Delta t \tag{SL.1}$$

Subject to:

$$P^{Min}_{s,j}+P^{G,RgC}_{s,j,t}\leq P^{G,E}_{s,j,t}\leq P^{Max}_{s,j}-P^{G,Rs}_{s,j,t}-P^{G,RgC}_{s,j,t} \qquad \forall j\in\mathcal{G},\forall t\in\mathcal{T} \text{ (SL.2)}$$

$$0\leq P^{G,Rs}_{s,j,t}\leq P^{Rs,ramp}_{s,j} \qquad \forall j\in\mathcal{G},\forall t\in\mathcal{T} \text{ (SL.3)}$$

$$0\leq P^{G,RsD}_{s,j,t}\leq f^{RsD}_{s,t}P^{G,Rs}_{s,j,t} \qquad \forall j\in\mathcal{G},\forall t\in\mathcal{T} \text{ (SL.4)}$$

$$0\leq P^{G,RgC}_{s,j,t}\leq P^{Rg,ramp}_{s,j} \qquad \forall j\in\mathcal{G},\forall t\in\mathcal{T} \text{ (SL.5)}$$

$$P^{G,RgC}_{s,j,t}\leq P^{G,RgM}_{s,j,t}\leq m_{s,j,t}P^{G,RgC}_{s,j,t} \qquad \forall j\in\mathcal{G},\forall t\in\mathcal{T} \text{ (SL.6)}$$

$$-O^{DE}_{i,t}\leq P^{B,E}_{s,i,t}\leq O^{SE}_{i,t} \qquad \forall i\in\mathcal{B},\forall t\in\mathcal{T} \text{ (SL.7)}$$

$$0\leq P^{B,Rs}_{s,i,t}\leq O^{Rs}_{i,t} \qquad \forall i\in\mathcal{B},\forall t\in\mathcal{T} \text{ (SL.8)}$$

$$0\leq P^{B,RsD}_{s,i,t}\leq f^{RsD}_{s,t}P^{B,Rs}_{s,i,t} \qquad \forall i\in\mathcal{B},\forall t\in\mathcal{T} \text{ (SL.9)}$$

$$0\leq P^{B,RgC}_{s,i,t}\leq O^{RgC}_{i,t} \qquad \forall i\in\mathcal{B},\forall t\in\mathcal{T} \text{ (SL.10)}$$

$$P^{B,RgC}_{s,i,t}\leq P^{B,RgM}_{s,i,t}\leq m_{s,i,t}P^{B,RgC}_{s,i,t} \qquad \forall i\in\mathcal{B},\forall t\in\mathcal{T} \text{ (SL.11)}$$

$$\sum_{j\in\mathcal{G}}P^{G,Rs}_{s,j,t}+\sum_{i\in\mathcal{B}}P^{B,Rs}_{s,i,t}\geq R^{Rs}_{s,t}:\pi^{Rs}_{s,t} \qquad \forall t\in\mathcal{T} \text{ (SL.12)}$$

$$\sum_{j\in\mathcal{G}}P^{G,RgC}_{s,j,t}+\sum_{i\in\mathcal{B}}P^{B,RgC}_{s,i,t}\geq R^{RgC}_{s,t}:\pi^{RgC}_{t} \qquad \forall t\in\mathcal{T} \text{ (SL.13)}$$

$$\sum_{j\in\mathcal{G}}P^{G,RgM}_{s,j,t}+\sum_{i\in\mathcal{B}}P^{B,RgM}_{s,i,t}\geq R^{RgM}_{s,t}:\pi^{RgM}_{s,t} \qquad \forall t\in\mathcal{T} \text{ (SL.14)}$$

$$\sum_{j\in\mathcal{G}|j=n}P^{G,E}_{s,j,t}+P^{G,RsD}_{s,j,t}+\sum_{i\in\mathcal{B}|i=n}P^{B,E}_{s,i,t}+P^{B,RsD}_{s,i,t}=P^{Load}_{s,n,t}+f^{RsD}_{s,n,t}R^{Rs}_{s,t}+$$
$$\sum_{w\in\mathcal{N}}H_{nw}(\theta_{n,t}-\theta_{w,t}):\pi^{E}_{s,n,t} \qquad \forall n\in\mathcal{N},\forall t\in\mathcal{T} \text{ (SL.15)}$$

$$-TL_{s,nw}\leq H_{s,nw}(\theta_{s,n,t}-\theta_{s,w,t})\leq TL_{s,nw} \qquad \forall (n,w)\in\mathcal{L},\forall t\in\mathcal{T} \text{ (SL.16)}$$

In the objective function of LLP, the cost of reserve deployment from other generators and BESS are added in comparison to previous frameworks. These costs are

calculated by energy market price offers of the market participant as it was assumed in the ULP that reserve deployment is compensated based on real-time energy market price. Also, the amount of spinning reserve deployment is added like a load to the right-hand side of the Constraint (SL.15). Note that the amount of reserve deployment in each bus and each hour of each scenario is modeled through a factor $f_{s,n,t}^{RsD}$ that multiplies to the spinning reserve requirement of that hour. In essence, it models what portion of the system's spinning reserve requirement is called due to contingency. Finally, Constraints (SL.4) and (SL.9) are added to ensure that the called spinning reserves of all units $P_{s,.,t}^{.,RsD}$ are not used toward satisfying system load and are only used for serving the deployed contingency reserve.

3.5 Solution Procedure of the Proposed Frameworks

The proposed bi-level optimizations are non-linear, non-convex, and hence, hard to solve. To find the solution to these problems, they are converted to a MILP by a similar procedure described in [34].

First, they are converted to a single-level optimization by writing the Karush-Kuhn-Tucker (KKT) conditions of the LLP as constraints for the ULP. The LLPs are linear and convex optimizations as the bids of BESS are not variables for these problems. So, the KKT conditions of the LLPs are necessary and sufficient to ensure their optimality. Thus, it is possible to include KKT conditions of the LLPs as constraints for the ULPs and convert the bi-level problem to a single-level one.

The resulting problems are called mathematical problems with equilibrium constraints (MPEC), and they have two sources of non-linearity. One is the complementary conditions that are within KKT equations, and the other one is the multiplication of variables in the objective function. It is possible to handle the former source of non-linearity with the Big-M method and replace each complementary condition with

two inequalities. On the other hand, it is possible to find the equivalent of non-linear terms in the objective functions by using the dual of the LLPs and some equations of the KKT conditions. Thus, replacing the non-linearities of objective functions with their equivalents will result in a MILP. Appendix A provides all of the equations for the conversion of the detailed optimization model to a MILP.

The MILPs are still non-convex and hard to solve, but it is possible to find their optimal solution if it exists using commercial solvers like Gurobi and Cplex [39, 42]. These solvers use branch and bound algorithms for solving this type of problem.

This chapter proposes two different optimization frameworks for the participation of a price-maker BESS in real-time energy and ancillary services markets. Both of the models are sophisticated enough to contain operational details of the BESS and structural aspects of markets. One of the models considers the degradation costs of the batteries while the other one neglects it. The next chapter is dedicated to simulation studies on these two models in order to not only compare them but also move toward the research goals of this work.

3.6 Approximated Solution Method for the Stochastic Framework

Stochastic optimizations in general are hard to solve as the introduction of uncertainty through various scenarios multiplies the size of the problem by the number of modeled scenarios and hence increases the optimization complexity. Stochastic modeling complexity in addition to the complexity of the discrete optimization in this work makes the proposed stochastic framework hard or even impossible to solve. Hence, this section proposes an approximation method for solving the stochastic framework in a timely manner.

The proposed method resembles the approximation in the value space of reinforcement learning which is implemented here through optimization relaxation. In

order to describe the proposed approximation it is needed to define the BESS market participation problem through the dynamic programming structure [19]. Following the Bellman Optimality principles, the stochastic problem of BESS participation in energy and ancillary services markets in each time interval can be defined as follows.

$$\arg\max_{O_t,\beta_t} E_{\mathcal{S}}\Big[Profit_t(SOC_{t-1}, O_t, \beta_t) + \sum_{\tilde{t}=t+1}^{T} Profit^*_{\tilde{t}}(SOC_{\tilde{t}-1}, O_{\tilde{t}}, \beta_{\tilde{t}})\Big] \tag{3.9}$$

where $profit$ is the total revenue of BESS from various markets minus its cost similar to (SU.1), and O and β are BESS's quantity and price offers for energy and ancillary services markets in time t.

If we were dealing with a deterministic and discrete problem, the dynamic programming approach could start from the last interval and calculates profit-to-go functions $J^*_t = \sum_{\tilde{t}=t+1}^{T} Profit^*_{\tilde{t}}(SOC_{\tilde{t}-1}, O_{\tilde{t}}, \beta_{\tilde{t}})$ till the first interval. Subsequently, a forward algorithm could find the optimal bidding sequence $\{[O^*_1, \beta^*_1], \ldots, [O^*_T, \beta^*_T]\}$. However, for stochastic and continuous problems like ours, this approach cannot solve the problem due to the curse of dimensionality.

A fundamental approach in reinforcement learning, called approximation in value space, solves (3.9) by replacing the optimal profit-to-go function J^*_t with an approximation of it $\hat{J}_t$. Different model-based or model-free methods may be used to find $\hat{J}_t$. In this work, we propose an approximation for $\hat{J}_t$ based on the binary relaxation of the MILP as detailed in Algorithm 1.

The proposed approximation method solves a sequence of less complex MILPs instead of the exact conversion of the stochastic bi-level framework to a MILP. The main source of complexity in the converted MILP of the stochastic framework is the existence of a large number of binary variables. These binaries are used for modeling charge/discharge in each AGC dispatch sub-interval and handling nonlinearities of

complimentary slackness conditions of LLP's KKT. The proposed method reduces the complexity of the MILP by approximating the profit-to-go function J_t^* with its binary relaxed optimization. Hence, in each iteration of Algorithm 1, the following problem solves while $\sum_t^{t+l} Profit_t(SOC_{t-1}, O_t, \beta_t)$ is modeled with binary variables, and binary variables of $\hat{J}_{t+l} = \sum_{t+l+1}^{T} Profit_t(SOC_{t-1}, O_t, \beta_t)$ are relaxed.

$$\arg\max_{O_t, \beta_t} \; E_{\mathcal{S}}\Big[\sum_{t}^{t+l-1} Profit_t(SOC_{t-1}, O_t, \beta_t) + \hat{J}_{t+l} \Big] \tag{3.10}$$

Note that lookahead step size l affects the accuracy of the results and also the solution time. A larger l results in higher approximation accuracy as more intervals are modeled with binary variables and inevitably increases the solution time of each sub-problem due to complexity increment. However, setting a higher l value may reduces the total solution time of the algorithm as it causes to solve fewer sub-problems. For example, in a 24-interval simulation, $l = 1$ results in solving 24 less complex sub-problems, while $l = 4$ solves 6 more complex sub-problems.

Algorithm 1 Optimization-based approximation in value space for stochastic participation of BESS in energy and ancillary services markets

1: Set lookahead step size l
2: Define the MILP of the stochastic framework (SU.1 - SU.22) based on Section 3.5
3: $t \leftarrow 1$
4: **while** $t < T$ **do**
5: Relax all binary variables of the MILP problem from interval $t + l$ to T
6: Call the solver (Gurobi/CPLEX) to solve the semi-relaxed MILP problem
7: Fix the variables of t to $t + l$ intervals to be equal to their solution
8: Enforce binary condition on all binary variables of MILP
9: $t \leftarrow t + l$
10: **end while**

Chapter 4

CASE STUDIES

In this chapter, numerical studies are performed on both of the proposed optimization frameworks in order to investigate the following issues.

- Evaluate the performance of each of the optimization models for the participation of BESS in real-time energy and ancillary services markets and compare them.
- Analyze how a more detailed model can affect the simulation results and relative conclusions, and if it is required to use a detailed model for research on this topic or not.
- Investigate the behavior and optimal capacity allocation of a price-maker BESS across multiple markets.
- Study the impact of a price-maker BESS on the markets' outcomes and grid operations and analyze whether it benefits the system or not.
- Inspect the effect of some critical parameters on the BESS's operation and the sensitivity of the simulation results to those parameters.
- Verify the accuracy of the proposed approximation method for the stochastic farmwwork.
- Analyze the effect of uncertainty modeling on the simulation results.

For having reasonable simulation results and valid conclusions, synthetic data based on real-world grid and market information are used for doing simulations on

the frameworks. Section 4.1 explains the details of the test case system and BESS operational parameters. The results of various case studies on the preliminary and detailed models are presented and discussed respectively in Sections 4.2 and 4.3. Finally, Section 4.4 does some analysis on the effect of BESS's size and batteries' cost on the simulation results.

4.1 Test Case System

The information of the test case system is divided into three categories. The first category is gird and system data, which consist of the test case system's grid topology, number of buses, and demand and ancillary services requirements. The second category contains information regarding the conventional generators that are participating in the markets. The last subsection talks about BESS's specific operation data.

4.1.1 Grid and System Data

The latest update of IEEE's reliability test system (RTS), which is called the RTS-Grid Modernization Laboratory Consortium (RTS-GMLC), is used in this work [17]. The full description of this test system is available at [9].

RTS-GMLC is made of three IEEE RTS 24-bus systems, which are connected through several tie lines. In this work, simulations are done just using the data of the RTS-GLMC's third area, and two other areas along with the tie lines, are neglected. Thus, the test system grid consists of 24 buses and 38 transmission lines. Figure 4.1 illustrates the test case grid topology along with the number and size of generators in each generation bus. Additionally, the share of each load bus from the system total load is also given in Figure 4.1. Information of the transmission lines is presented in Table B.2 of Appendix B.

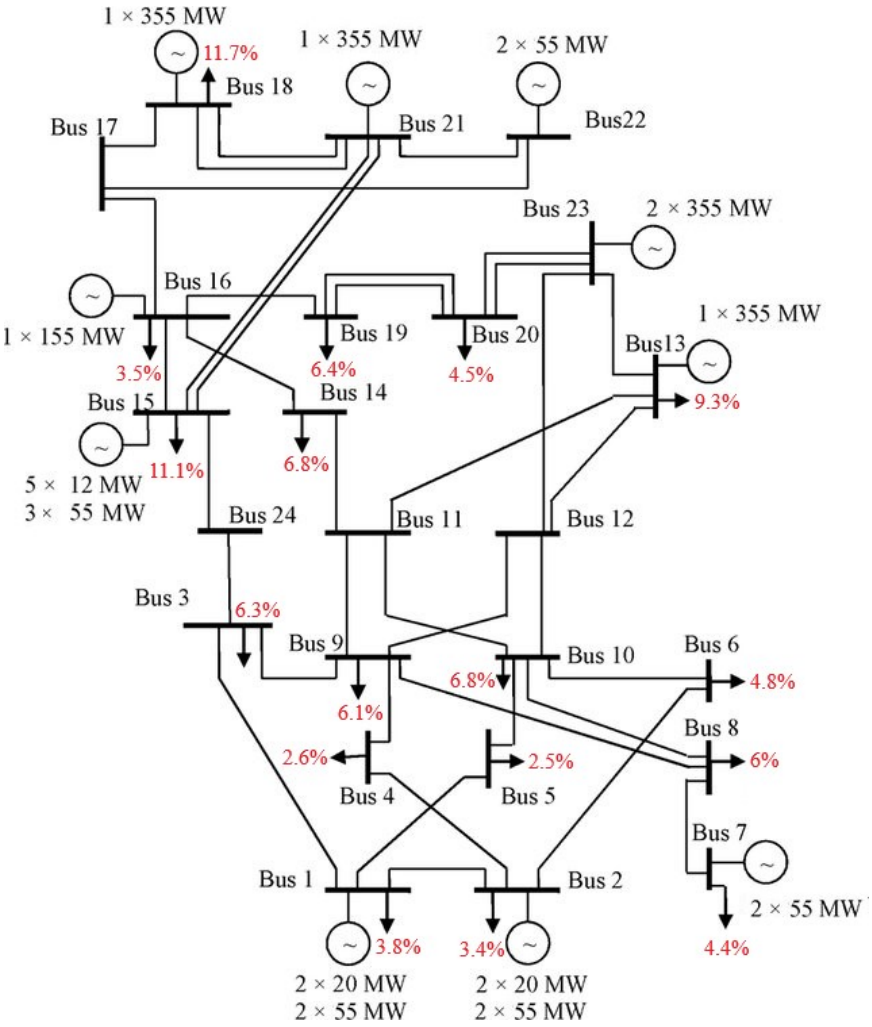

Figure 4.1: Topology of the Test Case Grid.

The simulation horizon is 24 hours consisting of 96 market-clearing intervals. The length of each interval is 15 minutes, and AGC signals are dispatched every 20 seconds instead of four seconds to reduce the computational burden of the simulations.

The average of RTS-GLMC's third area real-time load over the summer period (June to August) is used for creating the system load for each time interval of simulations. Reserve and regulation capacity requirements of each time interval are also calculated similarly. The regulation mileage requirement in each time interval is set to be around 1.5 times the regulation capacity requirement, which is a typical require-

ment [65]. Figure 4.2 shows the system total load and ancillary services' requirements over the 24-hour horizon.

According to the black curve of this figure, the highest load of the system occurs around hours 11 to 18, and hours zero to six have the lowest demand. It is expected that the energy market price is lower in off-peak hours and higher in peak-hours, and hence this phenomenon affects the BESS operation, which will be discussed when results are presented.

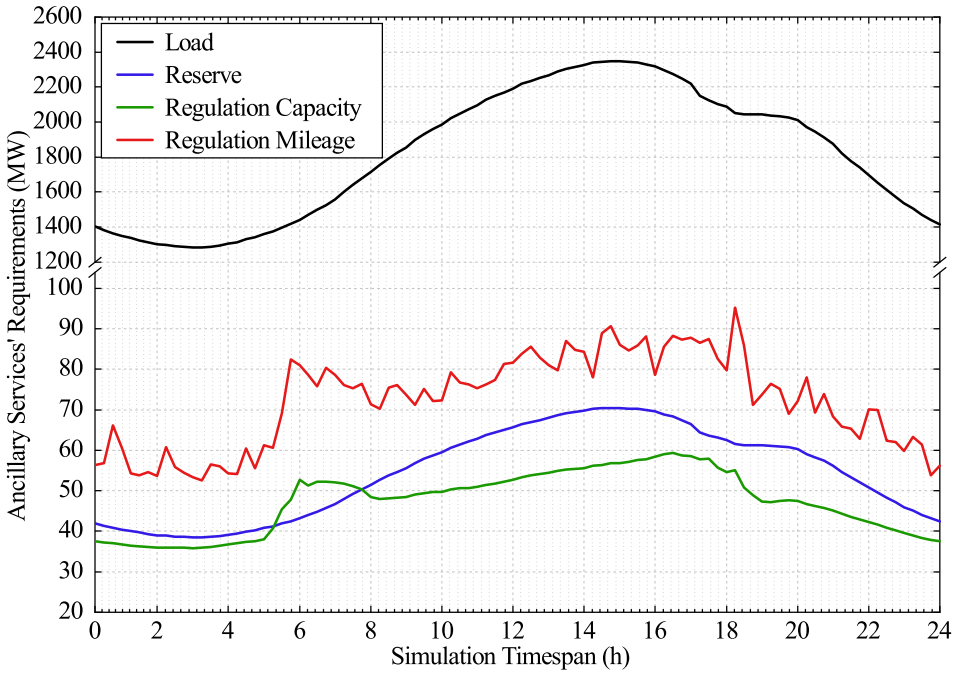

Figure 4.2: Test Case System Load and Ancillary Services Requirements.

Observe that in Figure 4.2, the ratio of regulation mileage requirement to regulation capacity is not exactly 1.5 in each interval, it changes from 1.3 to 1.7, but its average over simulation period is 1.5. Additionally, it is assumed that all of the regulation market participants had similar historical performance in following AGC signals, and their mileage multiplier in each time interval is just limited by (3.4).

The sample AGC set points provided by ISO New England (ISO-NE) are used for modeling AGC signals in the simulations [2]. We modified the AGC signals in a way

that summation of signal changes in each period, calculated by (3.2), is equal to the system's regulation mileage requirement in that period. Furthermore, AGC signals are modified to fit 20-second dispatching criteria and have zero-mean in each interval. AGC signals are used for the detailed model and they are not required to have zero-mean, but we modify them in this way as this type of signal is more appealing for BESSs. As AGC signals have zero-mean in each interval, the battery's SOC does not change by following AGC signals, but the degradation cost of the AGC deployment is captured in the degradation cost model. This is one of the advantages of the detailed framework over the preliminary one.

4.1.2 Market Participants Data

As it is shown in Figure 4.1, the test case system has 26 generators. It is assumed that generators' price offer in the energy market is equal to their generation costs. Additionally, historical ancillary services' price of the PJM market is used for making synthetic price offers for generators in reserve and regulation markets [6]. Extracted from PJM 2018 historical data, average ratios of reserve price, regulation capacity price, and regulation mileage price to the energy price are 0.15, 0.4, and 0.07 respectively. Therefore, generators' generation costs in each time interval are multiplied by 0.15, 0.4, and 0.07 to respectively create their price offers for the reserve, regulation capacity, and regulation mileage services. The operational data of the conventional generators along with their price offers are presented in Table B.1 of Appendix B.

4.1.3 BESS Data

The BESS's unit is lithium-ion battery storage and is placed on Bus 13. Its operational parameters are shown in Table 4.1.

According to this table, the capacity of the battery unit is equivalent to a 4-

Table 4.1: Operational Information of the BESS

P^{Rate} (MW)	Capacity (MWh)	SOC^{Min} (MWh)	SOC^{Max} (MWh)	SOC^{Init} (MWh)	η (%)
50	200	20	180	90	95

hour operation, which is a normal capacity for utility-scale BESSs, and its maximum charge/discharge cycle depth is 80%. This type of battery cells have cycle life of 6000 cycles at 80% charge/discharge cycle depth [5] and their replacement cost is around 200,000 $/MWh [33].

Based on the cycle depth stress function of lithium-ion batteries [51] and the replacement cost, the degradation cycle depth cost function for BESS's units is shown in (4.1), where δ is the charge/discharge cycle's depth. For implementation of the cost function model in the detailed optimization framework, this near quadratic function is approximated with a 16-segment piecewise linear function.

$$C(\delta) = 52.4\,\delta^{2.03} \tag{4.1}$$

For doing case studies of this chapter, both models are implemented using Python and solved with Gurobi optimization solver [39]. The simulations are done on an octa-core Intel-i7 3-GHz personal computer with 64 GB of RAM memory, while the MIP-gap is set to 1%.

4.2 Case Studies on the Preliminary Framework

The proposed preliminary optimization framework for the participation of the BESS in various markets is tested under four different cases. Each case represents a particular market participation policy for the BESS. In Case 1, the BESS is allowed to participate in the energy market only and perform energy arbitrage between different hours. In Case 2, BESS is allowed to participate in both of the energy and

reserve markets while participation in both energy and frequency regulation markets is modeled in Case 3. Finally, Case 4 simulates the participation of BESS in all of the energy, reserve and frequency regulation markets. After presenting the simulation results of these four cases in individual subsections, a comparison between BESS' revenue in each of the cases and its effect on the system's operation is presented in the last subsection of this part.

4.2.1 Case1: Energy Market

Scheduled power and SOC of a BESS that is participating in the real-time energy market across the 24-hour horizon is illustrated in Figure 4.3. In this figure, the black curve indicates BESS's scheduled power in the energy market across the simulation horizon; the grey area, which is plotted on the right axis, indicate the SOC of the BESS at different market clearing interval. Note that minimum and maximum SOC are indicated on the right axis with red horizontal lines.

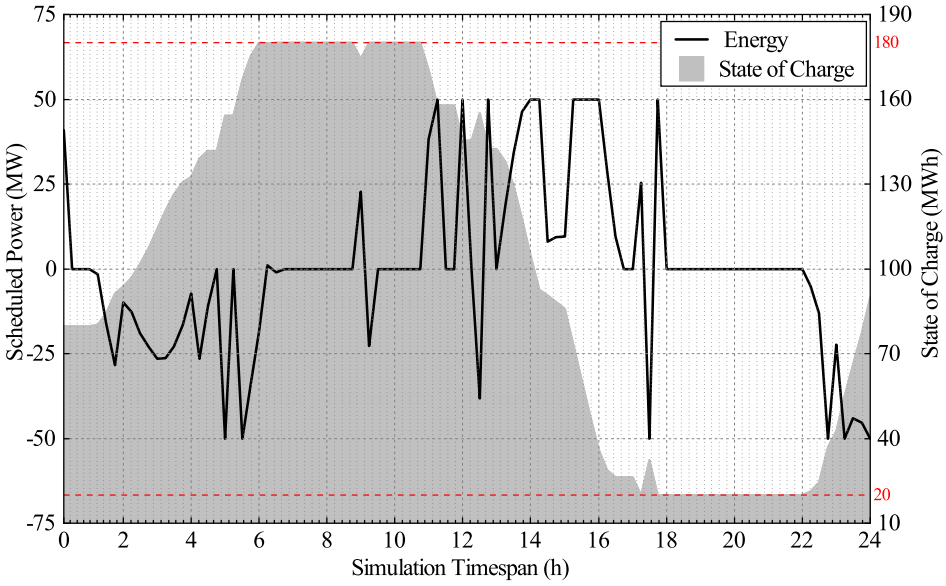

Figure 4.3: Simulation Results of the First Case Study on the Preliminary Model.

It is shown in the Figure 4.3 that the BESS mostly charges or buy energy during

off-peak hours (hours zero to six) when the energy price is low, and discharges or sell energy during peak hours (hours 11 to 18) when the energy price is higher. In the last hours of the day (22 to 24), the BESS buys energy to charges itself and reaches the initial SOC. Note that the last hours should also have low energy prices based on the demand curve (Figure 4.2).

The SOC curve of Figure 4.3 (gray area) shows that BESS uses all of its capacity to maximize its profit. It means that it charges itself up to 180 MWh in off-peak hours, and during peak-hours discharges to 20 MWh and sell the whole 160 MWh stored energy. This form of operation is equivalent to deep charge/discharge cycles as it is shown in the figure and will cause considerable life loss and degradation cost on the unit. In the preliminary framework, as degradation cost is not modeled, going through this deep charge/discharge cycle when it is participating in the energy market is the most profitable option for BESS, but it may not be the best option in reality.

According to Figure 4.3, BESS's SOC is at its maximum or minimum limit for at least one-third of the operation hours (gray curve in hours 6 to 10 and 18 to 22), while its output power (black curve) reaches the charge/discharge rate (50 MW or -50 MW) just in several market clearing intervals. Thus, energy capacity is the limiting parameter of the BESS while it is participating in the energy market. In other words, while BESS is just participating in the energy market, increasing BESS's energy capacity can result in more profit growth for it in comparison to increasing the unit's charge/discharge capability.

In this case study, BESS is just participating in the energy market and is able to do energy arbitrage between different hours. By participating in other markets simultaneously, it may be able to practice other types of arbitrages. This issue will be analyzed in the following case studies.

4.2.2 Case 2: Energy and Spinning Reserve Markets

In Case 2, the BESS is allowed to participate in both energy and reserve markets. Figure 4.4 presents its 24-hour scheduled powers and SOC under this scenario. In this figure, the black and blue curves indicate BESS's revenue from the energy market and reserve market, respectively; the grey area indicates the BESS's SOC at different market clearing interval and is plotted on the right axis.

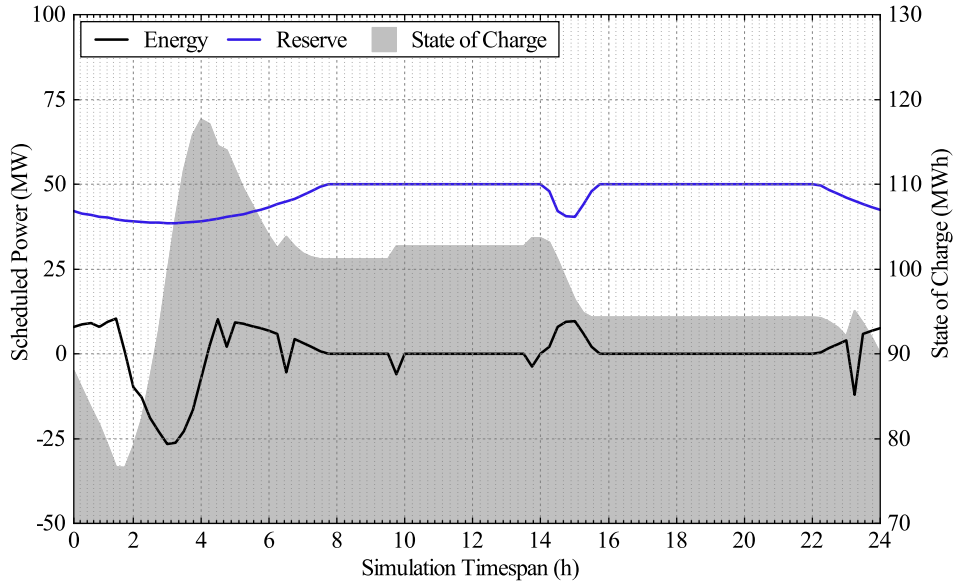

Figure 4.4: Simulation Results of the Second Case Study on the Preliminary Model.

According to Figure. 4.4, participation in the reserve market has more priority for the BESS than the energy market, hence its scheduled power in the reserve market (blue curve) is more than its scheduled power in the energy market (black curve) all over the simulation horizon.

A comparison between blue curves of this figure and Figure 4.2 shows that BESS provides all of the system reserve requirements in the intervals in which the requirements are less than 50 MW (i.e., the output capability of BESS). When the system reserve requirement is more than 50 MW (hours 8 to 22), the scheduled power of

BESS's in reserve market is fixed at its maximum output, except for a period between hours 14 to 16.

The system peak load happens around hour 15 (see Figure 4.2), hence generators with higher costs are marginal in these hours and energy price is higher. As a result, BESS finds that it is profitable to reduce its share in the reserve market and participate in the energy market. In the initial and last hours of the day when reserve requirement is not more than BESS's output limit, BESS participates in the energy market and do energy arbitrage. It again charges itself in initial hours to sell the stored capacity in other hours with higher energy prices.

The gray area of Figure 4.4 shows that less capacity of BESS is used in comparison to the previous case study. the maximum SOC reached by the BESS is 118 MWh and the deepest change in SOC is around 40 MWh. It means that a BESS with less capacity can also have the same profit, and batteries have less degradation compared to the previous case.

Although BESS does not reach its SOC limits in this case, its output power is always at its maximum. Thus, in contrast to the previous case, the charge/discharge power capability of the BESS is the limiting parameter here. It means that an increase in the charge/discharge capability of the BESS can result in its profit growth, but an increase in energy capacity may not affect the BESS's revenue.

4.2.3 Case 3: Energy and Frequency Regulation Markets

The scheduled power and SOC of BESS when it is participating in the real-time energy and pay as performance frequency regulation markets are presented in Figure 4.5. Similar to previous figures, BESS's scheduled power in the energy market is the black curve, and its SOC is the gray area that is plotted on the right axis. Additionally, green and red curves are respectively scheduled power of BESS for

regulation capacity and regulation mileage services.

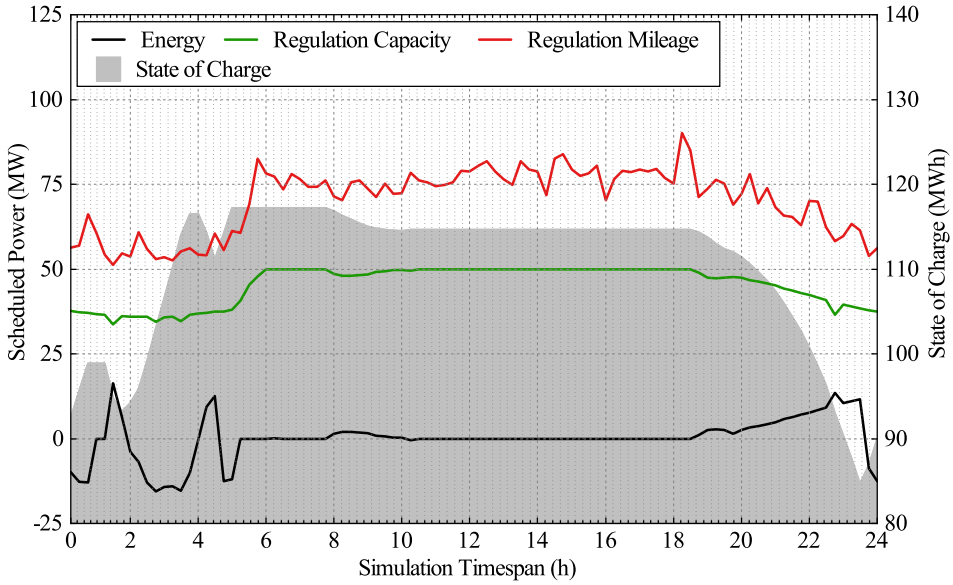

Figure 4.5: Simulation Results of the Third Case Study on the Preliminary Model.

Based on Figure 4.5, BESS prefers to participate more in the frequency regulation market than the energy one. The green curve of this figure is similar to the green curve of Figure 4.2 for the intervals during which regulation requirements are less than 50 MW. For the hours when system regulation requirements are more than BESS's output capability, its share is fixed at its output limit (50 MW).

In the initial and last hours when BESS output capacity is higher than the system regulation requirements, BESS participates in the energy market to arbitrage energy. It charges in initial hours and discharges in the hours with higher prices.

Similar to Case 2, participation in the frequency regulation market also results in using less capacity of BESS. According to Figure 4.5, the maximum SOC reached by the BESS is 118 MWh and largest change in SOC is around 30 MWh. The limiting parameter at this case is also BESS's output capability, and an increase in it will result in more revenue for BESS.

4.2.4 *Case 4: Energy, Spinning Reserve, and Frequency Regulation Markets*

Figure 4.6 shows the simulation results of the case that BESS is participating in the real-time energy and all of the ancillary services markets. In this figure, black, blue, green and red curves are respectively BESS's scheduled powers for energy, reserve, regulation capacity, and regulation mileage. Furthermore, the gray area that is plotted on the right axis is BESS's SOC.

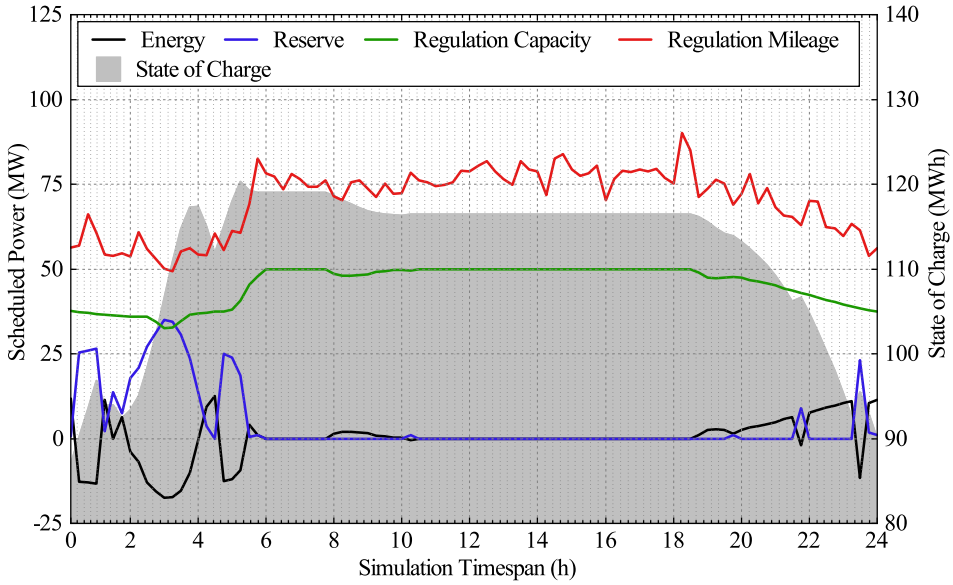

Figure 4.6: Simulation Results of the Fourth Case Study on the Preliminary Model.

It is obvious in Figure 4.6 that the frequency regulation market is the primary source of revenue for BESS. In hours that regulation market capacity requirements are less than 50 MW, the unused output capability of BESS is divided between reserve and energy markets. The share of the reserve market is more than that of the energy market, and the reserve market is the second option for BESS's market participation.

It is observed in Figure 4.5 that during the charging periods, the BESS simultaneously purchases energy from the energy market and sells all or part of its purchased energy to the reserve market (for reserve capacity provision). This represents the

BESS's arbitrage activities between the energy and reserve markets at the same market clearing interval. To clarify, consider the 12th interval (first interval of hour 3) when BESS is buying 17.5 MW from the energy market and also selling 35 MW and 32.5 MW in respectively reserve and regulation capacity markets. The summation of the scheduled power for ancillary services markets is 67.5 MW, which is 17.5 MW more than the BESS's charge/discharge limit. It means that if in a contingency situation, the ISO requires the BESS to inject the scheduled reserve (35 MW) to the grid; it provides 17.5 MW of it by not charging itself from the grid and decreasing the system load. It also provides the other half by discharges 17.5 MW to the grid as it has output power available in excess to its share in the regulation capacity market ($50 - 32.5 = 17.5$ MW).

The maximum SOC that BESS reaches is 120 MWh and deepest change in SOC is around 30 MWh. Therefore, the results of this case also show that participation in ancillary services markets causes redaction in battery capacity usage and respectively having less degradation cost. It is also apparent that a BESS unit with higher output charge/discharge rate and the same capacity could make more profit in this case.

The next subsection concludes the analysis of the preliminary model by providing a comparison between BESS's revenues in each case and reporting the system's total cost in each of the cases.

4.2.5 Discussion

For concluding the analysis on the proposed preliminary model for BESS participation in real-time energy and ancillary services markets, total revenue of BESS from each of the markets in each of the case studies is illustrated in Figure 4.7.

Figure 4.7 shows that participation in more markets provides more sources of revenues for BESS and result in having higher profit. It is worth mentioning that the

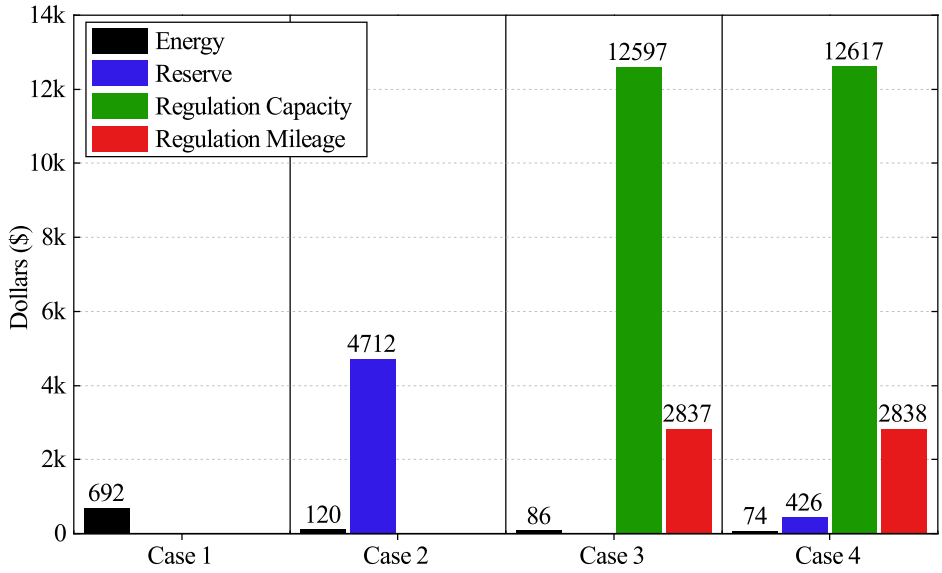

Figure 4.7: Bess's Total Revenue from Each Market in Each of the Case Studies.

SOC curves of previous figures also show that an increase in the number of markets that BESS is participating in leads to less usage of its capacity and charge/discharge cycles with lower depth. Therefore, the portfolio of BESS across various markets not only results in having more revenue streams but also decreases the BESS's investment costs as less capacity is needed. It also reduces BESS's degradation costs as less charge/discharge cycles happen.

It is obvious in Figure 4.7 that the frequency regulation market is the most profitable market for the BESS. In cases that BESS is allowed to participate in the regulation market (cases 3 and 4), almost all of the BESS's revenue comes from this market. This observation agrees with the BESS operating patterns in real-world practices [7] and verifies the accuracy of the model and the data.

Comparison between total revenues in cases 3 and 4 verifies the previous observation that the reserve market is the second option for BESS after the regulation market and has priority over the energy market. Additionally, it can be seen that by participation in the reserve market in case 4, the share of BESS in the energy market

does not change a lot from case 3. This happens due to the same interval energy arbitrage that can happens between these two markets.

To better understand the operation of a price-maker BESS and its effects on the system, Figure 4.8 shows the system's total operating cost in each of the previous case studies along with the operating cost of the system when BESS does not exist in it.

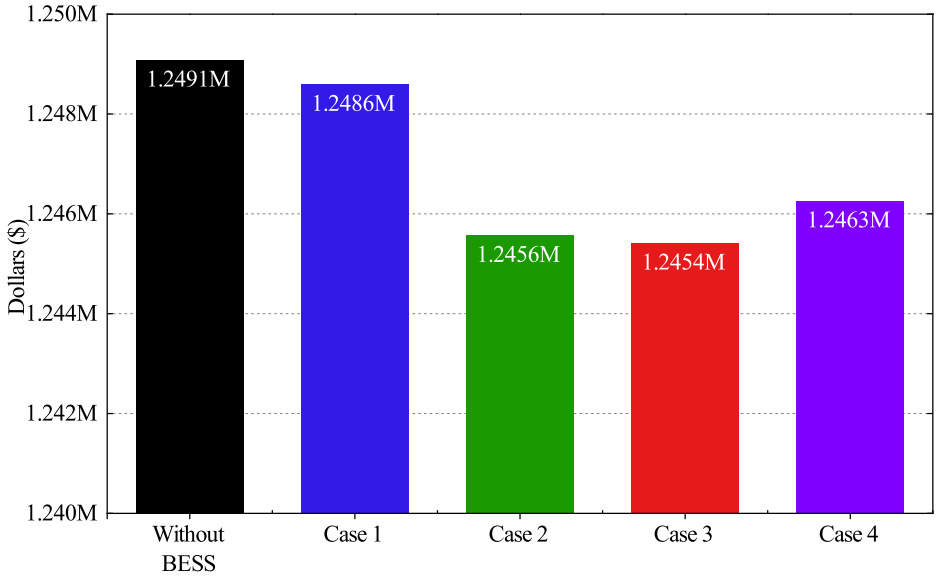

Figure 4.8: System Total Cost with and Without Bess.

According to Figure 4.8, although a price-maker BESS seeks to maximize its profit, its operation is beneficial and the total system costs in all the four the cases are less than the system costs without BESS. This cost reduction is small in comparison to the total system cost, but it must also be considered that BESS's output power is just 1.8% of the system total available generation.

In Figure 4.8, the addition of ancillary services markets to the energy market in Cases 2 and 3 causes more system cost reduction. System costs in Case 3 shows that the frequency regulation market is not just a better option than the reserve market for BESS. Also, it is more beneficial for the system when BESS provides regulation

services rather than reserve services.

An interesting observation in Figure 4.8 is the increase in the system cost for Case 4 compared with Cases 2 and 3. It shows that participation in more markets enables a price-maker BESS to leverage its power and affect the market outcomes. As a result, in Case 4, the total system cost is higher than costs in Cases 2 and 3 in which BESS is limited to participating in just one of the ancillary services markets. Note that even though BESS is affecting the markets and leveraging its price-maker characteristics, the total system cost in Case 4 is still less than that in Case 1 and also less than the system cost without BESS. Thus, in this reasonably realistic test system, the BESS price manipulation is limited, and its operation is generally in-line with the ISO goal (minimizing system cost). However, these results show that it is needed to improve the market structures for the participation of BESSs in a way that the system benefits the most from BESSs' technical capabilities while BESSs also maximize their profit.

4.3 Case Studies on the Detailed Framework

Similar to the previous section, four different case studies are performed with the detailed optimization framework first to analyze the operation of the BESS while degradation cost and AGC signal deployments are considered. Second, the performance of the proposed model for the participation of a price-maker BESS in various markets is evaluated. This section also compares different case study results and presents the effect of BESS on the system costs.

4.3.1 Case 1: Energy Market

Scheduled power and SOC of a BESS, which is only participating in the energy market are shown in Figure 4.9. Scheduled power is the black curve and SOC is a gray area that is plotted on the right axis.

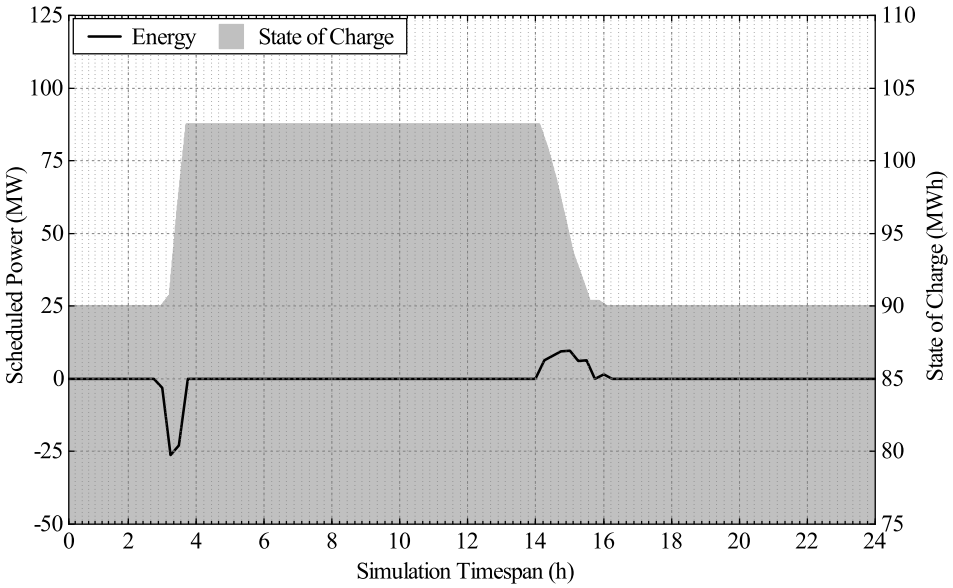

Figure 4.9: Simulation Results of the First Case Study on the Detailed Model.

It is obvious in Figure 4.9 that consideration of degradation cost totally affects the operation of BESS. The impact of degradation cost on BESS operating patterns can be observed by comparing this case with Case 1 of the preliminary model. Energy arbitrage between hours is no longer profitable for BESS. In this case, BESS only performs energy arbitrage for a total amount of 12 MWh, which is stored by the BESS during low-price hours and sold during peak hours.. Based on these results, it can be observed that participation in only the energy market is not profitable for a BESS if it considers its degradation costs in the decision-making process.

4.3.2 Case 2: Energy and Spinning Reserve Markets

Simulation result for a case that BESS is participating in the spinning reserve market besides the energy market is illustrated in Figure 4.10. In this figure, scheduled power for energy and reserve markets are respectively black and blue curves, and the gray area plotted on the right axis is the BESS's SOC.

In this scenario, BESS is just participating in the spinning reserve market, and its

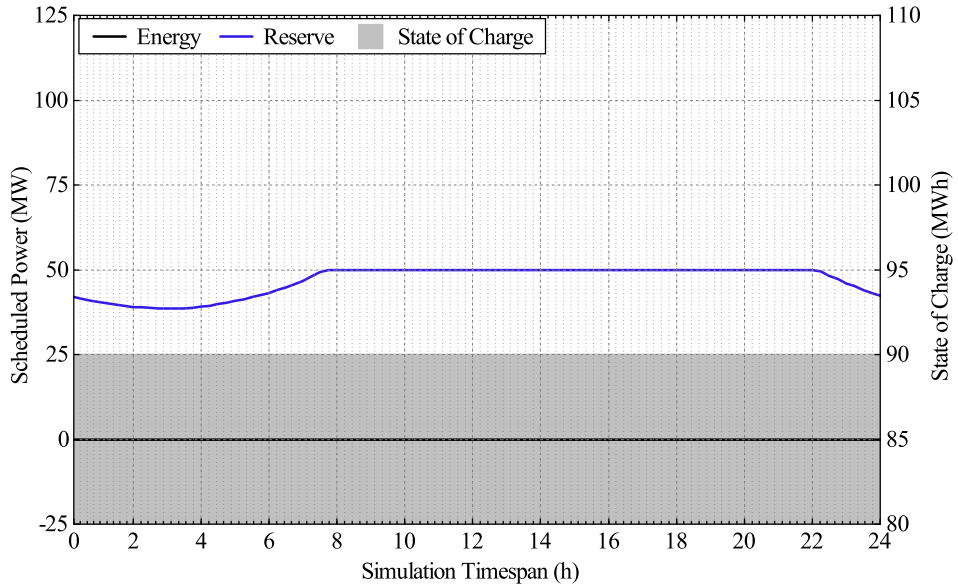

Figure 4.10: Simulation Results of the Second Case Study on the Detailed Model.

share in the real-time energy market is zero. This happens because reserve deployment is not modeled, hence by providing reserve services, BESS does not charge or discharge and does not incur degradation cost. Therefore, BESS participates in the reserve market as much as possible due to the charge/discharge limit. In contrast to Case 2 of the preliminary model, it does not allocate its unused output power to the energy market in the initial and last hours when system reserve requirements are less than 50 MW because of degradation cost that occurs by participating in the energy market.

In Case 2 of the previous model (Figure 4.4), BESS prefers to decrease its share in the reserve market for some of the intervals in the peak hours when the energy price is higher. However, in this case, although the energy price is still higher during peak hours, the degradation cost associated with energy market participation makes it nonprofitable for BESS to participate in the energy market. Furthermore, as a result of participating in the reserve market only, BESS's SOC does not change and remains at 90 MWh.

4.3.3 Case 3: Energy and Frequency Regulation Markets

In this case, BESS is allowed to participate in the energy and frequency regulation markets. Its scheduled power and SOC are depicted in Figure 4.11, where black, green and red curves are respectively scheduled power for energy, regulation capacity, and regulation mileage, and gray area is SOC and is plotted on the right axis.

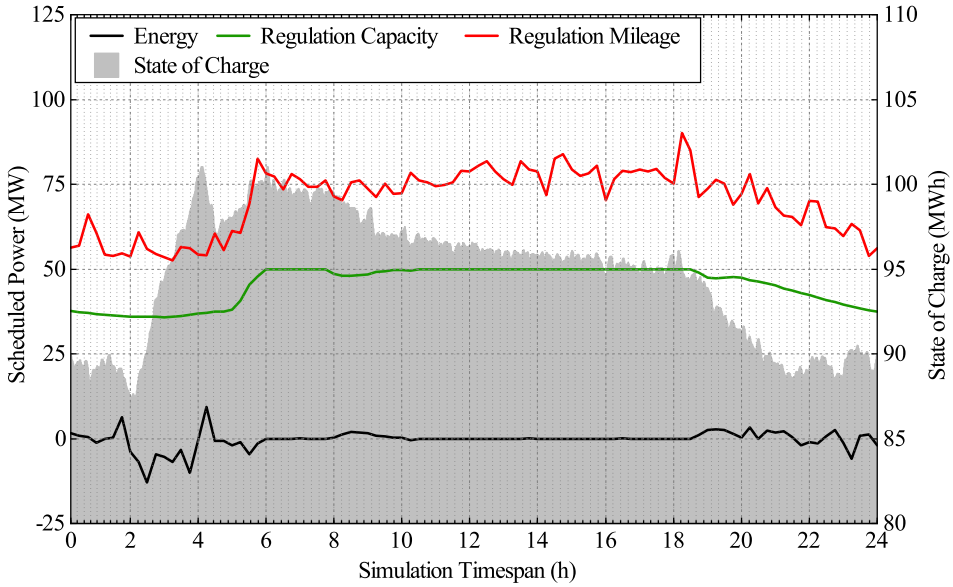

Figure 4.11: Simulation Results of the Third Case Study on the Detailed Model.

In Figure 4.11, BESS is allocating all of its output power to the regulation market in the hours when system regulation requirements are greater than or equal to 50 MW. In the initial hours, the system regulation requirement is less than 50 MW, and energy price is also low, the BESS charges itself. This stored energy is mostly used throughout the day for following AGC signals. Note that although AGC signals are modified to have zero-average in each interval, their average is not exactly zero, and the charge/discharge efficiency of the batteries also lead to BESS capacity usage for following AGC signals.

The gray area in Figure 4.11 shows the BESS's SOC across all of the sub-intervals.

It is apparent in the figure that charge/discharge cycles due to following AGC signals have low cycle depth. Hence, following AGC signals do not incur a high degradation cost on the BESS. As a result, the degradation cost of participation in the regulation market does not overcome its revenue, and the pattern for BESS's participation in this market is similar to the previous model (Figure 4.5).

The participation of BESS in the energy market is mostly for charging, and it has a minimal share in selling energy and its revenue from this market is negative. Additionally, the deepest SOC change in this case is around 12 MWh, which is less than half of the SOC change in Case 3 of the preliminary model and is again due to degradation cost modeling. In this case, similar to the previous case and Cases 2, 3 and 4 of the preliminary model, the limiting parameter is BESS's output rate, and an increase in it could result in profit growth.

4.3.4 Case 4: Energy, Spinning Reserve, and Frequency Regulation Markets

Figure 4.12 shows the simulation results for the condition that BESS is participating in all of the ancillary services markets besides the energy market. Scheduled power for energy, reserve, regulation capacity and regulation mileage are respectively black, blue, green and red curves, while BESS's SOC is the gray area, which is plotted on the right axis.

As was expected, when BESS can participate in all of the markets, the frequency regulation market is the first priority and the second option is the reserve market. According to Figure 4.12, it participates in the reserve market in the initial and last hours during which it has more output capability compared to the system regulation requirements.

Scheduled power of BESS in the energy market is mostly negative, hence BESS charges itself in hours with lower energy prices to provide other services throughout

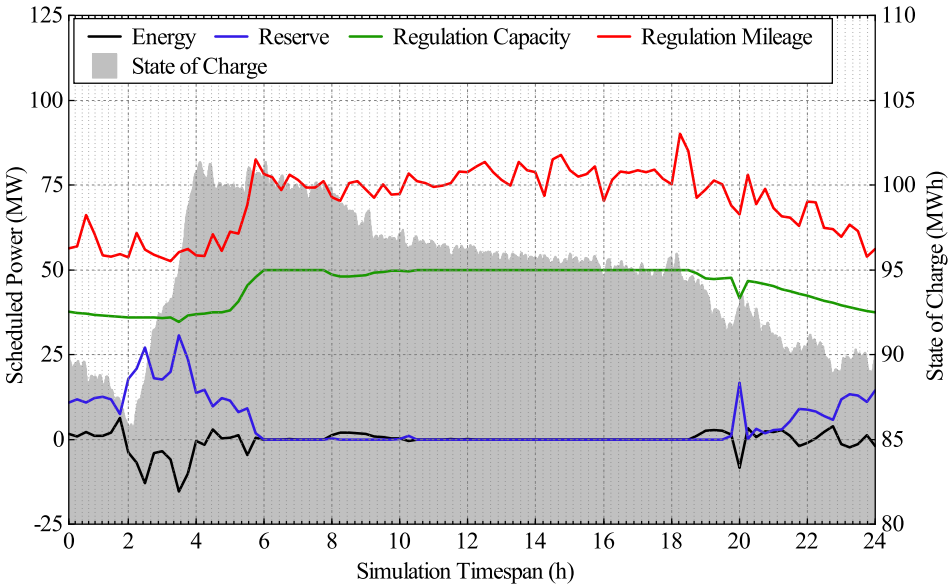

Figure 4.12: Simulation Results of the Fourth Case Study on the Detailed Model.

the day. It is worth mentioning that the same interval arbitrage between energy and reserve market also happens in this case during the charging periods.

BESS's SOC changes are mainly due to AGC signal following, which does not cause a high degradation cost for the BESS. The deepest change in the SOC is around 15 MWh and is similar to the previous case in which the BESS does not use a large portion of its storage capacity. In other words, a BESS with lower energy capacity is also able to gain the same profit. Although an increase in energy capacity does not cause growth in BESS's revenue, an increase in the unit's charge/discharge capability can result in gaining more profit for BESS as it is the limiting parameter.

4.3.5 Discussion

Total revenues of BESS from each of the markets in each of the four case studies that are done on the detailed optimization framework are presented in Figure 4.13 to provide an overall comparison and conclude this section. The total degradation cost of the batteries in each case are also shown in this figure.

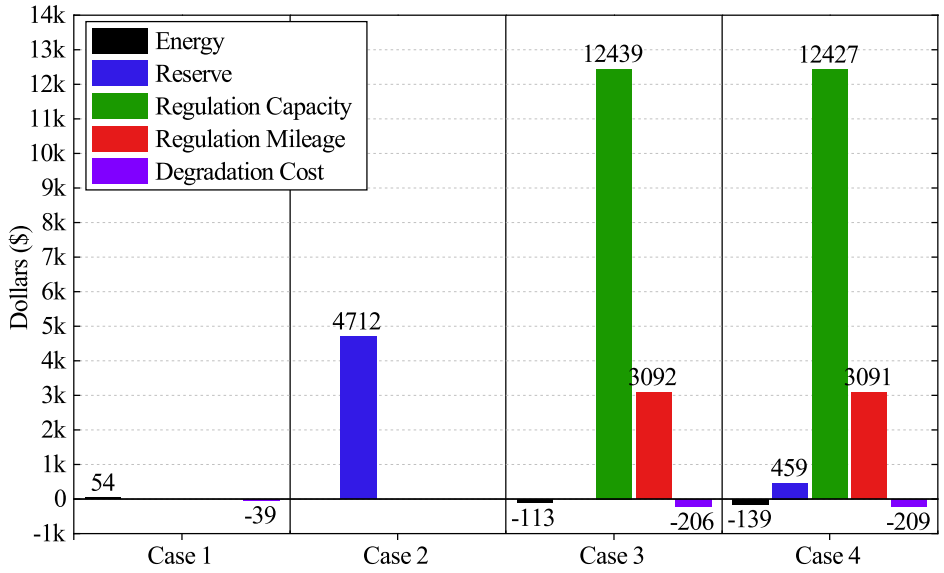

Figure 4.13: Bess's Total Revenue from Each Market in Each of the Case Studies along with Its Degradation Cost.

As the addition of the degradation cost model is the main difference between detailed and preliminary models, and degradation cost does not affect the share of BESS in ancillary service markets; Figure 4.13 is very similar to Figure 4.7. Figure 4.13 fortifies the previous observation that consideration of degradation cost mostly affects the behavior of BESS in the energy market and reduces BESS's revenue from this market.

In addition to all of the conclusions that are mentioned in Section 4.2.5, which are also valid for Figure 4.13, this figure has important information regarding the BESS participation modeling approach. These results show that the degradation costs of the batteries are negligible in comparison to the total revenue of the BESS in Cases 3 and 4. On the other hand, these degradation costs are incurred due to the AGC signal following. Thus, it is possible to neglect the cost of following AGC signals but still have similar results.

Based on this observation, we are able to develop a less sophisticated model for the participation of BESS in various markets while still capturing the features of the

detailed model. The new model is something between the preliminary framework and the detailed one. The model must have the degradation cost model in the objective function, but the AGC signal deployment model is not needed. As a result, the existence of the cost model prevents BESS from going through large charge/discharge cycles that happen mostly in the energy market, while the degradation cost of the small cycles resulting from participation in the regulation market is neglected. By not modeling AGC signal deployment, it is no longer needed to consider sub-intervals for each market clearing horizon, which causes a huge reduction in problem size and complexity. Therefore, having a less sophisticated model with almost similar accuracy enables us to add other details to the framework like consideration of other markets than these three.

Finally, Figure 4.14 shows the system's total cost without BESS and its cost for each of the simulation scenarios. This figure is also similar to the matching figure for the preliminary model (Figure 4.8).

Based on Figure 4.14, in this realistic test case system, system cost reduces even by the participation of a price-maker BESS. However, in the detailed model (Figure 4.14), system cost reductions in Cases 2 and 3 are more than that in the preliminary model (Figure 4.8). This is caused by the degradation cost limitation on the BESS. Hence, BESS cannot take advantage of being a price-maker like the preliminary framework. Using this model, the system operating cost increases in Case 4, compared to Cases 2 and 3, due to BESS price manipulation. Thus, developing a better market structure for the participation of BESS in various markets is an important goal for taking advantage of BESS technology.

In this section, the results of various simulations on both of the proposed preliminary and detailed optimization frameworks are presented and relevant conclusions are drawn. The next section provides some insights into the effect of BESS's size and

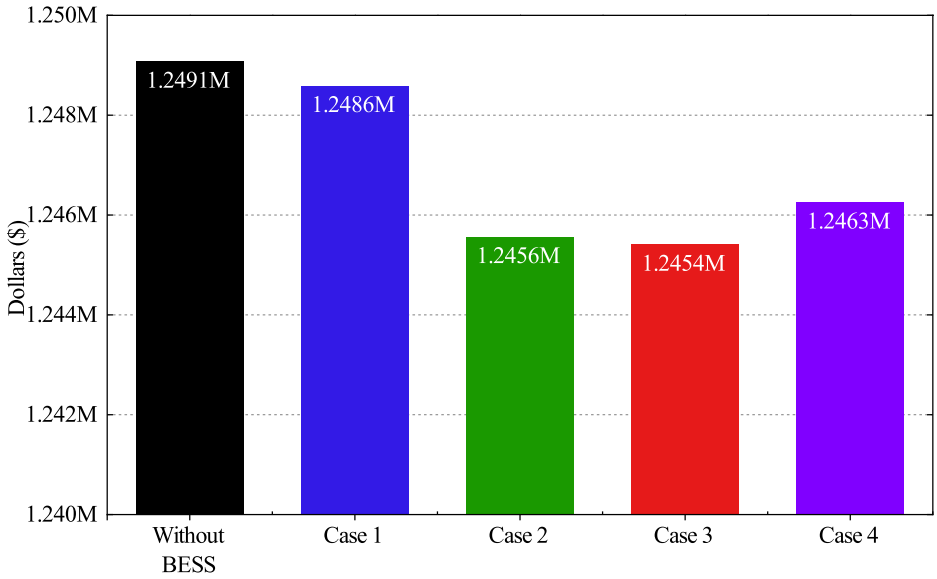

Figure 4.14: System Total Cost with and Without Bess.

degradation cost on its operation.

4.4 Effect of BESS's Size and Degradation Cost changes on its operation

Operation of a large-scale price-maker BESS dependents on different parameters. Among these parameters, BESS's capacity and degradation cost are primary drivers of its profit. On the one hand, it is crucial to analyze the role of BESS's size on its strategic behavior in the markets. On the other hand, the battery manufacturing cost is decreasing due to mass production and technology development, and it is expected that the battery cost reduces to less than 70,000 $/MWh by 2030 [21]. Hence, the effect of this cost reduction on the BESS operation must also be evaluated.

Independently considering the effect of these two parameters on the simulation results may cause misleading conclusions. Thus, a bi-parametric analysis of the BESS's size and degradation cost is performed in this section to gain an in-depth understanding of the BESS's operation in the markets.

In this analysis, the capacity of the BESS unit is changed from 100 MWh to

2000 MWh with a 100 MWh step size. As it is a 4-hour operation BESS, the charge/discharge capability of the unit (charge/discharge rate) also changes simultaneously from 25 MW to 500 MW with a 25 MW step size. Additionally, for each of the BESS capacity, 200,000 $/MWh, 150,000 $/MWh, 100,000 $/MWh, 50,000 $/MWh, 25,000 $/MWh and 1,000 $/MWh values are considered for the replacement cost of the batteries, and degradation cost function (4.1) is changed respectively. It is worth mentioning that in order to have the same accuracy in cost modeling, the number of segments for cost function approximation is also changed with respect to the size changes.

In total, 120 simulations are done to cover the above-mentioned variations in the parameters. For each replacement cost, the revenue of BESS in each market versus its size is depicted in Figure 4.15. In this figure, Total revenue and each market's revenue are depicted with specific patterns, and each curve is depicted in different colors representing various battery replacement costs. For example, the dotted black curve is the energy market revenue for a BESS with 1k$/MWh replacement cost. Note that the horizontal axis is labeled with both capacity (MWh) and output capability (MW).

The first and most important observation in Figure 4.15 is that the revenue curves of various replacement costs are overlapping with each other except for the total revenue and energy market revenue curves of the BESS with 1,000 $/MWh replacement cost (respectively solid and dotted black curves). It shows that the reduction of BESS's cost to 25,000 $/MWh does not affect the share of BESS in various markets.

In Figure 4.15, the regulation market revenue curve (dash-dot curve) increases with BESS's size increase until the 300 MWh. At that point, the whole system regulation requirements are provided by BESS, so the regulation market revenue curve for various battery costs do not change after 300 MWh (75 MW output). After

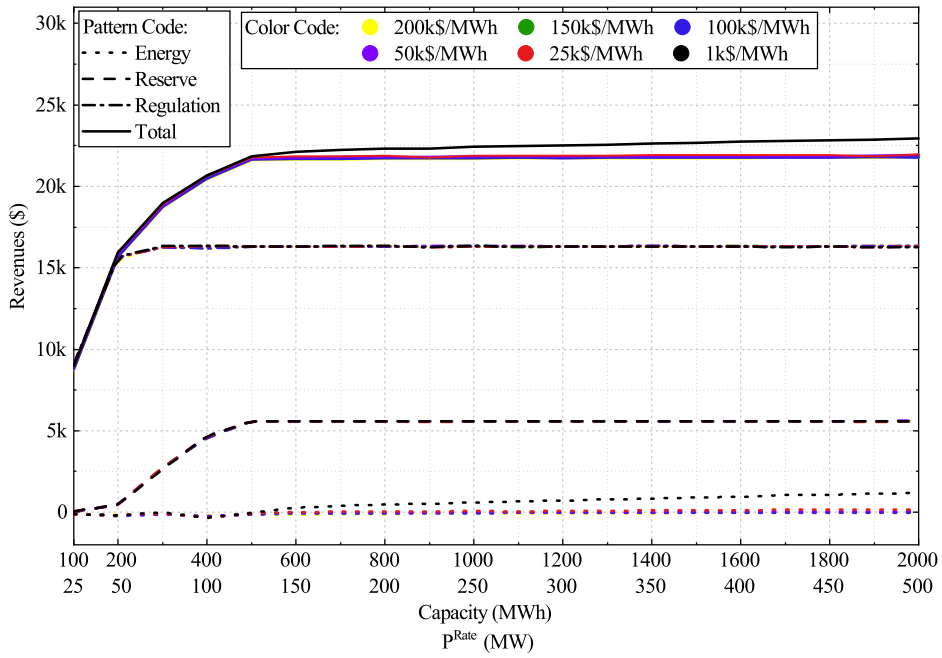

Figure 4.15: Bess's Revenues Versus Its Size for Different Replacement Costs.

the saturation of the regulation market, an increase in the size of BESS resulted in the growth of its share in the reserve market. When BESS's output capability reaches 125 MW (simultaneously its capacity reaches 500 MWh), it can provide all of the reserve requirements of the system. Hence the dashed curves do not change beyond that. After the saturation of ancillary services markets, the total revenues of BESS (solid lines) do not considerably increase by size growth except for the case with 1,000 $/MWh cost (black curve). It means that for batteries with a replacement cost of 25,000 $/MWh or higher, the degradation cost incurred by participation in the energy market does not worth its income.

For 1,000 $/MWh replacement cost, participation in the energy market is profitable, and after saturation of ancillary markets, BESS allocates its unused capacity to the energy market. Note that BESS's size growth does not have the same effect on various markets' revenues. For example, in the black curves, regulation market revenue increment from one step growth in size is much more than energy market

revenue increment from 15 steps growth in BESS's size.

These results show that regardless of battery cost, regulation, and reserve markets are BESS's first and second priorities while choosing the energy market is dependent on the degradation cost. Additionally, for ancillary services markets, the BESS's output capability is the limiting parameter, and BESS can have the same revenue in them with the same charge/discharge rate but less capacity. In contrast, the increment of BESS's revenue from the energy market is dependent on its storage capacity.

This chapter performs several case studies on both of the proposed preliminary and detailed optimization frameworks for the participation of a BESS in the energy and ancillary services markets. The relevant analysis is also done on the results, and interesting observations are discovered. The next chapter summarizes all of the outcomes of this research and also provides a road map for the continuation of research in this direction.

4.5 Case Studies on the Stochastic Framework

This section's case studies are focused on the stochastic framework and the proposed approximation methods for solving it. Initially, the accuracy of the approximation approach is evaluated on deterministic cases and a relatively small stochastic case. Once its accuracy is demonstrated, the approximation method is used to solve the strategic participation problem of the BESS in energy and ancillary services markets while uncertainties are imposed on the load, ancillary services requirement, services deployment, grid model, and other market participants' offers and operational parameters. The Gurobi solver is used for solving optimizations in this section with a MIPgap of 0.01, but unlike previous case studies, simulations are performed with a Mac book Pro personal computer with the M1 Pro processor and 16 GB memory.

4.5.1 Case 1: Approximation Method Performance on a Single Scenario Problem

Before dealing with stochastic problems, the approximation method is evaluated on a single scenario (deterministic) problem. The optimal participation of a BESS in energy, reserve, and frequency regulation markets is modeled through the stochastic framework, defined in Section 3.4, while there is only one scenario. This scenario is called the base scenario and its detail is presented in Section 4.1, which is the test case system used in previous case studies on preliminary and detailed frameworks. The added data to the test case system for this study is the reserve deployment as it was not modeled in the previous frameworks and studies. The reserve deployment is modeled as a percentage of the reserve capacity requirement and a uniform random value is assigned to it for each interval of the simulation horizon in the base scenario.

Figure 4.16 shows the simulation results of the case that BESS is participating in the real-time energy and all of the ancillary services markets. In this figure, black, blue, orange, green, and red curves are respectively BESS's scheduled powers for energy, reserve, reserve deployment, regulation capacity, and regulation mileage. Furthermore, the gray area that is plotted on the right axis is BESS's SOC.

Comparing Figure 4.16 with Figure 4.12, one can see that reserve deployment modeling does not affect the participation strategy of the BESS. The frequency regulation market is still the first priority for BESS, and it participates in energy and reserve markets only in the initial and last intervals that it has excess capacity to the frequency regulation market.

The main purpose of this case study is to evaluate the proposed approximation method. Hence, the stochastic model on the base scenario is solved several times through the proposed approximation approach with different values for lookahead l windows. The solution time and accuracy of these approximations are compared

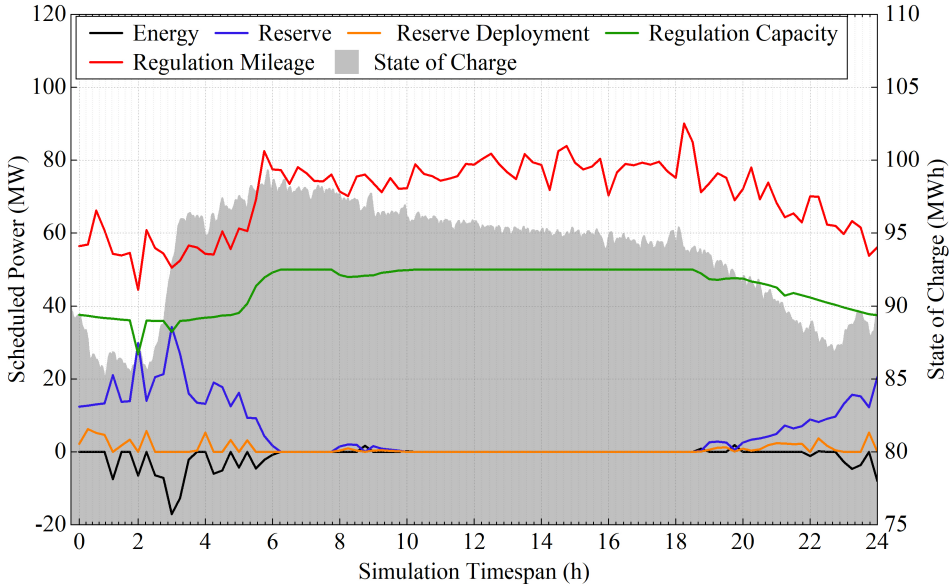

Figure 4.16: Exact Simulation Results of the Base Scenario Case Study.

against the exact solution in Table 4.2. Note that the exact MILP has 370753 constraints, 272640 continuous variables, and 38112 binary variables. The approximation approach reduces the number of binary variables in each sub-problem by relaxing a portion of them based on the lookahead step size.

Table 4.2: Base Scenario Result Approximations Versus Exact Solution

Lookahead Steps	Solution Time (Sec)	Solution Time Reduction (%)	Objective Value ($)	Error (%)
Exact	10828	–	15686.9	–
$l = 1$ step	1290	88.0%	15022.2	4.23%
$l = 2$ steps	944	91.2%	15441.6	1.56%
$l = 4$ steps	561	94.8%	15482.4	1.30%
$l = 16$ steps	405	96.2%	15652.7	0.21%

The comparison provided in Table 4.2 clearly shows that the approximation method reduces the solution time of the problem drastically while there is a small error in the objective values compared to the exact model. As it was expected, the approximation

accuracy increases by increasing the number of lookahead steps. Also, for all approximations, the decrease in the solution time as a result of solving fewer sub-problems for larger lookahead steps overcomes the increase of each sub-problem solution time. Hence, the total solution time of the algorithm always decreases with the increase of lookahead step sizes. For example, considering 96 intervals of simulation horizon, 4 sub-problem with an average solution time of 101 seconds are solved when the lookahead step size is 16, while 24 sub-problem with an average solution time of 23 seconds are solved for the four steps lookahead approximation.

The highest accuracy happens at 16 steps of lookahead approximation where the approximation error is less than one percent. Considering that the MIPgap of the solver is set to one percent, the result of approximation with 16 steps lookahead size is similar to the optimal solution. Note that as each interval duration is 15 minutes, 16 step lookahead is equivalent to 4 hours, which is the energy capacity duration of the BESS. Although the 16-step approximation has a small solution time and high accuracy, sub-problems with this number of lookahead steps may have a large solution time once more than one scenario is modeled. Hence, for the remainder of this dissertation, 4-step is used for the lookahead step size of approximations. Based on Table 4.2, 4-step approximation significantly reduces solution time by almost 95% while its error is only 1.3%.

To better represent the accuracy of approximation with 4 step lookahead size, approximated simulation results for the base scenario model using a 4-step lookahead size are presented in Figure 4.17. In this figure, black, blue, orange, green, and red curves are respectively BESS's scheduled powers for energy, reserve, reserve deployment, regulation capacity, and regulation mileage. Furthermore, the gray area that is plotted on the right axis is BESS's SOC.

Comparing this Figure with the exact results (Figure 4.16) shows that except for

several intervals, the scheduled powers are very similar to each other across these two figures. As a result of one of those discrepancies in scheduled energy between the exact result and the simulated one in initial periods, the SOC curves of these two figures are not similar to each other. However, the total change in SOC (difference between SOC's minimum and maximum) for both figures is around 10 MWh. It shows that the used portion of BESS's capacity in the approximated results is similar to the exact one.

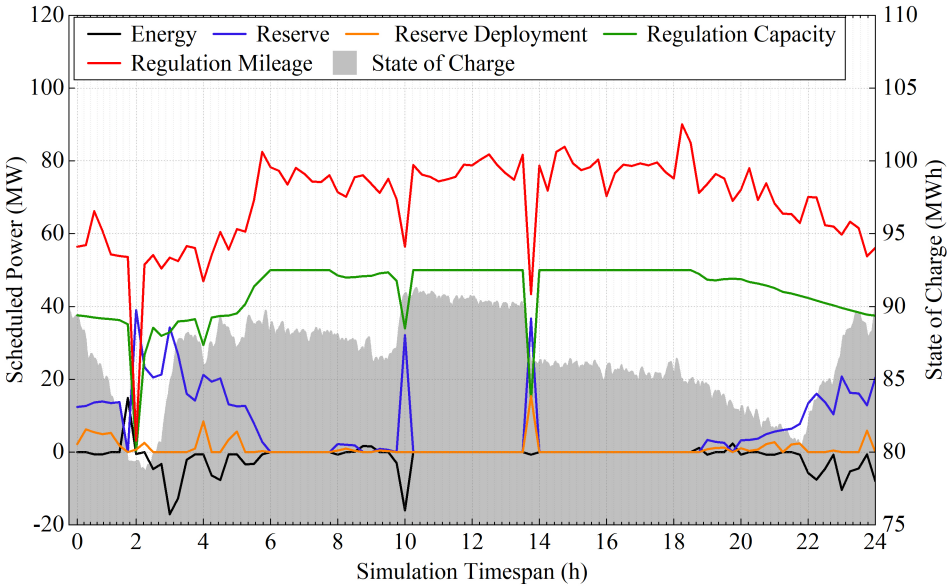

Figure 4.17: Approximated Simulation Results of the Base Scenario Case Study with 4-step Lookahead Size.

This case study showed that the proposed approximated method reduces the solution time of the problem significantly while it imposes an insignificant error on the results.

4.5.2 Case 2: Approximation Method Performance on a Small Stochastic Problem

The first case study showed that the proposed approximation approach finds the solution to the deterministic problem with high accuracy and low solution time. It

also demonstrated that the lookahead step size of four has a good balance between accuracy and solution time. Before using the 4-step approximation method for solving the stochastic participation of BESS, the accuracy of this approximation is analyzed in this case study on a small stochastic problem.

In order to be able to solve the exact stochastic model and compare its results with approximated one. The proposed stochastic framework is used to model BESS in energy and ancillary services markets in a 10-hour simulation horizon with 2 scenarios. Based on the described modeling procedure, the 10-hour horizon is modeled with 40 market clearing intervals. One of the modeled scenarios is the base scenario as described in the previous case study. The second scenario imposes a 30% error on the forecasted values for load and ancillary services requirements. Also, the probability of each scenario is 0.5.

The exact stochastic problem of this case is solved in 6861 seconds and the optimal objective value is \$203419. The objective function value is very high as in several intervals BESS has been able to exercise market power and manipulate regulation capacity prices. However, as this case study is only focused on the evaluation of the approximation method, price manipulation is not further discussed.

The exact simulation results for each scenario of this small stochastic problem are presented in Figure 4.18. In this figure, black, blue, orange, green, and red curves are respectively BESS's scheduled powers for energy, reserve, reserve deployment, regulation capacity, and regulation mileage. Furthermore, the gray area that is plotted on the right axis is BESS's SOC. Note that BESS has one quantity and price offer for each service for both of these scenarios, but scheduled powers resulting from these offers are different in each scenario.

On the other hand, this small stochastic model was solved through the approximation algorithm lookahead step size of four in 395 seconds. Additionally, the ap-

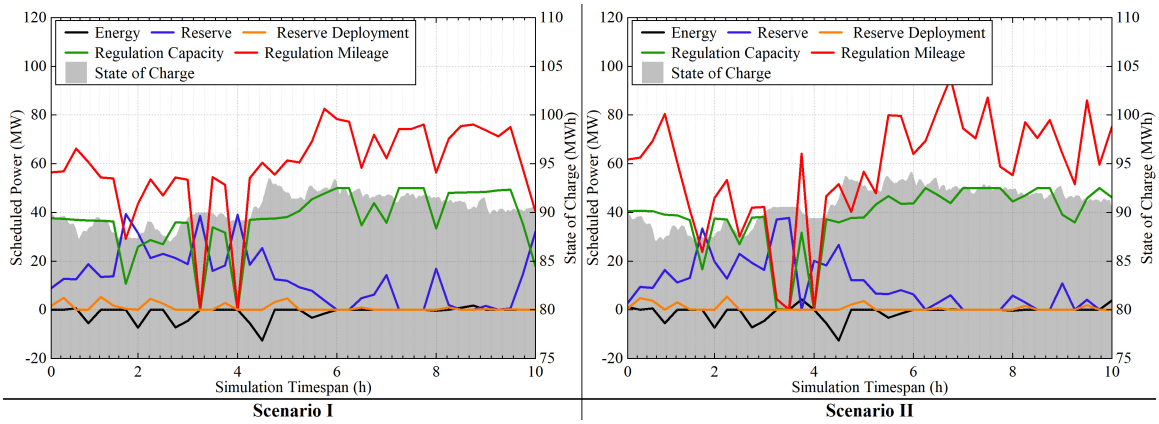

Figure 4.18: Exact Simulation Results for the Small Stochastic Case Study.

proximated objective value is \$197460. Hence, the proposed method with a 4-step lookahead size approximated the results with a 2.9% error while its solution time is 94.2% lower.

To complete the comparison, the approximated scheduled powers for each scenario are demonstrated in Figure 4.19. In this figure, black, blue, orange, green, and red curves are respectively BESS's scheduled powers for energy, reserve, reserve deployment, regulation capacity, and regulation mileage. Furthermore, the gray area that is plotted on the right axis is BESS's SOC.

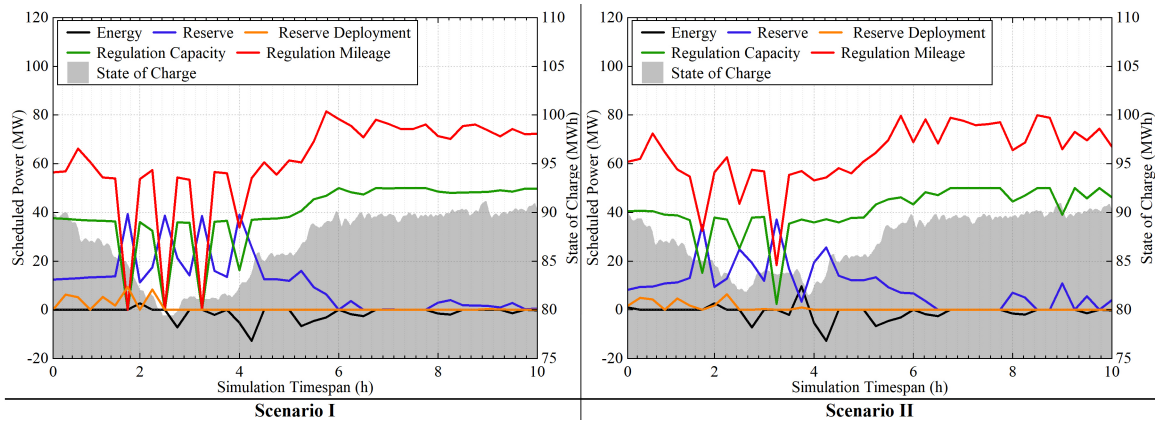

Figure 4.19: Approximated Simulation Results for the Small Stochastic Case Study.

Comparison between Figure 4.18 and 4.19 shows that the approximated schedule powers are close to the exact ones for most of the intervals. More importantly, the

participation priority for various markets is similar between these two figures even if the scheduled powers are not exactly similar. Thus, this case study, similar to the previous one, emphasized that the proposed method has high accuracy with a low simulation time.

4.5.3 Case 3: BESS Participation in Energy and Ancillary Services Markets under Uncertainties

The previous case studies showed that the proposed approximation method has good accuracy in solving stochastic optimization. As a result, this section uses the proposed method to implement the stochastic framework for the participation of the BESS in energy, spinning reserve, and frequency regulation markets while considering degradation costs.

In stochastic optimization, four different scenarios are considered for modeling uncertainties on various parameters and assumptions. These scenarios are described in Table 4.3.

Table 4.3: Scenario Description for the Stochastic Case Study

Scenario Number	Probability	Description
Scenario 1	0.3	Base scenario with the data described in Section 4.1
Scenario 2	0.25	Modeled 10% error in load and ancillary services forecasts
Scenario 3	0.25	Modeled 30% error in AGC signal and reserve deployment forecasts
Scenario 4	0.2	Modeled 20% error in grid and other participants parameters predictions

The first scenario is the base one with the same data as Sections 4.3.4 and 4.5.1, which has a relatively higher probability than other scenarios. The second scenario imposes errors in the load and ancillary services requirement forecasts as there is always uncertainty in these forecasts. Note that the modeled error is higher than the usual load forecast errors in markets to make sure that the results consider extreme cases. As AGC signal and reserve deployment are hard to forecast and have a huge impact on the BESS operation, the third scenario imposes a high 30% error on these forecasted values. Note that Scenario 2 also modeled a 10% error on ancillary services deployment as a part of load forecast error modeling but in Scenario 3 the error is only imposed on the services deployment forecast while load and services' requirements forecasts are similar to the base scenario. Scenario 3 helps to better model the most uncertain parameters in the BESS participation problem. Finally, Scenario 4 models a 20% error in the prediction of other market participants' offers and their operational parameters as well as gird models like transmission line limits and each bus load share. The last scenario has a relatively lower probability as one's prediction over these parameters gets more accurate over time.

These four scenarios are modeled through the stochastic framework detailed in Section 3.4 and solved using the proposed approximation method in Section 3.5. The approximation algorithm was executed in around 22 hours and the approximated objective value is \$15676.4, which is the weighted average of BESS net revenue in each of the four scenarios based on their probability. The breakdown of BESS's revenues in different scenarios is shown in Figure 4.20.

Figure 4.20 clearly shows that the participation pattern of BESS in various markets does not change under uncertainties. In all scenarios, similar to the previous deterministic case (Sectio 4.3.4), the frequency regulation market is the main revenue stream for BESS and the spinning reserve has the second priority. Note that these

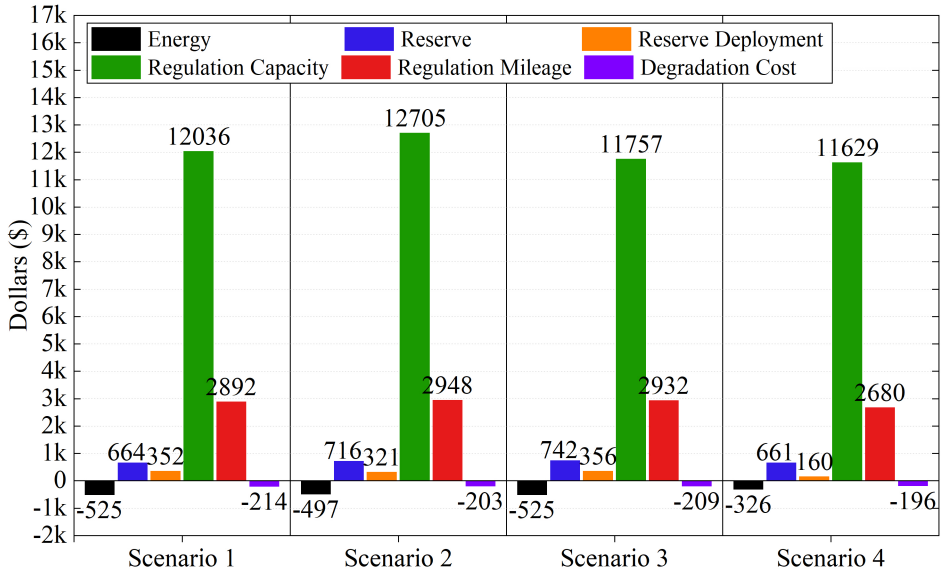

Figure 4.20: Bess's Total Revenue from Each Market in Each Scenario along with Its Degradation Cost.

scenarios are not independent of each other and are modeled in a single stochastic optimization problem. Meaning that BESS has picked a single set of quantity and price offers that results in this participation pattern over all different scenarios. This participation priority is happening as the provision of regulation services causes the least degradation cost for the battery due to shallow charge/discharge cycles.

Figure 4.21 shows the scheduled power and SOC of the BESS for each of the four scenarios. In this figure, black, blue, orange, green, and red curves are respectively BESS's scheduled powers for energy, reserve, reserve deployment, regulation capacity, and regulation mileage. Furthermore, the gray area that is plotted on the right axis is BESS's SOC. The scheduled powers for BESS are following the same pattern over all scenarios, which is prioritizing participating in the frequency regulation market. The reserve and energy market participation are the second and third priorities and happens in hours that BESS has an excess capacity over the regulation market. One important observation in Figure 4.21 is that BESS scheduled power for the reserve deployment is nearly zero in all scenarios, which is happening as providing reserve

services would cause deep charge/discharge cycles and hence high degradation costs.

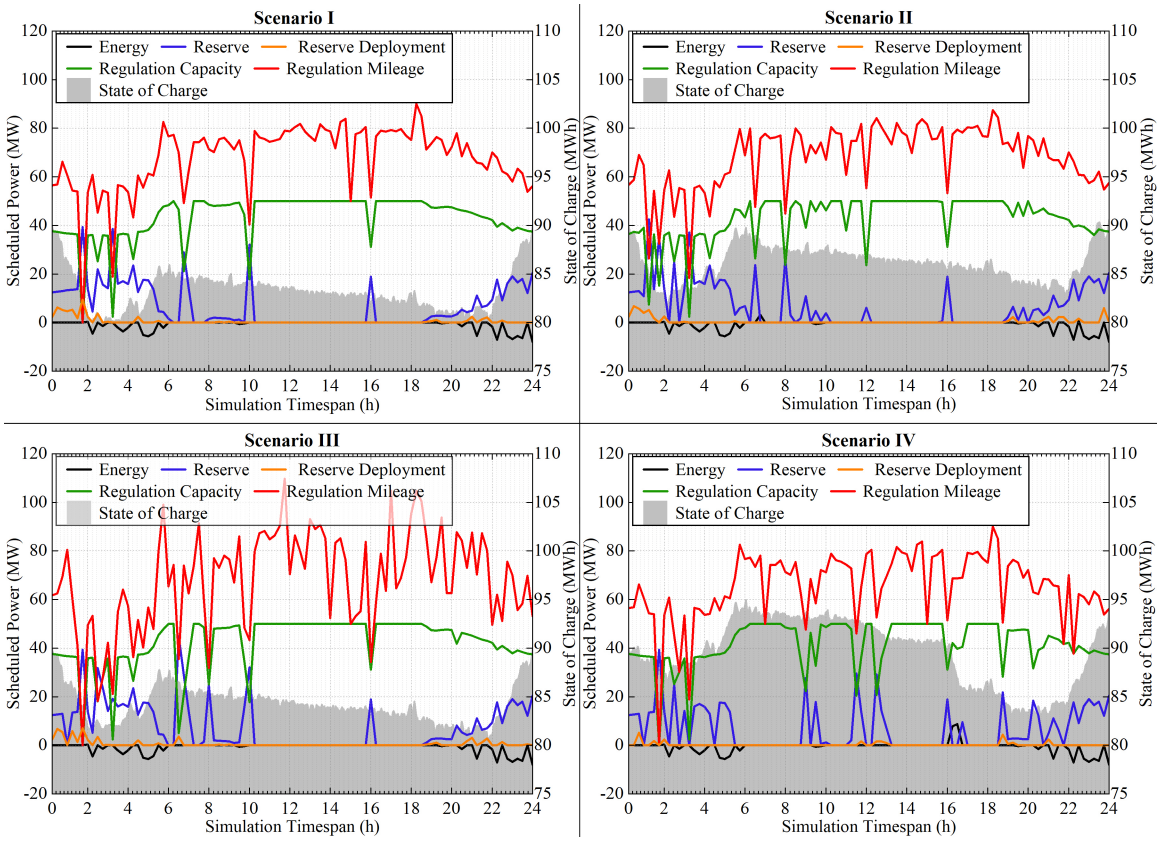

Figure 4.21: Simulation Results for the Stochastic Case Study.

In the third scenario results of Figure 4.21, the dispatched power for regulation mileage (red curve) has high fluctuation. This is happening because in this scenario a high error is modeled in AGC signals causing fluctuation in the regulation mileage requirement of the grid. BESS is providing most of the frequency regulation requirements of the system and follows those fluctuations.

Finally, Figure 4.21 shows that in all scenarios, BESS does the same interval arbitrage across reserve and energy markets if it is participating in the reserve market. This same interval arbitrage was also happening in the deterministic cases as it lets BESS utilize its capacity more profitably.

Chapter 5

CONCLUSION AND FUTURE WORK

This work proposed three optimization frameworks for the participation of a utility-scale price-maker BESS in real-time energy, spinning reserve, and pay as performance frequency regulation markets. All the proposed frameworks are bi-level optimizations. In their ULP, BESS maximizes its profit while operational details of the batteries are considered. In the LLP, ISO joint market clearing process is simulated with an accurate representation of each market. The preliminary framework does not consider battery degradation costs, and AGC signal deployment is handled through the choice of market clearing intervals' duration. On the other hand, the proposed detailed framework uses a participation factor for accurate AGC signal modeling. It also considers batteries' degradation cost using a piecewise linear cost approximation. Lastly, the third framework introduces uncertainty in the problem and model spinning reserve deployment. The third framework is solved through a reinforcement learning approximation approach.

Several case studies are done on the models using real-world data to evaluate the models, analyze the effect of BESS operation on the market/grid, and also study the optimal allocation of BESS's capacity across various revenue resources. The main outcomes of the performed studies are summarized in the first section of this chapter. The second section discusses potential future research directions.

5.1 Conclusion

The simulation results showed that regardless of consideration of degradation cost, the participation of BESS in more markets will result in more profit. This result is

expected as economic concepts recommend it, and previous works also have shown it. Furthermore, by participating in more markets, BESS experiences charge and discharge cycles with less cycle depth, and also it does not need to use a significant portion of its capacity. It is equivalent to having less degradation cost and also requiring fewer investment costs for building BESS when it participates in several markets.

Letting BESS gain revenue from various markets also enables it to do different forms of arbitrage and increase its profit. On the other side, simulation results showed that the participation of BESS in more markets could also be beneficial for the system and reduces the total system cost even when BESS is a price-maker unit in the markets.

Participation in the ancillary services markets is more appealing for the BESS no matter whether degradation cost is considered or not. Among the ancillary services markets, the frequency regulation market is more profitable than the reserve market for the BESS. Hence, participation in the frequency regulation market is the priority for BESS and the reserve market is the second option. It is worth mentioning that participation in the frequency regulation market and following AGC signals do not cause high degradation costs as BESS goes through charge/discharge cycles with small depth.

If both of the ancillary services markets are saturated, which means that BESS has unused output power compared to system reserve and regulation requirements, its participation in the energy market depends on the batteries' cost. Our simulation results showed that the energy market is not profitable for batteries with a replacement cost of 25 \$/kWh or higher.

Another important outcome from the simulations is the required technical capability of the BESS for each market. In the ancillary services markets, the role of

BESS' output power limit is more critical for gaining profit. It means that for two BESSs with the same energy capacity, the one with higher output power will gain more profit in the ancillary services markets. This fact is not valid in the energy market, this market requires BESS to use its capacity for performing energy arbitrage. Hence, gaining profit in the energy market is more dependent on the BESS's energy capacity while output power is also an essential factor. Considering this fact in the design of BESSs for grid applications may result in investment cost reduction.

Simulation results showed that at least in the fairly realistic test case system of this work, even the existence of a price-maker BESS is beneficial and reduces the total system cost. However, as the BESS participates in more markets, it gains more power to affect the markets and the reduction in the system cost may not be as expected. Thus, ISOs need to modify their market structure further to benefit the most from BESSs, while the independent operation of BESSs is not affected.

In general, the comparison between our results with the existing literature in this field and also the comparison between the proposed preliminary and detailed frameworks showed that neglecting batteries' degradation cost can lead to results that are not realistic. To the best of our knowledge, our proposed detailed optimization framework is the first one that considers degradation cost for the participating of a price-maker BESS in various markets. Although the addition of the accurate degradation cost model increases the size and complexity of the problem, the results are more credible. Hence, this model enables us to better analyze BESS's operation and its effects on the markets.

Finally, the stochastic framework results showed that the mentioned outcomes regarding BESS operation in various markets are valid even if there are errors or uncertainties in the price-maker model assumptions. Also, the proposed approximation method for solving stochastic framework showed high accuracy while reducing

solution time drastically. This approximation approach may be used for applications outside this work.

5.2 Future Work

Expansion of BESSs into the grid, especially the large-scale ones, is happening currently, and it is a new phenomenon. Although researchers have been working on this area for several years, there are still a large number of non-touched topics in this field. This chapter mentions some of them as possible future directions of this research work.

BESSs can provide many other services that are not considered in proposed frameworks or other models in the literature. Chapter 1 explained various power grid services which can be provided by BESSs. Modeling other services besides reserve and frequency regulation can increase the profit of BESS and also enhance its effect on the market/grid operations. This addition can happen in the form of a market product like the flexible ramp market or as a non-market application like the co-location of BESSs with other resources.

In this dissertation, BESS is the only strategic unit in the markets, which is a controversial assumption. Considering more strategic or price-maker units in the markets gets the optimization framework closer to the game that happens between participants in reality. In the case of considering several or all market participants as strategic, the problem is converted to an equilibrium problem with equilibrium constraints (EPEC), which have higher computational complexity comparing to the proposed models. However the market equilibrium of this model is more realistic, so the EPEC model is better for doing analysis from the ISOs' perspective.

Finally, simulation results showed that the existing market mechanism needs to be modified for more beneficial participation of BESSs. Doing further mathematical

analysis on the effect of the BESSs on the LMPs and ancillary services prices is a valid future direction for this work. Using these analyses, it is possible to better understand the role of price-maker participants in the markets. Hence, it may result in designing a better market mechanism for the participation of BESSs or other new participants like renewable fleets, aggregators, and DERs.

Part II

BIDDING OBJECTIVE IDENTIFICATION OF ELECTRICITY MARKET PARTICIPANTS THROUGH ADVERSARIAL INVERSE REINFORCEMENT LEARNING

Chapter 6

INTRODUCTION

Data-driven methods advancement in recent years besides the transparency implementation and bidding data availability in the electricity markets has led to a new research topic, which is the identification of market participants' bidding objectives from their historical bidding data. The bidding objective identification (BOI) has been a prominent research question since the electricity market deregulation due to its importance for system operators as well as market participants. However, the introduction of data-driven methods to this field provides the opportunity to extract bidding objectives directly from the market performance data without biasing the objective identification by relying on any presumption for the market participant's behavior. The application of data-driven methods for BOI is in its incipient phase and needs improvement. This research work tries to address some of the most important shortcomings in the existing works in this field by doing BOI through adversarial inverse reinforcement learning (AIRL). Before getting into the details of this research work, this section initially reviews the importance of the BOI research area. Subsequently, an overview of reinforcement learning (RL) and inverse reinforcement learning (IRL) concepts is provided. Finally, the motivations and contributions of this work are discussed before detailing the arrangement of the contents in the remainder of the dissertation.

6.1 Bidding Objective Identification Importance

Bidding behavior modeling and analysis are two fundamental problems for both market participants and system operators. Independent system operators (ISOs) can

perform bidding behavior modeling and analysis to improve market design and market efficiency, as well as detect fraudulent bidding strategies and market power exercises. On the other hand, a market participant can perform bidding behavior modeling and analysis using historical bidding data of other participants to design its own bidding strategies.

The above problems of bidding behavior modeling and analysis can be solved through bidding objective identification (BOI). All behavior modeling approaches, including bi-level optimization [35] and reinforcement learning (RL) [23] methods, maximize the bidding objective function (reward function) of the market participant. Therefore, successful identification of the underlying bidding objective leads to accurate bidding behavior modeling. Additionally, finding the underlying objective of an observed bidding behavior is the main approach for market participant behavior analysis.

Besides operating the electricity market and grid, ISOs always seek the best market design upgrades and optimal grid expansion plans. Any market or grid changes require extensive analysis of the effect of the changes on the market and grid operation. For these analyses, market participants' behavior under new grid expansion or market rule changes should be modeled. ISOs need to know or identify the bidding objective of the market participants in order to model them under the grid and market changes. Additionally, by knowing the bidding objective behind the market participants' bidding data, an ISO can easily identify fraudulent bidding behaviors or market power execution.

From the market participants' perspective, identifying the bidding objective of other market participants can have several benefits. They can model their interactions with other participants in the market and find the optimal bidding strategy. Also, they can use an identified bidding objective to replicate a certain behavior.

Traditionally, a cost-based bidding objective has been considered for market participants based on a rational bidding paradigm. However, besides the existing information barriers for retrieving the cost of a market participant, different studies and real-world observations have shown that cost is not the only factor that affects the market participants' behavior [37]. The widespread expansion of renewable and storage resources and the adoption of carbon reduction policies have introduced new complexities to the bidding problem that traditional definitions of bidding objectives are not able to capture.

The historical bidding data transparency implementation in electricity markets has created an opportunity to use data-driven methods for BOI. Unlike the traditional definitions, data-driven approaches require minimal or no presumption of the objective function structure and rely solely on available data for extracting bidding objectives. Inverse RL (IRL) can be adapted to the electricity market for BOI as it tries to find the reward underlying an observed behavior. Adversarial IRL is a novel IRL method that has shown prominent improvement over other IRL methods in various applications [14]. This method is used in this work to identify the bidding objective of market participants while addressing the shortcomings of existing works.

6.2 Reinforcement Learning and Inverse Reinforcement Learning

This section provides a brief overview on the RL and IRL topics.

6.2.1 Reinforcement Learning

Reinforcement learning (RL) as a sub-field of artificial intelligence (AI) is built upon the idea that an agent can learn how to act optimally by interacting with its environment and getting feedback in a form of a reward or penalty that shows how well it has performed. As a result, various problems like optimal bidding can be

tackled with RL. In a general description, an RL agent interacts with an environment sequentially. At each time step sequence, the agent selects an action by observing the current state of the environment, based on its current policy. The policy is a set of rules that specify how the agent should behave. As a result of the selected action, the agent receives a reward or penalty based. The goal of the agent is to maximize the cumulative reward over time, which it tries to achieve by learning the optimal policy.

Methods for solving the RL problem can be categorized as model-free and model-based approaches. A model-based approach tries to learn a model of the environment, including transition dynamics and reward function, and use it to inform its actions (policy). On the other hand, model-free approaches learn the optimal policy directly from the experience without any explicit modeling of their environment.

Having a sequential structure, the Markov decision process (MDP) is often used for modeling RL problems. The specific MDP of the BOI problem is defined in the following chapters of the dissertation. In general, three main functions are usually used across various RL methods: the state-value function, the action-value function, and the advantage function. The state-value function shows the expected cumulative reward of a certain state by following the current policy. Similarly, the action-value function shows the expected cumulative reward of a certain action in a state by following the current policy. Finally, the advantage function is the subtraction of the action-vale function from the state-value function showing how good that action is compared to the baseline reward expectation. Model-free and model-based RL methods try to estimate, learn, or calculate one or combinations of these functions to find the optimal policy.

Common RL approaches can be categorized in dynamic programming (following Bellman equations as it was described in the previous part), Monte Carlo methods, temporal-difference learning methods, and policy gradient methods [78]. Each of these

categories contains various approaches, and reviewing them is out of the context of this dissertation. However, the ones that are needed are reviewed in the following chapters.

RL has applications in a wide range of fields, including robotics, game playing, control systems, finance, and power systems. The application of RL in power systems covers various topics from dynamic stability to the electricity markets. These applications are reviewed in the second chapter of this part.

6.3 Inverse Reinforcement Learning

Inverse reinforcement learning (IRL) aims to understand the reward function that motivates the observed behavior and justify it. It was mainly developed to learn the reward function of an expert (human) by observing its performance in a given task and reusing the reward for training a non-human agent [58]. The idea behind it is that learning a reward function of observed actions can help us to improve the policy or transfer the knowledge to another agent. For example, in the context of BOI, we can learn the reward (bidding objective) of a market participant from its actions (bidding data), and then use this reward for analyzing the performance of the market participant, modeling it, or training another agent to act like similarly.

Learning a reward function based on the Maximum causal entropy (MaxEnt) concept is the main approach for IRL [87]. MaxEnt IRL tries to find a reward function that maximizes the entropy of the policy distribution, subject to the constraint that the policy is consistent with the observed behavior of the agent. The intuition behind this approach is that the reward function that leads to the observed behavior should be the one that maximizes the entropy of the policy distribution. Another IRL approach is Bayesian IRL, which models the reward function as a distribution over possible reward functions rather than a single function.

AIRL [32] is a novel IRL method that implements the maximum entropy (MaxtEnt) IRL through generative adversarial (GAN) [36] training. This method is used in this research work to identify the bidding objectives of electricity market participants based on their historical bidding data. MaxEnt IRL is truly reviewed in the third chapter in order to introduce and customize AIRL for the BOI application.

6.4 Motivation for Bidding Objective Identification through AIRL

As it is reviewed in the next chapter, all the existing IRL methods for BOI in electricity markets use discrete variables for modeling the problem and identifying the bidding objective. Hence, the historical market data including bidding records and market clearing results need sophisticated preprocessing to be discretized for the use of current IRL approaches. These preprocess introduce complexity to the IRL models and make their real-world applications challenging. Also, there is a high risk of information loss in a discretization that affects the identified bidding objective. Furthermore, the unique multi-segment bidding structure of electricity markets, where participants may have various prices for different capacity portions, is not directly modeled in the existing IRL methods. This phenomenon may also cause inaccuracy in the BOI. More importantly, existing literature on BOI in electricity markets through IRL does not provide analytical or empirical evidence on the robustness of their identified bidding objectives. Ideally, we want to identify bidding objectives that are robust to the changes in the environment. E.g., the bidding objective of a storage unit that performs energy arbitrage should not change if the peak load of the system moves from the afternoon to the morning. Identifying a robust bidding objective results in legitimate bidding behavior analysis and successful bidding behavior modeling in various environments. For instance, by having a robust bidding objective, an ISO may analyze the effect of gird and market changes on the participants' behavior.

Recognizing the existing shortcomings in the literature, this paper proposes a robust BOI framework through AIR which works in the continuous domain and complies with the unique bidding structure of the electricity markets. The main contributions of this work are listed below.

- A data-driven approach for identifying robust bidding objectives for electricity market participants based on their historical bidding data is proposed.
- AIRL is introduced and customized for performing BOI in electricity markets without variable discretization.
- Necessary modifications in the problem definition and AIRL structure are proposed to ensure the robustness of the identified bidding objective from the environment.
- The robustness of the identified bidding objective through the proposed AIRL-BOI method is proven.
- A special policy structure that complies with multi-segment bidding rules of electricity markets is proposed, which may be used for RL applications beyond this paper.
- Two approaches for electricity market environment modeling in RL/IRL problems based on data availability and type of market participants are proposed.
- Training stability and convergence of the AIRL in BOI application is improved by introducing gradient penalty and data sampling expansion.
- Comprehensive case studies are designed to ensure the accuracy of the proposed method and validate the robustness of the identified bidding objective over syn-

thetic and real data. The case studies also provide a diverse set of examples for the application of AIRL-BOI from users with different levels of data availability.

6.5 Summery of Content

In the remainder of the dissertation, Chapter 7 reviews the application of IRL in electricity markets and describes the existing gap in the literature. Chapter 8 is dedicated to the methodology and formulation of the AIRL method for BOI. This chapter formulates the BOI problem by defining its main elements including the policy structure and electricity market modeling approaches. MaxEnt IRL and GAN are also reviewed in Chapter 8 to provide some background for the proposed method. Subsequently, AIRL in the electricity market is discussed in Chapter 8 along with method customization, proof of the identified bidding objective's robustness from the environment, policy structure, and algorithmic improvements. Chapter 8 also proposes a policy structure that complies with electricity market rules and can be used in RL applications beyond this dissertation. Chapter 9 designs three independent sets of case studies to extensively evaluate the performance of the proposed AIRL-BOI method. It also verifies the robustness of the identified bidding objective in each of the case studies. Finally, Chapter 10 concludes this part of the dissertation and discusses future works.

Chapter 7

LITERATURE REVIEW

In contrast to the RL whose application in various aspects of power systems has been extensively explored in recent years [23, 70, 76], the application of IRL in power systems is a relatively new research area, and a limited number of research works exist in this field. This section reviews the literature in the field of BOI through IRL to describe their shortcoming, which emphasizes the advantages of the proposed AIRL-BOI method.

7.1 Bidding Objective Identification through Inverse Reinforcement Learning

The IRL concept was first introduced to the electricity markets and BOI topic in [85], where the parameters of a linear risk preference model for a market participant are extracted with IRL. This work is built upon one of the earliest IRL methods [58]. This IRL method assumes a linear structure for the reward function and learns its parameters in order to maximize the probability of the observed action over all possible actions. Hence, there is a presumption of linearity for the reward function which limits the possibility of identifying the exact reward function. As a result, Zhao et al., have done risk preference analysis through this IRL method instead of BOI [85].

A cluster-based method for historical bidding data pattern extraction is proposed in [37], which is only focused on bidding behavior interpretation, not BOI. This work uses the adaptive k-medoid approach for clustering the bidding data of electricity market participants. Although this does not do BOI, it is fundamental for the other research works that do BOI. The proposed clustering method provides a discretization

approach for bidding data, that is used in other works as all of them work on the discrete domains [38, 73, 72].

Built upon [37], authors in [38] introduce deep IRL to the electricity markets. In this work, the bidding objective function is represented through a neural network to capture complexities and nonlinearities. Hence, the bidding objective is identified without imposing a predefined structure (e.g. linear, quadratic) on it. The parameters of the bidding objective's neural network are learned through the MaxEnt IRL [87] algorithm. As mentioned, [38] uses discrete state and action spaces for BOI as it uses the very first MaxEnt algorithm, which cannot handle continuous domains. Hence, the bidding data of market participants are discretized through the method proposed in [37], which not only adds to the complexity of the BOI problem but also introduces the risk of information loss to the BOI process. Additionally, this work does not provide any empirical or theoretical evidence on the robustness of its identified bidding objective.

Built upon [37, 38], the IRL applications to multi-market [73] and multi-task [72] BOI problems are proposed. The bidding objective of a storage unit participating in the energy and ancillary services markets is extracted in [73]. Although this work provides useful insight into the participation strategies of storage units across various markets, it suffers from the same shortcomings as the previous one [38]. In essence, the IRL algorithm of [73] is similar to [38], and hence it needs discretization and does not guarantee robustness. A similar IRL algorithm is used in [72] to extract the bidding objective of various tasks. In this work, the historical bidding data are divided into several tasks and discretized using the same clustering methods as [37]. Subsequently, the discretized actions are fed into the MaxEnt IRL algorithm to learn the bidding objectives. Task categorization in this work helps to better model the market participant bidding objective. However, similar to the other works of this

research group, their method only works on discretized domains and the robustness of the bidding objectives are not discussed.

The IRL is not the only method that has been used for BOI in electricity markets. An inverse optimization method is presented in [22] to find the parameters of a market participant's quadratic cost function. The opt-net concept is used in [20] to represent optimization as a neural network and identify the bidding objective by training the network. The use of the opt-net concept helps to better identify the market participant's constraints but the bidding objective is limited to a fixed structure e.g. quadratic functions.

Chapter 8

METHODOLOGY AND FRAMEWORK

Bidding objectives identification (BOI) through AIRL implements Maximum Entropy (MaxEnt) IRL in the adversarial training structure as the direct implementation of MaxtEnt IRL may not be the most efficient approach [30]. Also, this indirect implementation may benefit from the existing rich literature in the adversarial training domain. This chapter provides details on the proposed AIRL-BOI algorithm. In the following, the Markov decision process is tailored for BOI application; Two different electricity market environment approaches are proposed; Some background is provided on generative adversarial training (GAN) and MaxEnt IRL; The AIRL for BOI is introduced; Nessecarly modifications are made to learn a bidding objective that is robust from changes in the environment and this robustness is proved; Finally, the structure of AIRL-BOI is reviewed and its algorithm is proposed along with some augmentations for convergence improvements.

8.1 Bidding Objective Identification Framework

Markov decision process (MDP) is the mathematical structure for modeling sequential decision-making problems such as RL and IRL [71]. This section reviews the MDP modeling concept and tailors certain MDP components for the studied BOI problem.

8.1.1 Markov Decision Process for Bidding Objective Identification

MDP can be described by a tuple $(\mathcal{S}, \mathcal{A}, \mathcal{T}, r, \gamma)$. Each element of the tuple for the electricity market bidding problem is defined as follows.

State space $\mathcal{S}$:

Each state s is an array containing the data that informs the market participant's decision. State space may vary depending on the market and type of the participant modeled for BOI. It may contain information like market price, dispatch power, state of charge (SOC), current load, and forecasted load, but it is not limited to these data points.

Action space $\mathcal{A}$:

The market participant's bid (offer) is the action a in this problem. According to the bidding structure of the electricity market, action a may be a scaler or an array in case of multi-segment quantity and price bidding. The state and action spaces of the proposed AIRL-BOI method are both continuous, which enables it to handle historical bidding data directly without complex pre-processing and discretization.

State transition distribution or dynamics $\mathcal{T}$:

Given a state s, $\mathcal{T}$ provides a distribution over the transitioning states when taking action a. $\mathcal{T}$ should satisfy Markov properties [71]. This dynamic is represented through the electricity market environment (EME) discussed in the next section.

Reward function or bidding objective r:

This function associates a scalar reward value to each state $r(s)$ or state and action pair $r(s, a)$. An RL agent maximizes the expected cumulative reward over time, while the IRL learns a reward function that justifies the observed behavior of an expert [58]. For the AIRL-BOI problem, the bidding objective is equivalent to the reward function, which should be identified through the historical bidding data of a market participant. In this work, the bidding objective function is modeled by a NN

to capture the nonlinearities and complexities of the market participant's bidding objective. The cumulative reward includes a discount factor $\gamma \in [0, 1)$ to set the importance of immediate rewards versus future rewards.

8.1.2 Electricity Market Environment (EME)

The electricity market is the environment for the BOI problem. The market participant which can be modeled as a RL agent submits bids (actions) and collects market clearing results (states) to/from this environment. Our proposed AIRL-BOI method is based upon model-free RL without requiring prior knowledge of the environment. This mimics the real-world market participant's bidding process without knowing the confidential market model. Being model-free is an advantage as the EME is exogenous to the method, and hence the AIRL-BOI method can be used for BOI in any market by implementing a relevant EME model. Based on different levels of data availability, two different approaches are proposed for establishing the EME for a certain electricity market, which can be utilized to cover various application scenarios.

Exact EME Model

Solving the BOI problem from the independent system operator (ISO) perspective, operational data of the grid and other market participants' bids are available along with the historical bidding data of the market participants. Thus, the EME can be implemented through an optimization replica of the market i.e., DC optimal power flow (DC-OPF). The EME gets the market participant RL agent's actions and minimizes the market clearing objective, with regard to the grid's operational constraints. Subsequently, cleared market price and dispatch of the agent beside any other relevant data are returned to the agent as a state. This market model is implemented through

optimizations similar to the one that was formulated as the lower-level problem of frameworks in Part I of this dissertation (Section 4.4.2).

Simplified EME Model

An exact market model is the most accurate way of EME modeling, but it may not be possible if the BOI problem is solved from the market participant's perspective due to data availability. The simplified model arranges the EME around the historical data of the market based on the market operation concept. This model only needs the price of the market participant's bus, which is contained in the bidding data. Subsequently, the simplified EME model works by only clearing the agent's bid (action) for the segments (in case of a multi-segment bidding structure) that are less than the market price, and the dispatch is determined accordingly. This modeling approach is analogous to the price-taker modeling concept as it is inherent in the simplified EME model that the market participant's bids do not affect market outcomes, and it is a valid assumption in the ideal market situation. This EME model along with the exact one is explored in the case study section.

8.1.3 Policy

The policy is a mapping from states to actions $\pi : \mathcal{S} \rightarrow \mathcal{A}$, indicating the action that the agent (market participant in this problem) should take in each state. Hence, the goal of the agent is to find an optimal policy. Policy gradient methods are common approaches for tackling continuous RL problems, where the policy is usually represented by a neural network π_α and parameters of the network α are learned by a policy optimizer in order to maximize the expected cumulative reward over time. While policy optimizer is discussed in a separate section, the policy structure used in this work is paraphrased below.

The Gaussian policy structure is used for dealing with continuous state and action spaces of our BOI problem. In the Gaussian policy, the probability distribution of actions is represented by a normal distribution $\pi_\alpha(a|s) = \mathcal{N}(\mu(s), \sigma(s))$. Where the mean vector $\mu(s)$ indicates the expected action, and standard deviation function $\sigma(s)$ represents the variability of the actions around the mean, which trades off between exploration and exploitation for action selection. In each state, the market participant action is determined by drawing a sample from the learned normal distribution based on the specific value of mean $\mu(s)$ and standard deviation $\sigma(s)$ in that state. It is a straightforward policy model, but it cannot be used by an electricity market participant.

In electricity markets, participants may submit multi-segment bids/offers, meaning that instead of a single quantity (MW) and price ($) value, they can have piecewise supply or demand curves by submitting various prices for different portions of their capacity. However, supply curves must be monotonically increasing, while demand curves must be monotonically decreasing to have a convex market [35]. Hence, for a k-segment bid/offer $[(a_1^p, a_1^\lambda), (a_2^p, a_2^\lambda), ..., (a_k^p, a_k^\lambda)]$, the condition in (8.1) should hold, where a_i^p and a_i^λ are respectively quantity and price values for each offer segment. This condition does not necessarily hold for the actions from the described Gaussian policy.

$$\begin{aligned} &\text{Supply offer: } a_i^\lambda \geq a_{i-1}^\lambda;\ a_i^p > a_{i-1}^p \quad \forall i \in \{2, 3, ..., n\} \\ &\text{Demand bid: } a_i^\lambda \leq a_{i-1}^\lambda;\ a_i^p > a_{i-1}^p \quad \forall i \in \{2, 3, ..., n\} \end{aligned} \tag{8.1}$$

A new Gaussian policy structure is proposed here to fit in the electricity markets' rules. The proposed structure adds a clipping filter to the output of the baseline Guassiam policy. The filter traverses through the quantity and price values sequentially and ensures that condition (8.1) holds. The proposed clipping filter for a supply

offer is described in (8.2), where each segment's action value is clipped to be more than the previous section's value and less than the maximum possible action value. In (8.2), $a_i^{\cdot}$ is the raw output (quantity a_i^p or price a_i^λ) of the Gaussian policy, $\hat{a}_i^{\cdot}$ is the clipped action value (the output of the proposed policy structure), and $\hat{a}_0^{\cdot} = fl^{\cdot}$. The $fl^{\cdot}$ and $cl^{\cdot}$ are respectively minimum (floor) and maximum (ceiling) action values. For a^p, the fl^p and cl^p are the minimum and maximum capacity of the unit; while for a^λ, the fl^λ and cl^λ are set by the ISO.

$$\hat{a}_i^{\cdot} = \text{clip}(a_i^{\cdot}, \hat{a}_{i-1}^{\cdot}, cl^{\cdot}) = \min(\max(a_i^{\cdot}, \hat{a}_{i-1}^{\cdot}), cl^{\cdot}) \tag{8.2}$$

Equation (8.2) applies to the price and quantity segments of the supply bid and the quantity segments of the demand bid. For the demand bid, to ensure a monotonically decreasing curve, the proposed output filter for price segments a^λ changes to $\hat{a}_i^\lambda = \text{clip}(a_i^\lambda, fl^\lambda, \hat{a}_{i-1}^\lambda)$, where $a_0^\lambda = cl^\lambda$.

The proposed policy structure complies with the electricity market rules for multi-segment bids/offers and its application is not limited to this paper's AIRL-BOI method. This structure can be used in any electricity market bidding problems for having a realistic policy model. Also, the proposed policy works for single-value bids as in that case the action value will be clipped between zero and the maximum possible value, and the filter only imposes boundaries on the output.

8.1.4 Proximal Policy Optimization

There are variations of policy gradient methods for optimizing the policy network [79]. Among them, proximal policy optimization (PPO) has shown outstanding performance in various real-world problems importantly the ones with continuous and multi-dimensional action domains like the BOI problem. Hence, we have used PPO as the policy optimizer element of our proposed AIRL-BOI method. This section pro-

vides a brief overview of the PPO as one of the main components of the AIRL-BOI algorithm.

The PPO approach is a variant of the actor-critic policy gradient method. In this work, the described policy structure is the actor and the critic is a policy value function V_υ that can be represented through a neural network. In each training epoch of PPO, the value function's parameters υ update to predict the expected return of states under the current policy, which defines as follows.

$$V^{\pi}(s_t) = E_{\pi_\alpha}\left[\sum_{k=0}^{T}\gamma^k r_{t+k}\middle| s_t\right] \tag{8.3}$$

On the other hand, the policy's parameters α update to maximize the following surrogate objective function.

$$\mathcal{J}(\alpha) = E_t\Big[\min\Big(\rho_t(\alpha)A^{\pi_{\alpha_{old}}}(s_t,a_t), \text{clip}\big(\rho_t(\alpha), 1-\epsilon, 1+\epsilon\big)A^{\pi_{\alpha_{old}}}(s_t,a_t)\Big)\Big] \tag{8.4}$$

Where $\rho_t(\alpha)$ is the probability ratio of updated policy to the old one $\rho_t(\alpha) = \frac{\pi_\alpha(a_t|s_t)}{\pi_{\alpha_{old}}(a_t|s_t)}$ and indicate the extent of changes in the updated policy. Additionally, $A^{\pi}(s_t,a_t)$ is the advantage function that measures how much a certain action is better than average $A^{\pi}(s_t,a_t) = V^{\pi}(s_t) - Q^{\pi}(s_t,a_t)$. State-action value function $Q^{\pi}(s_t,a_t)$ is the expected return of a state under a certain action which defines as follows.

$$Q^{\pi}(s_t,a_t) = E_{\pi_\alpha}\left[\sum_{k=0}^{T}\gamma^k r_{t+k}\middle| s_t, a_t\right] \tag{8.5}$$

The minimization term in the policy optimization objective (8.4) imposes a pessimistic bound by ignoring probability ratios that are making improvements to the objective. Subsequently, the clip function limits the amount that the policy can change in a single update step ensuring that the updated policy is not too far away from the old policy, which prevents policy divergence. Detail on PPO can be found in [67].

8.2 Background

Generative adversarial networks (GANs) and maximum entropy (MaxEnt) IRL are reviewed before dealing with AIRL in electricity markets as in essence AIRL implements the MaxEnt IRL concept through GAN training.

8.2.1 Generative Adversarial Networks

Generative adversarial networks are an approach to generative modeling, where two networks, generator G and discriminator D, are trained simultaneously. The discriminator is tasked to distinguish whether its input is a sample from a generator (fake data) or a sample from an underlying distribution p (real data). On the other hand, the generator's objective is to output a sample that the discriminator cannot differentiate from the real data [36]. Thus, The discriminator's loss is the average log probability it assigns to the correct classification evaluated on an equal mixture of real and fake data as below.

$$\mathcal{L}_D = E_p\Big[-\log D_\theta(x)\Big] + E_G\Big[-\log\big(1 - D_\theta(x)\big)\Big] \tag{8.6}$$

The generator loss can be defined in several similar ways, following is a common loss function that provides a strong gradient signal in the early stages of generator training [36].

$$\mathcal{L}_G = E_G\Big[-\log D_\theta(x)\Big] + E_G\Big[\log\big(1 - D_\theta(x)\big)\Big] \tag{8.7}$$

For a fixed generator with a q density, the optimal discriminator value is $D^* = p(x)/(p(x) + q(x))$ [36]. Representing p with a parametrized function p_θ, and defining discriminator output as follows, where $q(x)$ is filled in with its known values, θ parameters can be learned through GAN training [30].

$$D_\theta(x) = \frac{p_\theta(x)}{p_\theta(x) + q(x)} \tag{8.8}$$

8.2.2 Maximum Entropy Inverse Reinforcement Learning

Considering the MDP formulation of the BOI problem, the historical bidding data of an electricity market participant can be assembled into a set of multiple bidding trajectories $\mathcal{D}^h = \{\tau_1^h, ..., \tau_n^h\}$, where each bidding trajectory (may also be called demonstration trajectory) is a sequence of states and actions $\tau^h = (s_0, a_0, ..., s_T, a_T)$. Given a historical bidding trajectory τ^h of a market participant which is assumed to act near-optimally, IRL seeks the bidding objective function underlying the demonstrated behavior[58]. MaxEnt IRL associates Boltzmann distribution to the historical trajectory stating that the probability of each trajectory is exponentially related to its reward value under maximum entropy hypothesis[87].

$$p_\theta(\tau^h) = \frac{1}{Z} \exp\big(r_\theta(\tau^h)\big) \tag{8.9}$$

Where r_θ is the bidding objective parameterized by θ, and Z is a partition function, integral of $\exp(r_\theta(\tau^h))$ over the set of historical bidding trajectories $\mathcal{D}^h = \{\tau_1^h, ..., \tau_N^h\}$, ensuring that sum of all probabilities is equal to one. Under this model, the IRL problem can be interpreted as solving a maximum likelihood problem and have the following loss function.

$$\mathcal{L}(\theta) = E_{\mathcal{D}^h}\big[-\log(p_\theta(\tau^h))\big] = E_{\mathcal{D}^h}\big[-r_\theta(\tau^h)\big] + \log Z \tag{8.10}$$

For large or continuous action and state spaces, like the BOI problem, partition function Z estimation is computationally difficult or even intractable. As a result, existing works [38, 73, 72] have reduced the BOI problem to the discrete domain and computed Z directly with dynamic programming similar to the first application of MaxEnt IRL [87].

Guided Cost Learning

Guided cost learning (GCL)[31] overcomes the Z estimation challenge by training a sampling distribution $q(\tau)$, which learns demonstrations density, and samples from it for estimating Z in the MaxEnt IRL. Once having the sampling distribution $q(\tau)$, based on (8.9), the Z in the MaxEnt IRL loss function (8.10) can be replaced by $E_q[\frac{\exp(r_\theta(\tau))}{q(\tau)}]$. However, the trained distribution $q(\tau)$ may have poor coverage over demonstrations in the early stages of training and cause high variance in sampling. This issue can be addressed by drawing samples from a mixture of currently learned demonstration density $\tilde{p}_\theta(\tau)$ and sampling distribution $q(\tau)$. Let this mixture distribution be $\xi(\tau) = \frac{1}{2}\tilde{p}_\theta(\tau) + \frac{1}{2}q(\tau)$, thus the GCL loss function is as follows.

$$\mathcal{L}(\theta) = E_{\mathcal{D}^h}\big[-r_\theta(\tau^h)\big] + \log\left(E_\xi\left[\frac{\exp\big(r_\theta(\tau)\big)}{\xi(\tau)}\right]\right) \tag{8.11}$$

The sampler learns the demonstrations' distribution, so its goal is minimizing the KL divergence between $q(\tau)$ and $\frac{1}{Z}\exp(r_\theta(\tau))$ and have the following loss function. Note that $E_q[\log Z]$ is omitted in the sampler's loss function as it is a parameter of IRL and is fixed for sampler training.

$$\mathcal{L}(q) = D_{KL}\big(q(\tau)||p_\theta(\tau)\big) = E_q\big[\log q(\tau) - r_\theta(\tau)\big] \tag{8.12}$$

GCL algorithm alternate between optimizing these two loss functions, (8.11) and (8.12), in order to solve the IRL problem. The next section paraphrases how our BOI problem with continuous action and state spaces can be solved through AIRL[32], resembling the GCL approach for solving MaxEnt IRL.

8.3 Adversarial Inverse Reinforcement Learning for Bidding Objective Identification

Solving BOI problem through AIRL casts optimization of (8.11) as a GAN training. We can define the discriminator output as (8.13), where the probability of each

state and action is exponentially associated with their reward value similar to maximum entropy hypothesis and replaced as real data (historical data) distribution p_θ in (8.8). Also, the generator's distribution of (8.8) q is represented by the policy structure $\pi(a|s)$ that was introduced in Section 8.1.3. We show that GAN training over this definition of discriminator resembles solving the GCL MaxEnt IRL for BOI of a electricity market participant.

$$D_\theta(s,a) = \frac{\exp\big(r_\theta(s,a)\big)}{\exp\big(r_\theta(s,a)\big) + \pi_\alpha(a|s)} \tag{8.13}$$

8.3.1 Discriminator Training

Substituting discriminator's loss function (8.6) with (8.13), and defining a mixture distribution as $\xi = \frac{1}{2}\mathcal{D}^h + \frac{1}{2}\pi_\alpha$, we have.

$$\begin{aligned}
\mathcal{L}_D(\theta) =& \sum_{t=0}^{T} E_{\mathcal{D}^h}\Big[-\log \frac{\exp\big(r_\theta(s,a)\big)}{\exp\big(r_\theta(s,a)\big) + \pi_\alpha(a|s)}\Big] + \\
& E_{\pi_\alpha}\Big[-\log \frac{\pi_\alpha(a|s)}{\exp\big(r_\theta(s,a)\big) + \pi_\alpha(a|s)}\Big] \\
=& \sum_{t=0}^{T} E_{\mathcal{D}^h}\Big[-r_\theta(s_t,a_t)\Big] + E_{\pi_\alpha}\Big[-\log\big(\pi_\alpha(a_t|s_t)\big)\Big] + \\
& 2E_\xi\Big[\log\big(\exp\big(r_\theta(s_t,a_t)\big) + \pi_\alpha(a_t|s_t)\big)\Big]
\end{aligned} \tag{8.14}$$

Taking derivative of $\mathcal{L}_D$ w.r.t θ,

$$\frac{\partial}{\partial\theta}\mathcal{L}_D(\theta) = \sum_{t=0}^{T} E_{\mathcal{D}^h}\Big[-\frac{\partial}{\partial\theta} r_\theta(s_t,a_t)\Big] + E_\xi\left[\frac{2\exp\big(r_\theta(s_t,a_t)\big)}{\exp\big(r_\theta(s_t,a_t)\big) + \pi_\alpha(a_t|s_t)}\frac{\partial}{\partial\theta} r_\theta(s_t,a_t)\right] \tag{8.15}$$

Multiplying top and button of the second expression in (8.15) by the state marginal $\pi_\alpha(s_t) = \int_a \pi_\alpha(s_t,a_t)$, and rearranging terms results in.

$$\frac{\partial}{\partial\theta}\mathcal{L}_D(\theta) = \sum_{t=0}^{T} E_{\mathcal{D}^h}\Big[-\frac{\partial}{\partial\theta} r_\theta(s_t,a_t)\Big] + E_{\hat{\xi}}\left[\frac{\hat{p}_{\theta,t}(s_t,a_t)}{\frac{1}{2}\hat{p}_\theta(s_t,a_t) + \frac{1}{2}\pi_\alpha(s_t,a_t)}\frac{\partial}{\partial\theta} r_\theta(s_t,a_t)\right] \tag{8.16}$$

Where $\hat{p}_{\theta,t}(s_t, a_t) = \exp(r_\theta(s_t, a_t))\pi_\alpha(s_t)$, and $\hat{\xi}$ denotes a mixture of policy π_α and $\hat{p_\theta}$ as it is written in the denominator of the second expression.

On the other hand, by taking the derivative of the GCL loss function (8.11) w.r.t θ, we have:

$$\frac{\partial}{\partial\theta}\mathcal{L}(\theta) = E_{\mathcal{D}^h}\Big[-\frac{\partial}{\partial\theta}r_\theta(\tau^h)\Big] + E_\xi\Big[\frac{\frac{1}{Z}\exp\big(r_\theta(\tau)\big)}{\xi(\tau)}\frac{\partial}{\partial\theta}r_\theta(\tau)\Big] \tag{8.17}$$

Expanding the reward function over states and actions $r_\theta(\tau) = \sum_{t=0}^{T} r_\theta(s_t, a_t)$, we can rewrite the above equation as (8.18), where $p_\theta(s_t, a_t) = \int_{s_{i\neq t}, a_{i\neq t}} p_\theta(\tau)$ denotes the state-action marginal at time t. Note that ξ is a mixture of p_θ and q as written in the denominator of the second expression.

$$\frac{\partial}{\partial\theta}\mathcal{L}(\theta) = \sum_{t=0}^{T} E_{\mathcal{D}^h}\Big[-\frac{\partial}{\partial\theta}r_\theta(s_t, a_t)\Big] + E_\xi\Big[\frac{p_\theta(s_t, a_t)}{\frac{1}{2}p_\theta(s_t, a_t) + \frac{1}{2}q(s_t, a_t)}\frac{\partial}{\partial\theta}r_\theta(s_t, a_t)\Big] \tag{8.18}$$

In (8.16), as π_α reaches optimality, we have $\hat{p}_\theta(s, a) = p_\theta(s, a)$. Hence, if we show that training the sampler q in GCL is equivalent to the generator training (policy π_α optimization) in AIRL, we can show that (8.16) and (8.18) are equivalent.

8.3.2 Generator Training

Replacing D_θ in (8.7) with the discriminator definition of AIRL (8.13), results in equation (8.19). As the generator is the policy network for the BOI problem, the following loss function is similar to passing $[\log D_\theta(s_t, a_t) - \log(1 - D_\theta(s_t, a_t))]$ as a reward to the policy optimizer (PPO).

$$\begin{aligned}\mathcal{L}_G &= \sum_{t=0}^{T} E_{\pi_\alpha}\Big[-\log\frac{\exp\big(r_\theta(s, a)\big)}{\exp\big(r_\theta(s, a)\big) + \pi_\alpha(a|s)} + \log\frac{\pi_\alpha(a|s)}{\exp\big(r_\theta(s, a)\big) + \pi_\alpha(a|s)}\Big] \\ &= \sum_{t=0}^{T} E_{\pi_\alpha}\big[\log\pi_\alpha(a_t|s_t) - r_\theta(s_t, a_t)\big]\end{aligned} \tag{8.19}$$

It is apparent that equation (8.19) matches (8.12) once the bidding objective is extended over states and actions, with π_α serving as q. Subsequently, it leads to the

equivalency of (8.16) and (8.18) as discussed before, which proves that solving the BOI problem through AIRL resembles MaxEnt IRL GCL. Note that, unlike GCL, AIRL is not trajectory-centric and is applied over the state and action pairs, which leads to a more efficient learning process [32].

Based on the GAN concept [36], once AIRL converges to the optimal solution, discriminator output is equal to 0.5, hence $r^*_\theta(s,a) = \log \pi^*_\alpha(a|s)$. Also, knowing that $\log \pi(a|s) = A(s,a)$, we can learn the advantage function of a market participant by solving the BOI problem through AIRL. Although the advantage function is a valid reward (bidding objective) for a RL agent (market participant in BOI problem) to optimize, this bidding objective is highly dependent on the dynamics of the market environment as advantage evaluates each action based on the baseline policy. Hence, the current setting for BOI encourages mimicking historical bidding trajectories. Learning a robust bidding objective that can lead to the desired behavior even with changes in the market environment is our goal in this work. The next section describes how we can learn a robust bidding objective using AIRL through a specific structure of the r_θ, and state and action space definitions.

8.3.3 Identifying a Robust Bidding Objective with AIRL

A bidding objective is robust or disentangled from the market environment if changes in the environment do not affect the optimal policy (desired behavior) resulting from optimizing the bidding objective. For example, consider a storage unit that does energy arbitrage in the electricity market. The observed bidding behavior of it in a typical afternoon-peaking market is charging in the morning and discharging in the afternoon. Learning the underlying bidding objective of such behavior, we want the bidding objective to always lead to a policy that charges in hours with high prices and discharges in low-price hours regardless of the time of the day. Thus, optimizing

this robust bidding objective in a morning-peaking market will still lead to energy arbitrage behavior.

The reward shaping concept [57] states that without any prior knowledge of the environment, the following reward transformation is the only class of reward transformation that leads to policy invariance. It means that optimal policy learned over r and $\hat{r}$ are similar for any shaping function $\Phi : \mathcal{S} \to \mathbb{R}$.

$$\hat{r}(s, a, \acute{s}) = r(s, a, \acute{s}) + \gamma\Phi(\acute{s}) - \Phi(s) \tag{8.20}$$

This concept was initially introduced to improve policy convergence by shaping the reward, but it also falls in the robust reward definition that we are pursuing here. However, this structure is not sufficient for learning a robust reward [32]. based to the disentangled reward theorems [32, Theorem 5.1 and 5.2], we have.

Corollary 1 *Given that the ground-truth bidding objective is only function of the state variables, and electricity market environment dynamic $\mathcal{T}$ satisfies the decomposability condition, identified bidding objective, with a structure similar to* (8.20)*, is disentangled from the environment if and only if it is solely function of the state variables.*

For Corollary 1 to hold, we need to prove the following statements.

Lemma 1 *Ground-truth bidding objective of an electricity market participant can be only function of the state variables.*

proof 1 *The bidding objective of a market participant is only function of the state variables if all information regarding its bidding behavior is modeled through state variables, even if they can be modeled as actions. Hence, the bidding objective being solely function of the state variables is entirely dependent on the MDP formulation of the problem. To paraphrase, consider a self-scheduling unit with a simple bidding*

objective which is the multiplication of its dispatched power and electricity price. The MDP of this unit's market participation can be modeled in two different ways. One way is defining the state space as $\mathcal{S} = [\lambda_t]$, and the action space as $\mathcal{A} = [a_t^p]$, where in each time interval t, λ_t is the electricity price and a_t^p is the unit's quantity offer in the market. The bidding objective under this definition is $r_t(s, a) = \lambda_t a_t^p$. The other MDP formulation variant has a similar action space, but a new variable, dispatched power, is added to the state space $\mathcal{S} = [\lambda_t, P_t]$. The bidding objective becomes $r_t(s) = \lambda_t P_t$. The simple change in the state space definition of the later MDP resulted in a state-only bidding objective, and following such methodology in MDP formulation proves this lemma.

Lemma 2 *The state transition distribution $\mathcal{T}$ of the electricity market environment satisfies the decomposability condition.*

proof 2 *A state transition distribution $\mathcal{T}$ satisfies the decomposability condition if the probability of transitioning from state s to s' by taking action a, $p(s'|s, a)$, through an interim state s'' can be decomposed into $p(s'|s, a) = p(s''|s, a) \times p(s'|s'', a)$. This condition is inherent in Markov properties [71] and is satisfied for the state transition distribution $\mathcal{T}$ of the electricity market environment as long as all states are linked with all other states. All states being linked means there is no state that is impossible to leave under any action (absorbing state). Such an absorbing state never happens unless the BOI problem is terminated and the market participant stops bidding in the market, which proves this lemma.*

Replacing the discriminator definition of (8.13) with the following equation.

$$D_{\theta,\phi}(s, a, \acute{s}) = \frac{\exp\big(f_{\theta,\phi}(s, \acute{s})\big)}{\exp\big(f_{\theta,\phi}(s, \acute{s})\big) + \pi_\alpha(a|s)} \tag{8.21}$$

$$\text{where } f_{\theta,\phi}(s, \acute{s}) = r_\theta(s) + \gamma h_\phi(\acute{s}) - h_\phi(s)$$

we can see that $f_{\theta,\phi}$ resembels the structure of (8.20) by having the shaping term h_ϕ. Also, the bidding objective $r_\theta(s)$ is a state-only function. Hence, based on Corollary 1 and lemmas 1 and 2, the identified bidding objective under this new definition of discriminator (8.21) is robust from changes in the environment.

8.4 Framework and Algorithm of AILR-BOI Method

Previous sections defined the main elements of the BOI problem through AIRL and paraphrased its concept. This section provides an overview of the AIRL-BOI framework to better describe how these elements interact with each other under the AIRL methodology to identify the bidding objective of an electricity market participant through its historical bidding data. Subsequently, the algorithm of the proposed AIRL-BOI framework is proposed along with augmentations for convergence improvement.

8.4.1 Framework of the AIRL-BOI Method

Fig. 8.1 depicts a schematic of the AIRL-BOI method. In this figure, the orange block represents the historical bidding data from which the market participant's underlying bidding objective (i.e., reward function) will be identified. Being historical, these data are superscripted with h. Building upon the adversarial training methodology, the AIRL-BOI method has a generator and discriminator pieces. The generator (shown in blue) is an RL agent with the defined policy structure π_α that maximizes its bidding objective through interactions with EME, while its bidding objective values come from the discriminator (shown in green). The value function V_v that involves in PPO is also part of the generator. The policy (agent) samples are superscripted with π. Historical bidding data and policy samples along with their actions' probability evaluated with the current policy are fed into the discriminator

where the bidding objective function is identified through the training of two NNs for the bidding objective r_θ and shaping term h_ϕ.

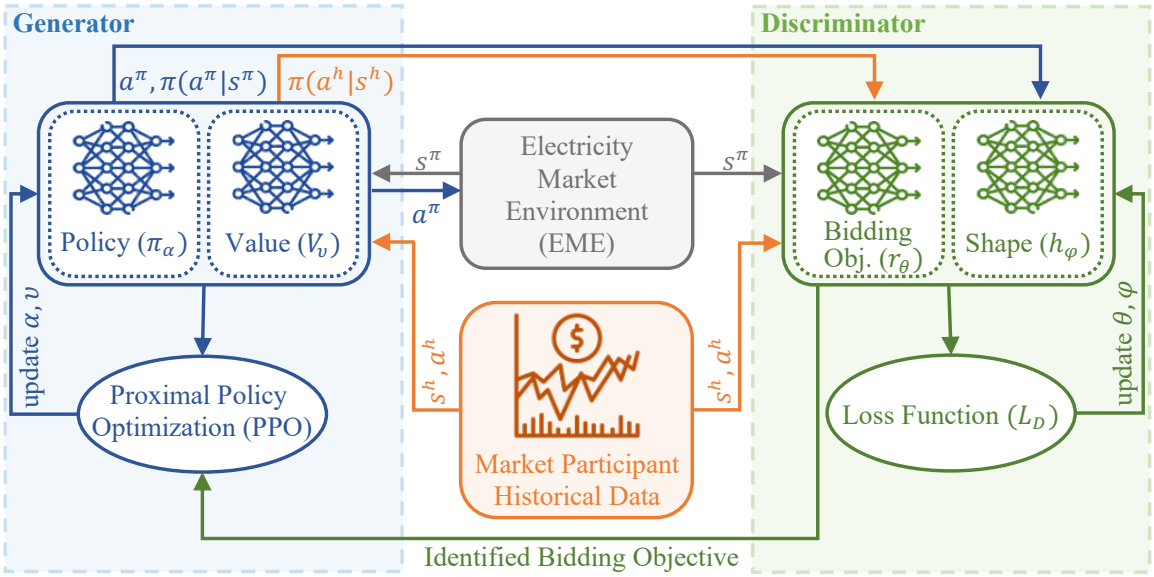

Figure 8.1: Framework of the AIRL-BOI Method.

It is worth mentioning that as the generator is a direct RL model, it is used in the case study section of this paper for evaluating the reward functions that are learned with the AIRL-BOI method. It is also used for generating bidding trajectories using a known bidding objective.

8.4.2 Algorithm of the AIRL-BOI Method

The entire training procedure for BOI of an electricity market participant through AIRL is detailed in Algorithm 2. The algorithm alternates between training a discriminator $D_{\theta,\phi}$ to classify historical bidding trajectories $\mathcal{D}^h$ from policy samples $\mathcal{D}^\pi$, and updating the proposed policy π_α through PPO to confuse the discriminator. Upon convergence, the algorithm outputs the robust bidding objective r_θ underlying market participant's historical bidding data and the optimal policy π_α^*. The policy structure π_α and EME model, besides value function V and PPO are the main elements that

interact through the AIRL-BOI method, and all of them have been discussed in previous sections. Despite their powerful performance, adversarial algorithms like AIRL can be hard to train [52]. Hence, several stabilizing methods have been augmented into the AIRL for the BOI algorithm to improve training and convergence, which are discussed below.

Algorithm 2 AIRL-BOI

Obtain historical bidding trajectories $\mathcal{D}^h = \{\tau_1^h, ..., \tau_n^h\}$
Initialize π_α, V_υ, $D_{\theta,\phi}$, EME, and $\mathcal{B}$
for episode in $\{1, ..., N\}$ **do**
    Collect $\mathcal{D}^\pi = \{\tau_1^\pi, ..., \tau_m^\pi\}$ by executing π_α in EME
    Store $\mathcal{D}^\pi$ in the buffer $\mathcal{B} \leftarrow \mathcal{D}^\pi$
    for epoch in $\{1, ..., N_d\}$ **do**
        update discriminator parameters θ, ϕ using the gradient of (8.22) over samples from $\mathcal{D}^h$ and $\mathcal{B}$
    end for
    Assign reward values to $\mathcal{D}^\pi$ using the current $D_{\theta,\phi}$
    $r(s, a, \acute{s}) \leftarrow \log D_{\theta,\phi}(s, a, \acute{s}) - \log(1 - D_{\theta,\phi}(s, a, \acute{s}))$
    for epoch in $\{1, ..., N_{ppo}\}$ **do**
        Update policy and value function parameters α, υ according to $r(s, a, \acute{s})$ with PPO method
    end for
end for

Policy Sample Expansion

At each discriminator training epoch of the original AIRL algorithm, parameters are updated using the gradient of loss function calculated over samples from historical

trajectories $\mathcal{D}^h$ and the most recent trajectories of the policy $\mathcal{D}^\pi$. Using recent $\mathcal{D}^\pi$ may overfit the discriminator on the latest policy samples and hence the bidding objective will not provide good training signals for the policy optimizer. As a result, neither the discriminator nor the policy will converge. To improve the BOI algorithm, similar to the background sampling in GCL [31], we used a buffer $\mathcal{B}$ to store policy samples $\mathcal{D}^\pi$ of the last k training episodes, and the discriminator is trained over samples from the buffer $\mathcal{B}$, instead of latest $\mathcal{D}^\pi$, and the expert data $\mathcal{D}^h$. Thus, it is provided with earlier learner data and will not overfit on the latest policy.

Gradient Penalty

There exists a rich literature on adversarial learning methods for stabilizing training and improving convergence [52]. Adding noise to the discriminator's input for smoothing probability distributions and avoiding overfitting is a wildly suggested empirical approach for convergence improvement. Kevin et al. [63] have shown that the addition of a zero-centered gradient penalty to the discriminator loss function is equivalent to training with the addition of noise to the input.

To enhance the training stability of the AIRL-BOI algorithm, we applied a zero-centered gradient penalty to the discriminator loss function, which the original AIRL algorithm [32] does not have. This noise-induced regularization method smooths the probability distributions and improves training stability by penalizing the discriminator for deviating from the nash-equilibrium [63]. Hence, equation (8.14) is changed to the following loss function to include the gradient penalty. Note that r_θ is replaced with $f_{\theta,\phi}$ based on the robustness section's discussion, and ω is the penalty weight.

$$\mathcal{L}_D(\theta,\phi) = \sum_{t=0}^{T} E_{\mathcal{D}^h}\Big[- f_{\theta,\phi}(s_t, \acute{s}_t)\Big] - E_{\pi_\alpha}\Big[\log\big(\pi_\alpha(a_t|s_t)\big)\Big]$$

$$+ 2E_{\xi}\Big[\log\big(\exp\big(f_{\theta,\phi}(s_t, \acute{s}_t)\big) + \pi_{\alpha}(a_t|s_t)\big)\Big]$$
$$+ \frac{\omega}{2}E_{\mathcal{D}}\Big[\nabla_s g_{\theta}(s) + \nabla_{\acute{s}} h_{\phi}(\acute{s}) + \nabla_s h_{\phi}(s)\Big] \tag{8.22}$$

Chapter 9

CASE STUDIES

This chapter evaluates the accuracy of the proposed method for bidding objective identification of electricity market participants and also verifies that the identified bidding objectives are robust from changes in the electricity market environment. Three independent case studies are designed in this section to generate historical bidding data for market participants and subsequently apply AIRL-BOI to identify the bidding objective. To the best of our knowledge, this is the first work in the field of BOI through IRL that its accuracy is validated against a known bidding objective. In the following, The first case study represents the application of the proposed AIRL-BOI method from the ISO perspective with full knowledge of the system, while the second one solves the BOI problem from a market participant standpoint with limited access to the market data. Finally, the third case study shows the application of the proposed method equipped with the designed policy structure on real-world market data with minimum data pre-processing and no discretization.

9.1 First Test Case

This case study is performed using simulated data of a market participant in a small grid model. Knowing the true bidding objective behind simulated demonstration trajectories, along with the simplicity of the model enables us to illustratively compare the identified bidding objective with the true one and assess the AIRL-BOI method's accuracy. Additionally, we are able to design the grid model such that there exists a unique optimal action for maximizing true bidding objectives, which is not common in continuous domain problems. Having a unique optimal action helps

us further evaluate the AIRL-BOI method by examining whether identified bidding objective guides the agent to the only possible optimal action or not.

Initially, the AIRL-BOI method is applied to the simulated bidding trajectories and the identified bidding objective is compared with the true one. Subsequently, the optimal actions that maximize true and identified bidding objectives are compared with each other. Finally, the identified bidding objective is used in a new grid model with changed parameters to verify that it is robust against the environment's changes. Details of this case study are described below.

9.1.1 Test Case and AILR-BOI Algorithm Information

EME Model

As it was mentioned, there are two different grid models in this case study. Grid model 1 is used for simulating the historical bidding data, and grid model 2 is used for identified bidding objective robustness verification.

Gird model 1 is a single node system with five different generators, which their operational parameters are presented in Table 9.1. The load in this model has a yearly peak of 1 GWh, and the load shape is mapped from the California ISO historical data [11].

The grid model 2 of this case study is shown in Figure 9.1. As this grid model is used to verify the bidding objective robustness, the grid structure and generator parameters are completely changed to make a new EME. The identified bidding objective is used over this grid model to verify that its results are similar to the true bidding objective. In grid model 2, the minimum power capacity of generators is zero and their maximum power is provided in Figure 9.1. Blue arrows in Figure 9.1 show the share of each bus in the total load of the system while the load shape is similar to

Table 9.1: Generators Parameters in Grid Model 1 of the First Test Case.

Generator Name	Minimum Power (MW)	Maximum Power (MW)	Generation Cost ($/MWh)
G1	0	200	10
G2	0	140	25
G3	0	160	60
G4	0	400	100
G5	0	600	8

gird model 1. All transmission lines have the same susceptance and their flow limit is written in Figure 9.1.

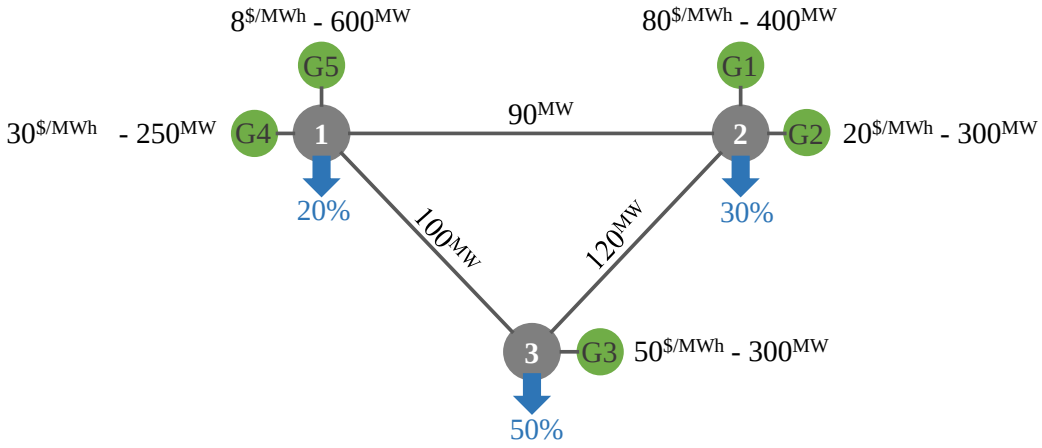

Figure 9.1: Grid/Market Structure of the Grid Model 2 in the First Test Case.

The proposed exact EME model (Section 8.1.2) is implemented using these grid models information. Generator 5 (G5) is the under-study market participant and its historical bidding trajectories are simulated for BOI. Hence, the EME model gets the action of G5, solves DC-OPF, and returns the state variables. It is assumed that all other market participants offer their maximum capacity and generation cost in the market.

State and Action Spaces

The state space of this case study is $\mathcal{S} = [P_t, \lambda_t, L_t]$, which are respectively dispatched power of G5, the price at the bus 1, and system total load at each time step t. Additionally, the action space contains a pair of power capacity and price offer for G5 in each time step $\mathcal{A} = [(a_t^p, a_t^\lambda)]$, while the price offer a_t^λ is always fixed at G5's generation cost.

Demonstration Trajectories

For simulating historical bidding trajectories, it is assumed that G5 has full knowledge of the system and its bidding problem is formulated through a bi-level optimization model, where G5's profit maximization is the upper-level problem and grid model (DC-OPF) is the lower-level problem similar to the Part I frameworks. Thus, G5 acts strategically by curtailing its capacity for manipulating market prices and maximizing its profit in various hours. Details on the bi-level optimization modeling and its solving procedure are presented in Part I of the dissertation.

Hyperparameters

In this test case, $\pi_\alpha, V_\upsilon, r_\theta, h_\phi$ are two-layer fully connected NNs with 20 hidden nodes per layer. The activation function of π_α is tanh, while V_υ has a linear activation function, and r_θ, h_ϕ has leaky ReLU for activation function. The length of τ^π and τ^h is 120 steps (five days), and buffer $\mathcal{B}$ size is 1. Other parameters of the AIRL-BOI algorithm are: $n = 600, m = 10, N = 500, N_d = 5, N_{ppo} = 40, \omega = 0, \gamma = 0.8, \epsilon = 0.2$.

9.1.2 Results

The identified bidding objective is compared with the true one in Figure 9.2. For depicting these figures, the state resulting from the G5's action in various loads of the

system is sent to the learned r_θ, and the output is compared with the true bidding objective value of the state (revenue minus generation cost). All reward shapes of this dissertation are depicted in normalized values for simplicity.

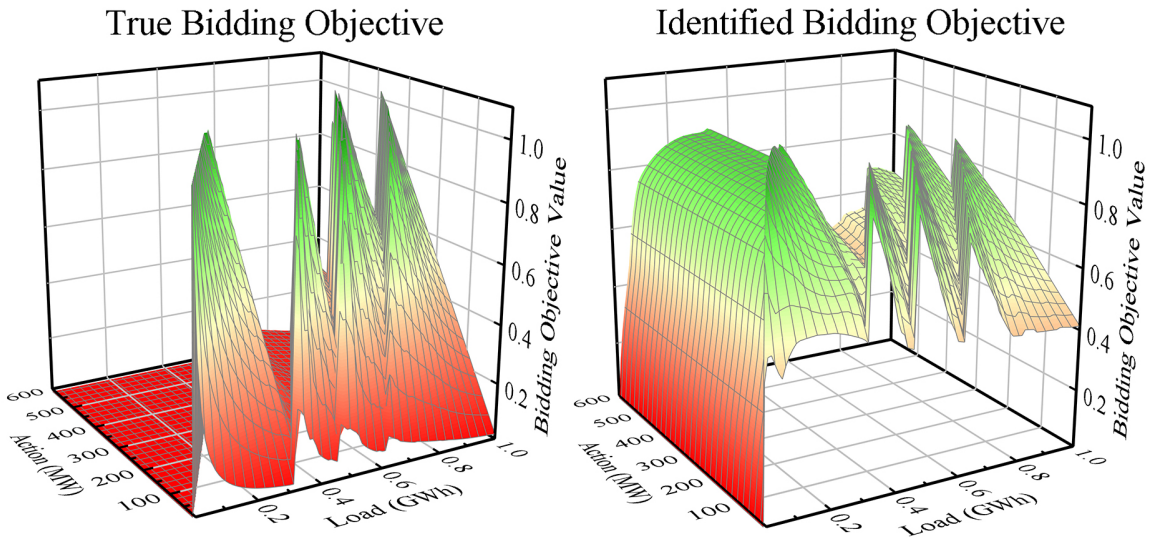

Figure 9.2: Identified and True Bidding Objectives in Model 1 of the First Test Case.

Figure 9.2 shows that the shape of the identified and true bidding objectives are very similar to each other. Note that the bidding objective value of each state relative to the others is the distinguishing factor that guides the agent. Hence, the identified bidding objective does not necessarily need to have the exact same shape as the true objective. It only needs to prioritize different states, resulting from actions, similar to the true one, even if it does not have an exactly similar shape. Considering this, Figure 9.2 shows that AIRL-BOI identifies bidding objectives with high accuracy.

The bidding objective identification accuracy is better shown in Figure 9.3, where optimal actions resulting from identified and true bidding objectives in the model 1 grid are depicted. These optimal actions are found through a search algorithm resembling greedy policy search methods. For each load value, the G5's actions are swiped to find the action with the highest state bidding objective value associated

with it under the identified and true objectives.

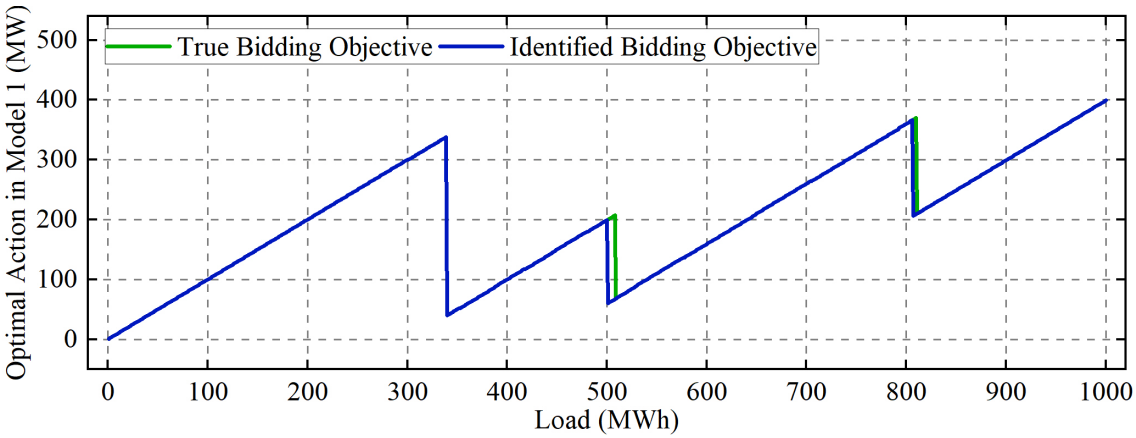

Figure 9.3: Optimal Actions Resulted from Ground-truth and Learned Rewards in the Grid Model 1 of the First Test Case.

The grid in Model 1 is a single-node market, and G5's price offer is equal to its generation cost, which is the lowest in the grid, hence the optimal action (quantity offer) for G5 is curtailing its capacity for keeping prices at the highest possible values to maximize its profit. The sudden action drops in Figure 9.3 happen at load values that G5's profit can be increased by curtailing capacity and forcing higher prices. According to this figure, the identified bidding objective optimal action is almost always similar to the true one, which is the only unique optimal action in this model. This action accuracy emphasizes the precision of the AIRL-BOI method.

In order to evaluate the robustness of the identified bidding objective, the learned objective over historical bidding trajectories of model 1 is applied to the grid model 2. Figure 9.4 compares the identified bidding objective shape in this model against the true one. Note that identified and true bidding objectives do not change between Figure 9.2 and Figure 9.4. The states resulting from the actions of the G5 are different in this new environment, which leads to different bidding objective shapes. We can see that the identified bidding objective is prioritizing states similar to the true objective even if their shapes are not exactly similar. It shows that the identified objective is

robust against changes in the environment and performs similarly to the true objective in a new environment.

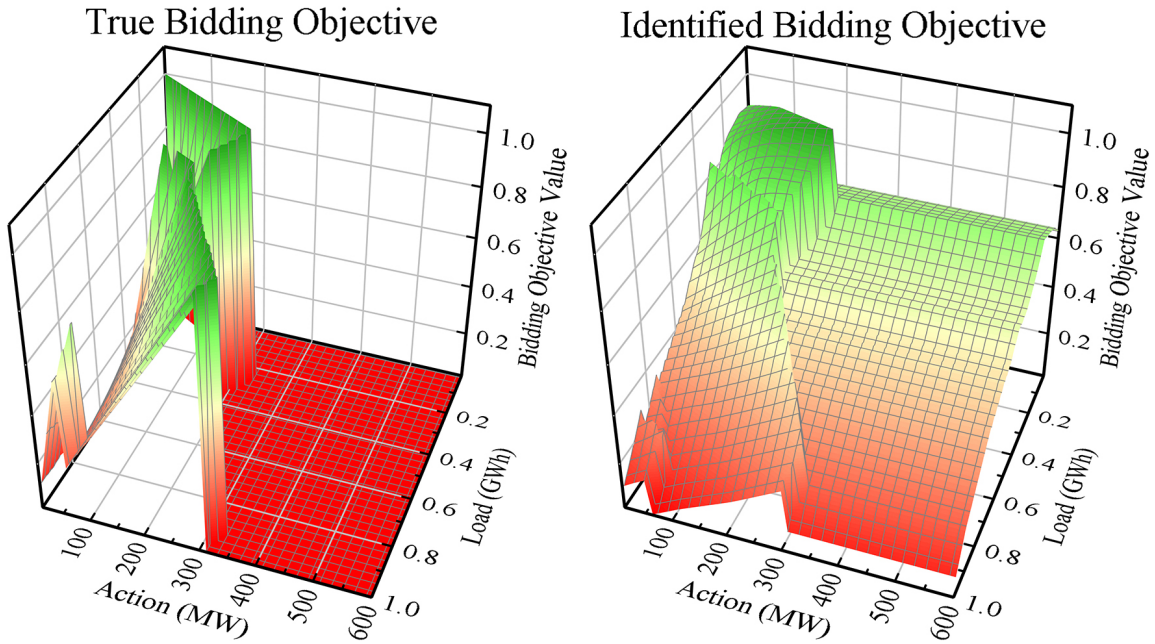

Figure 9.4: Identified and True Bidding Objectives in Model 2 of the First Test Case.

The robustness is further evaluated in the bottom figure of Figure 9.5 by comparing the resulting optimal action from these bidding objectives. In the grid of model 2, not only the operation parameters of other generators have changed, but also the transmission lines have flow limits and congestion may happen. Hence, G5 may affect the congestion part of energy price in addition to the generation cost part of it by performing curtailment. The parts with the negative slope in Figure 9.5 are curtailment actions that are happening to keep the transmission lines congested and causing higher prices. It is apparent in this figure that except for a short period the identified bidding objective results in the exact optimal action as the true objective, which accentuates the fact that AIRL-BOI identifies robust bidding objectives.

This test case is a good example of the AIRL-BOI method's application from the ISO perspective. It shows that an operator with full knowledge of the system can

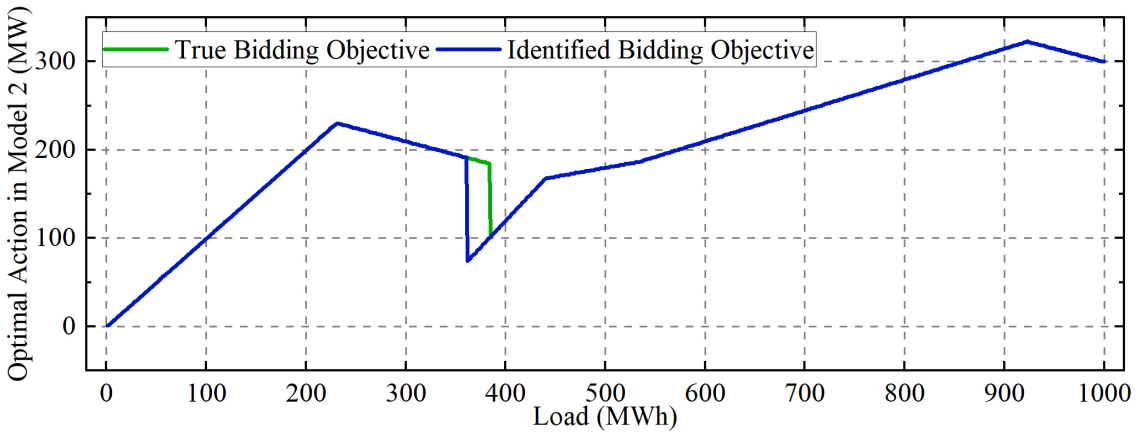

Figure 9.5: Optimal Actions Resulted from Ground-truth and Learned Rewards in the Grid Model 2 of the First Test Case.

find the bidding objective of market participants accurately to inspect their bidding behavior. Also, as the identified bidding objective is robust, the operator can use it for analyzing market participants' behavior under changes in the market or gird e.g. addition of a transmission line.

9.2 Second Test Case

This case study further evaluates the performance of the AIRL-BOI method by examining it over bidding trajectories that are simulated with a sophisticated objective in a real-world market model. In this test case, simulated bidding data of a price-taker energy storage unit that performs energy arbitrage in the ISO New England (ISO-NE) market is fed into the AIRL-BOI to learn the bidding objective. Unlike the previous test case, an illustrative comparison of objectives is not possible here due to the complexity of the model and bidding objective. Hence, similar to other works in the IRL field [14], identified bidding objective is used to train an agent in a direct RL algorithm (the blue part of Figure8.1 with identified bidding objective as the reward), and the optimal policy/action of it is compared with simulated trajectories to evaluate the performance of the AIRL-BOI method. Additionally, both identified and

true bidding objectives are used for training an agent in a different market (PJM) to analyze the robustness of the learned bidding objective. Test case components and results are presented below.

9.2.1 Test Case and AILR-BOI Algorithm Information

State and Action Spaces

The state space, in this study, is $\mathcal{S} = [P_t, \lambda_t, SOC_t]$, where P_t is the dispatched power of storage in the interval t and may change in $[-125, 125]$ as it can charge (buy) or discharge (sell), λ_t is the market price at storage's bus, and the storage's SOC is the last variable in $\mathcal{S}$ which cannot be more than storage capacity 500 MWh. Being a price-taker market participant, the action space $\mathcal{A} = [a_t^p]$ only contains power capacity offer of storage in each time step, which has similar limits as P_t.

EME Model

The proposed simplified EME model (Section 8.1.2) is used in this case study as the energy storage unit is a price-taker, and having a more complex EME model is redundant. In each interval, once the EME model gets the storage action a_t^p, it determines P_t according to (9.1), where η is the charge or discharge efficiency, and because of being a price-taker the equation states that the dispatched power of storage is equal to its offer unless it is limited by its SOC. Accordingly, $SOC_t = SOC_t + P_t$, and λ_t comes from the market data that EME is implemented on them. Historical (2019, 2020, 2021) energy prices of ISO-NE [12] and PJM [13] are used for implementing these ISOs' EME models in this test case. For PJM's EME model, the prices are shifted to have a morning-peaking system in contrast to the ISO-NE, and

evaluate robustness over more extreme environment changes.

$$P_t = \begin{cases} \eta^c \min(a_t^p, 500 - SOC_{t-1}), & \text{if } a_t^p \geq 0 \\ \frac{1}{\eta^d} \max(a_t^p, SOC_{t-1} - 500), & \text{if } a_t^p < 0 \end{cases} \tag{9.1}$$

Demonstration Trajectories

Historical bidding trajectories of this case study are generated by solving the direct RL problem for the storage in the ISO-NE EME using the following bidding objective, which is inspired by [83]. The direct RL implementation has been done through [61].

$$r_t = \begin{cases} -\beta P_t, & \text{if } P_t \geq 0 \\ (\lambda_t - C_t - \beta)|P_t|, & \text{if } P_t < 0 \end{cases} \tag{9.2}$$

where C_t represents the average cost of stored energy in the storage and calculates as follows, and storage's fixed wear and tear cost per MW is β.

$$C_{t+1} = \begin{cases} \frac{C_t SOC_t + \lambda_t P_t}{SOC_t + P_t}, & \text{if } P_t > 0 \\ C_t, & \text{if } P_t \leq 0 \end{cases} \tag{9.3}$$

Note that C_t only changes in the intervals with positive P_t, meaning that the average cost of stored energy updates whenever storage charges. According to (9.2), the storage bidding objective in charging hours is a negative value equal to its wear and tear, and in discharging hours, the objective can have a positive value if λ_t is higher than $C_t + \beta$. Hence, this bidding objective function guides the storage to perform energy arbitrage between hours. Note that the defined bidding objective is only a function of state variables as required by Corollary 1. The defined bidding objective is not only highly nonlinear but also it is dependent on previous hours λ_t and P_t through C_t, which adds to its complexity and makes it a good candidate for evaluating the AIRL-BOI method.

Hyperparameters

For this case study, $\pi_\alpha, V_\upsilon, r_\theta, h_\phi$ are modeled with two-layer fully connected tanh NNs with 64 nodes in each hidden layer, and π_α has tanh activation function also in its output layer. The length of τ^π and τ^h is 168 steps (one week), and $\mathcal{B}$'s size is 10. Other parameters of AILR-BOI method are: $n = 156, m = 10, N = 1000, N_d = 30, N_{ppo} = 80, \omega = 0, \gamma = 0.95, \beta = 0.75, \eta^c = 0.9, \eta^d = 0.95, \epsilon = 0.2$.

9.2.2 Results

To assess the performance of the AIRL-BOI method, the actions of an agent trained on identified bidding objective are compared with the actions of an agent trained on the true objective. Note that the later actions are historical bidding trajectories. These two sets of actions along with the ISO-NE prices over a sample week are demonstrated in Fig. 9.6.

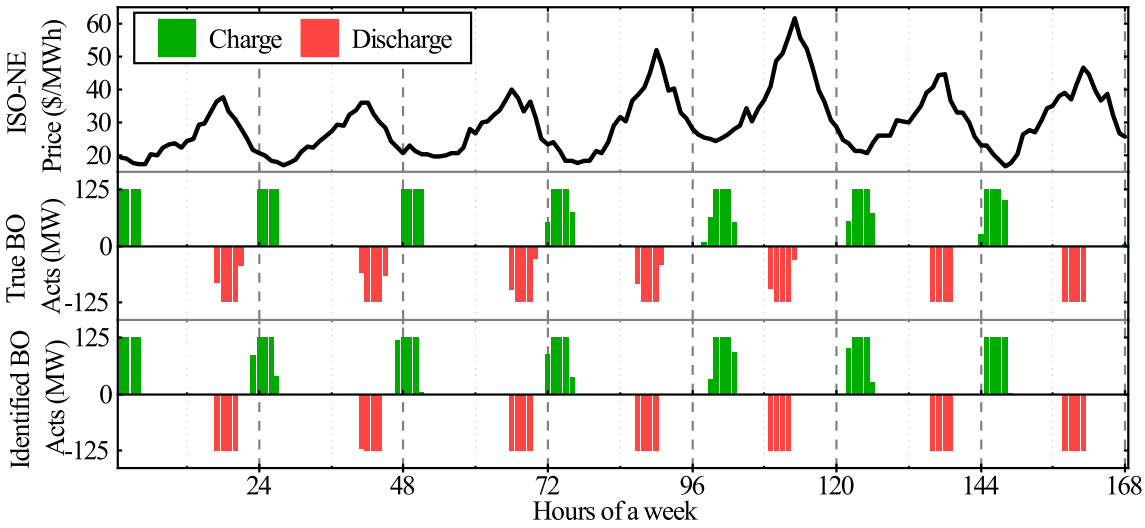

Figure 9.6: Actions (Acts) of a Storage Unit Trained with True and Identified Bidding Objectives (BOs) in ISO-NE Market over an Example Week.

Both agents in Fig. 9.6 perform energy arbitrage across hours. In contrast to the first test case, we do not expect the actions of these two agents to be exactly

similar as it is rare for policy optimizers to reach global optimality in problems with continuous action domains like this test case. However, we expect the identified bidding objective to guide the policy toward the energy arbitrage behavior as the true objective is designed for this. Fig. 9.6 clearly shows that identified bidding objective has high accuracy since the agent trained with it performs energy arbitrage very similar to the historical data.

To verify the robustness of the identified BO, the objective learned from the bidding trajectories of energy storage in ISO-NE is used for training an agent in the PJM market with shifted prices to a morning-peaking system. This agent's actions along with the actions of an agent trained with true objective are shown in Fig. 9.7. This figure shows that both agents wait for the first price valley to charge and perform energy arbitrage from that point on. Although the agents' actions are not identical, both are performing energy arbitrage in very similar ways in this new market. These results show that the identified bidding objective is robust and guides the agent to the desired behavior even in a market with different price ranges, shapes, and patterns.

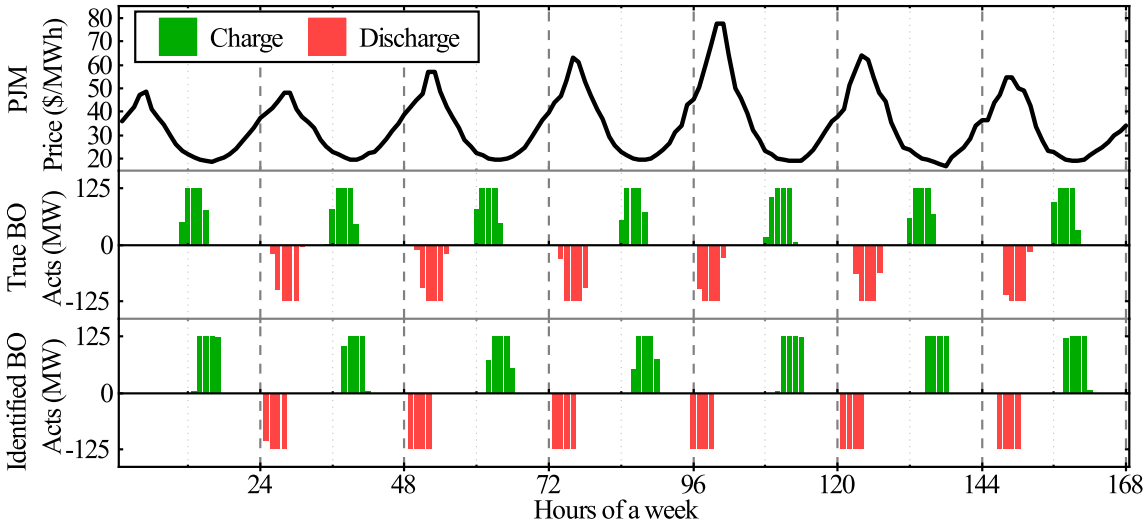

Figure 9.7: Actions (Acts) of a Storage Unit Trained with True and Identified Bidding Objectives (BOs) in PJM Market over an Example Week.

The second test case shows that the AIRL-BOI method identifies sophisticated and nonlinear bidding objectives with high accuracy and robustness. Also, this test case provides a good example of the proposed method's application for a non-ISO user. One with limited access to market data may still use the proposed framework to identify the bidding objective of a market participant and inform its own bidding strategy or imitate a desired behavior.

9.3 Third Test Case

Previous case studies elaborately assessed the performance of the AIRL-BOI method over different bidding objectives and EME models. This test case extends the studies to BOI of real-world market participants in the Midcontinent ISO (MISO) market using the AIRL-BOI method.

9.3.1 Test Case and AILR-BOI Algorithm Information

EME Model

Having limited access to the MISO market data, the proposed simplified EME model is used in this test case, where the participants' bids do not affect market prices. For each market participant, the EME model is implemented around its historical bidding data. Knowing the market price of each hour t from the historical data, the EME model only clears the agent's offer for the segments if their offering prices are less than the market price. Each EME model's accuracy is verified over historical offers of the participant to make sure that EME's outcome is the same as the historical market data.

State and Action Spaces

The state space of this test case is defined as $\mathcal{S} = [P_t, \lambda_t, L_t, P_t^{max}]$, where the first three variables are similar to the previous test cases. The new state variable P_t^{max} is the maximum available power capacity of a market participant, which is available in historical data and may affect the bidding strategy. Also, P_t^{max} is needed in the output filter of the proposed policy structure in (8.2). The action space of each market participant is $\mathcal{A} = [(a_1^{MW}, a_1^{\$}), ..., (a_k^{MW}, a_k^{\$})]$, where $a_\cdot^{MW}$ and $a_\cdot^{\$}$ can be any positive real number less than their limit for the power and price. The number of offer segments k is different for each participant, but k cannot be more than 10 in the MISO market.

Demonstration Trajectories

A year-long historical bidding data of two market participants in the MISO's energy market [3] is used in this test case. The masked unit codes of these market participants are 11098 and 8689 and their historical data contains their offers, the resulting dispatched powers, and energy prices at their buses. These data sets are arranged to make trajectories based on defined state and action spaces and omit data points with poor EME model performance.

Hyperparameters

For each market participant, $V_\upsilon, r_\theta, h_\phi$ are represented with two-layer fully connected tanh NNs with 64 nodes in each hidden layer, while π_α has the same structure but sigmoid activation function for all layers including the output layer. The length of τ^π and τ^h is 168 steps (one week), and $\mathcal{B}$'s size if 20. Other parameters of AILR-BOI method are: $n_{11098} = 45, n_{8689} = 40, m = 10, N = 2000, N_d = 25, N_{ppo} = 80, \omega = 0.1, \gamma = 0.9, \epsilon = 0.2, k = 2$.

9.3.2 Results

The identified bidding objectives of units 11098 and 8689 are presented respectively in Fig. 9.8 and Fig. 9.9. The price axis of these figures changes between 10 to 60 $/MWh as historical prices fall mostly in this range, and the power axis range is set according to each unit's minimum and maximum capacity.

Similar to the previous test case, identified bidding objectives are used to train a direct RL agent in their corresponding MISO EME models. Subsequently, the error between agents' resulting dispatch and historical data measures the BOI accuracy. The mean absolute percentage error (MAPE) between historical data and the RL agents' dispatch are 5.79% and 7.24% for units 11098 and 8689, respectively. Thus, the low error values ensure the accuracy of the identified bidding objectives.

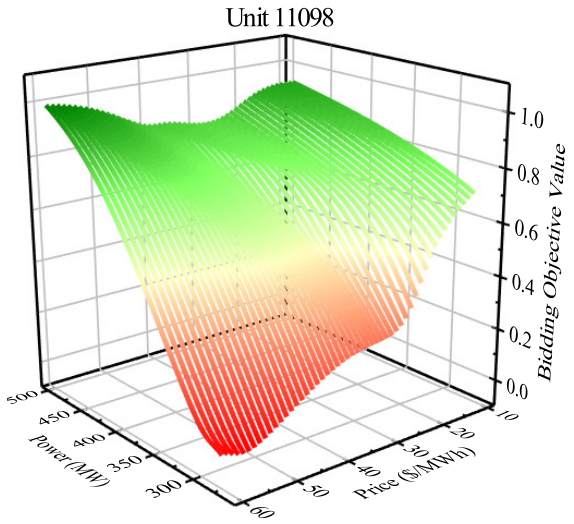

Figure 9.8: Identified Bidding Objective of Units 11098 in MISO Market.

Fig. 9.8 shows that at all prices, unit 11098 prefers to be dispatched at the highest output power. This is a valid bidding objective shape for a unit with low marginal generation cost, hence the objective promotes higher output power to gain more profit. Additionally, the slope of bidding objective across the power axis significantly increases as the prices get higher. That is, the difference between bidding

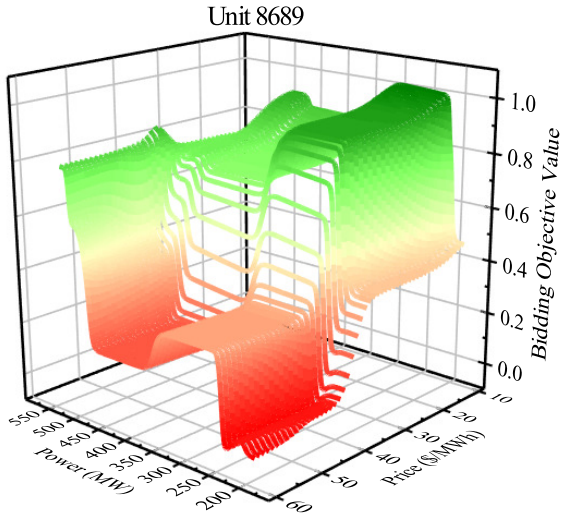

Figure 9.9: Identified Bidding Objective of Units 8689 in MISO Market.

objective values at 150 MW and 485 MW with 60 $/MWh price is much more than the corresponding difference with 10 $/MWh price. This observation is genuine as selling one more MW at 60 $/MWh price yields higher revenue than selling one more MW at 10 $/MWh price.

In contrast to unit 11098, the bidding objective of unit 8689 does not always have the highest bidding objective values at the maximum output power. Based on Fig. 9.9, for prices less than 30 $/MWh, the highest objective value for unit 8689 happens at 300 MW power. This observation means that the cost of generating above 300 MW is more than its revenue unless the price is higher than 30 $/MWh. Similar to the other unit, the difference between bidding objective value of minimum and maximum output power for unit 8689 is the most when the price is 60 $/MWh.

The third test case shows that the proposed AIRL-BOI method can be applied to real-world data without discretization and with minimum data preprocessing to identify the bidding objective of actual market participants. This is an advantage over existing methods that not only ease the application of this approach in the real-world but also eliminate the risk of information loss due to discretization.

Chapter 10

CONCLUSION AND FUTURE WORKS

This section concludes the second part of the dissertation dealing with the bidding objective identification (BOI) of electricity market participants through adversarial inverse reinforcement learning (AIRL). Directions for future work in this field are also depicted in this section.

10.1 Conclusion

This part of the dissertation presented a data-driven framework for BOI in the electricity market through AIRL. The proposed AIRL-BOI is the first deep IRL method in this area that directly works with continuous state and action spaces, without the need for discretization. Also, the proposed method is the first work in the field of RL that complies with electricity market bidding rules. Hence, the historical bidding data of market participants can be used in the proposed AIRL-BOI with a minimum amount of pre-processing, which reduces the chance of information loss in discretization and provides application-wise advantages in the real world.

The proposed method is a model-free RL approach which means that the bidding objective identification process is independent of the environment model. Hence, this approach may be used in any market by using an appropriate market model. This work proposed two different market modeling approaches to be used in the AIRL-BOI algorithm. These electricity market environment (EME) models may be used based on the data availability and complexity of the BOI problem. The exact EME model is suitable for the cases in that BOI is solved by one who has full knowledge of the system like an ISO. On the other hand, the simplified EME model is a suitable option

for solving BOI from a market participant perspective with limited data availability.

The unique bidding rules of electricity markets separate them from all other types of markets and hence affect the RL application in them. To the best of our knowledge, the proposed policy in this work is the first structure whose design is informed by the electricity market monotonicity rules. Hence, the application of the proposed policy structure in this dissertation expands beyond the AIRL-BOI method.

For the first time in the field of BOI with IRL, this work provides theoretical proof for the robustness of identified bidding objectives from the changes in the electricity market environment. Thus, the bidding objective identified through AIRL-BOI may be used in a different market or grid structure for simulating a similar bidding strategy. This advantage expands the application of this method in various analyses. For example, an ISO may use the identified bidding objective through AIRL-BOI to study the bidding behavior of its market participants under market or grid structure changes. Also, a market participant may use this method to transfer knowledge from a desired bidding behavior into its own bidding strategy.

Finally, the performance of the proposed AIRL-BOI method is extensively evaluated over synthetic and real-world data from different ISOs on various assumptions and data availability scenarios. The case studies show the accuracy and robustness of the identified bidding objectives and provide a diverse set of examples for the AIRL-BOI method's application in various scenarios in the electricity market.

10.2 Future Works

This part of the dissertation addressed several of the most important shortcomings of the existing literature in the field of BOI through IRL and paved the path for future investigation in this area. As a result, some of the possible future work directions are depicted here.

The proposed AIRL-BOI method is focused on the energy market, while a market participant may bid in various day-ahead and real-time energy markets as well as ancillary services markets. Further investigation on the application of the proposed method across various markets is needed. Also, some changes and augmentation may be needed to the proposed method to expand it into a multi-market field. Further research in this direction forfeits the benefits of a data-driven bidding objective identification method in electricity markets.

The proposed AIRL-BOI algorithm is built upon the single-agent RL concept. However, electricity markets can be better modeled through multi-agent RL approaches. Hence, future research work may expand the proposed method into multi-agent AIRL-BOI. Considering all other market participants in a multi-agent approach may not be possible, but modeling some of the prominent participants with multi-agent RL can improve the accuracy of bidding objective identification.

Finally, the proposed AIRL-BOI method can be expanded into a multi-task BOI method. In the multi-task IRL, it is assumed that an observed behavior may serve several goals (objectives) and hence reward functions associated with each of the goals are learned. Although, the identified bidding objective through the proposed method covers all possible goals of a market participant, identifying these goals separately can improve BOI accuracy and expand its applications. This multi-task BOI research direction may be combined with the first future research direction mentioned above about the application of AILR-BOI in various markets.

REFERENCES

[1] "California ISO", URL https://www.caiso.com/Documents/MSC-FinalOpinion-Pay-for-PerformanceRegulation.pdf (2012).

[2] "Simulated Automatic Generator Control (AGC) Setpoint Data", URL https://www.iso-ne.com/isoexpress/web/reports/grid/-/tree/simulated-agc (2014).

[3] "MISO market data", URL https://rb.gy/rtk4eq (2016).

[4] "Growth of battery storage for renewable energy", URL https://ihsmarkit.com/topic/growth-battery-storage-for-renewable-energy.html (2017).

[5] "Lithium-ion batteries for large-scale grid energy storage", URL https://researchinterfaces.com/lithium-ion-batteries-grid-energy-storage (2018).

[6] "PJM market data", URL https://dataminer2.pjm.com/list (2018).

[7] "U.S. Battery Storage Market Trends", Tech. rep., U.S. Energy Information Administration (2018).

[8] "Battery energy storage technology overview and co-op case studies", Tech. rep., NRECA (2019).

[9] "RTS-GMLC: Reliability Test System—Grid Modernization Lab Consortium", URL https://github.com/GridMod/RTS-GMLC (2019).

[10] "U.s. utility-scale battery storage power capacity to grow substantially by 2023", URL https://www.eia.gov/todayinenergy/detail.php?id=40072 (2019).

[11] "CAISO market data", URL https://rb.gy/qlp52 (2020).

[12] "ISO-NE market data", URL https://rb.gy/vylqai (2021).

[13] "PJM market data", URL https://rb.gy/066puv (2021).

[14] Arora, S. and P. Doshi, "A survey of inverse reinforcement learning: Challenges, methods and progress", Artificial Intelligence **297**, 103500 (2021).

[15] Arteaga, J. and H. Zareipour, "A price-maker/price-taker model for the operation of battery storage systems in electricity markets", IEEE Transactions on Smart Grid **10**, 6, 6912–6920 (2019).

[16] Atwa, Y. M. and E. F. El-Saadany, "Optimal allocation of ess in distribution systems with a high penetration of wind energy", IEEE Transactions on Power Systems **25**, 4, 1815–1822 (2010).

[17] Barrows, C., A. Bloom, A. Ehlen, J. Ikaheimo, J. Jorgenson, D. Krishnamurthy, J. Lau, B. McBennett, M. O'Connell, E. Preston *et al.*, "The ieee reliability test system: A proposed 2019 update", IEEE Transactions on Power Systems (2019).

[18] Benasciutti, D. and R. Tovo, "Spectral methods for lifetime prediction under wide-band stationary random processes", International Journal of fatigue **27**, 8, 867–877 (2005).

[19] Bertsekas, D., *Dynamic programming and optimal control: Volume I*, vol. 1 (Athena scientific, 2012).

[20] Bian, Y., N. Zheng, Y. Zheng, B. Xu and Y. Shi, "Demand response model identification and behavior forecast with optnet: A gradient-based approach", in "Proceedings of the Thirteenth ACM International Conference on Future Energy Systems", pp. 418–429 (2022).

[21] BloombergNEF, "A behind the scenes take on lithium-ion battery prices", URL `https://about.bnef.com/blog/behind-scenes-take-lithium-ion-battery-prices` (2019).

[22] Chen, R., I. C. Paschalidis, M. C. Caramanis and P. Andrianesis, "Learning from past bids to participate strategically in day-ahead electricity markets", IEEE Transactions on Smart Grid **10**, 5, 5794–5806 (2019).

[23] Chen, X., G. Qu, Y. Tang, S. Low and N. Li, "Reinforcement learning for selective key applications in power systems: Recent advances and future challenges", IEEE Transactions on Smart Grid (2022).

[24] Cui, H., F. Li, X. Fang, H. Chen and H. Wang, "Bilevel arbitrage potential evaluation for grid-scale energy storage considering wind power and lmp smoothing effect", IEEE Transactions on Sustainable Energy **9**, 2, 707–718 (2017).

[25] Ecker, M., N. Nieto, S. Käbitz, J. Schmalstieg, H. Blanke, A. Warnecke and D. U. Sauer, "Calendar and cycle life study of li (nimnco) o2-based 18650 lithium-ion batteries", Journal of Power Sources **248**, 839–851 (2014).

[26] Environmental and Energy Study Institute (EESI), "Fact sheet: Energy storage", URL `https://www.eesi.org/papers/view/energy-storage-2019` (2019).

[27] Fatemi, A. and L. Yang, "Cumulative fatigue damage and life prediction theories: a survey of the state of the art for homogeneous materials", International journal of fatigue **20**, 1, 9–34 (1998).

[28] Federal Energy Regulatory Commission, "Order no. 755. frequency regulation compensation in the organized wholesale power markets", (2011).

[29] Federal Energy Regulatory Commission, "Order no. 841. electric storage participation in markets operated by regional transmission organizations and independent system operators", (2018).

[30] Finn, C., P. Christiano, P. Abbeel and S. Levine, "A connection between generative adversarial networks, inverse reinforcement learning, and energy-based models", arXiv preprint arXiv:1611.03852 (2016).

[31] Finn, C., S. Levine and P. Abbeel, "Guided cost learning: Deep inverse optimal control via policy optimization", in "International conference on machine learning", pp. 49–58 (PMLR, 2016).

[32] Fu, J., K. Luo and S. Levine, "Learning robust rewards with adversarial inverse reinforcement learning", arXiv preprint arXiv:1710.11248 (2017).

[33] Fu, R., T. W. Remo and R. M. Margolis, "2018 us utility-scale photovoltaics-plus-energy storage system costs benchmark", Tech. rep., National Renewable Energy Lab.(NREL), Golden, CO (United States) (2018).

[34] Gabriel, S. A., A. J. Conejo, J. D. Fuller, B. F. Hobbs and C. Ruiz, *Complementarity modeling in energy markets*, vol. 180, p. 250 (Springer Science & Business Media, 2012).

[35] Gabriel, S. A., A. J. Conejo, J. D. Fuller, B. F. Hobbs and C. Ruiz, *Complementarity modeling in energy markets*, vol. 180 (Springer Science & Business Media, 2012).

[36] Goodfellow, I., J. Pouget-Abadie, M. Mirza, B. Xu, D. Warde-Farley, S. Ozair, A. Courville and Y. Bengio, "Generative adversarial networks", Communications of the ACM **63**, 11, 139–144 (2020).

[37] Guo, H., Q. Chen, Y. Gu, M. Shahidehpour, Q. Xia and C. Kang, "A data-driven pattern extraction method for analyzing bidding behaviors in power markets", IEEE Transactions on Smart Grid **11**, 4, 3509–3521 (2019).

[38] Guo, H., Q. Chen, Q. Xia and C. Kang, "Deep inverse reinforcement learning for objective function identification in bidding models", IEEE Transactions on Power Systems **36**, 6, 5684–5696 (2021).

[39] Gurobi Optimization, LLC, "Gurobi optimizer reference manual", URL `http://www.gurobi.com` (2020).

[40] He, G., Q. Chen, C. Kang, P. Pinson and Q. Xia, "Optimal bidding strategy of battery storage in power markets considering performance-based regulation and battery cycle life", IEEE Transactions on Smart Grid **7**, 5, 2359–2367 (2016).

[41] Huang, Q., Y. Xu, T. Wang and C. A. Courcoubetis, "Market mechanisms for cooperative operation of price-maker energy storage in a power network", IEEE Transactions on Power Systems **33**, 3, 3013–3028 (2018).

[42] IBM ILOG, "Ibm ilog cplex optimization studio cplex user's manual", URL `https://www.ibm.com/analytics/cplex-optimizer` (2020).

[43] International Renewable Energy Agency (IRENA), "Electricity storage and renewables: Costs and markets to 2030", URL https://www.irena.org/publications/2017/Oct/Electricity-storage-and-renewables-costs-and-markets (2017).

[44] International Renewable Energy Agency (IRENA), "Electricity storage valuation framework", URL https://www.energy.gov/sites/prod/files/2019/07/f64/2018-OTT-Energy-Storage-Spotlight.pdf (2020).

[45] Kassem, M., J. Bernard, R. Revel, S. Pelissier, F. Duclaud and C. Delacourt, "Calendar aging of a graphite/lifepo4 cell", Journal of Power Sources **208**, 296–305 (2012).

[46] Kazemi, M. and H. Zareipour, "Long-term scheduling of battery storage systems in energy and regulation markets considering battery's lifespan", IEEE Transactions on Smart Grid **9**, 6, 6840–6849 (2018).

[47] Kazemi, M., H. Zareipour, N. Amjady, W. D. Rosehart and M. Ehsan, "Operation scheduling of battery storage systems in joint energy and ancillary services markets", IEEE Transactions on Sustainable Energy **8**, 4, 1726–1735 (2017).

[48] Khalilisenobari, R. and M. Wu, "Optimal participation of price-maker battery energy storage systems (BESSs) in energy, reserve and pay as performance regulation markets", in "51st North American power symposium", vol. 1, pp. 1–6 (2019).

[49] Korpaas, M., A. T. Holen and R. Hildrum, "Operation and sizing of energy storage for wind power plants in a market system", International Journal of Electrical Power & Energy Systems **25**, 8, 599–606 (2003).

[50] Laresgoiti, I., S. Käbitz, M. Ecker and D. U. Sauer, "Modeling mechanical degradation in lithium ion batteries during cycling: Solid electrolyte interphase fracture", Journal of Power Sources **300**, 112–122 (2015).

[51] Laresgoiti, I., S. Käbitz, M. Ecker and D. U. Sauer, "Modeling mechanical degradation in lithium ion batteries during cycling: Solid electrolyte interphase fracture", Journal of Power Sources **300**, 112–122 (2015).

[52] Mescheder, L., A. Geiger and S. Nowozin, "Which training methods for gans do actually converge?", in "International conference on machine learning", pp. 3481–3490 (PMLR, 2018).

[53] Mitra, J., "Reliability-based sizing of backup storage", IEEE Transactions on Power Systems **25**, 2, 1198–1199 (2010).

[54] Mohsenian-Rad, H., "Coordinated price-maker operation of large energy storage units in nodal energy markets", IEEE Transactions on Power Systems **31**, 1, 786–797 (2015).

[55] Mohsenian-Rad, H., "Optimal bidding, scheduling, and deployment of battery systems in california day-ahead energy market", IEEE Transactions on Power Systems **31**, 1, 442–453 (2015).

[56] Muenzel, V., J. de Hoog, M. Brazil, A. Vishwanath and S. Kalyanaraman, "A multi-factor battery cycle life prediction methodology for optimal battery management", in "Proceedings of the 2015 ACM Sixth International Conference on Future Energy Systems", pp. 57–66 (2015).

[57] Ng, A. Y., D. Harada and S. Russell, "Policy invariance under reward transformations: Theory and application to reward shaping", in "Icml", vol. 99, pp. 278–287 (1999).

[58] Ng, A. Y., S. Russell *et al.*, "Algorithms for inverse reinforcement learning.", in "Icml", vol. 1, p. 2 (2000).

[59] Oudalov, A., D. Chartouni and C. Ohler, "Optimizing a battery energy storage system for primary frequency control", IEEE Transactions on Power Systems **22**, 3, 1259–1266 (2007).

[60] Pudjianto, D., M. Aunedi, P. Djapic and G. Strbac, "Whole-systems assessment of the value of energy storage in low-carbon electricity systems", IEEE Transactions on Smart Grid **5**, 2, 1098–1109 (2014).

[61] Raffin, A., A. Hill, A. Gleave, A. Kanervisto, M. Ernestus and N. Dormann, "Stable-baselines3: Reliable reinforcement learning implementations", The Journal of Machine Learning Research **22**, 1, 12348–12355 (2021).

[62] Ramadesigan, V., P. W. Northrop, S. De, S. Santhanagopalan, R. D. Braatz and V. R. Subramanian, "Modeling and simulation of lithium-ion batteries from a systems engineering perspective", Journal of the electrochemical society **159**, 3, R31–R45 (2012).

[63] Roth, K., A. Lucchi, S. Nowozin and T. Hofmann, "Stabilizing training of generative adversarial networks through regularization", Advances in neural information processing systems **30** (2017).

[64] Ruetschi, P., "Aging mechanisms and service life of lead–acid batteries", Journal of power sources **127**, 1-2, 33–44 (2004).

[65] Sadeghi-Mobarakeh, A. and H. Mohsenian-Rad, "Optimal bidding in performance-based regulation markets: An mpec", IEEE Transactions on Power Systems **32**, 2, 1282–1292 (2017).

[66] Schillemans, A., G. D. V. Serrano and K. Bruninx, "Strategic participation of merchant energy storage in joint energy-reserve and balancing markets", in "Seminar on business models and regulation for storage, Date: 2018/11/30-2018/11/30, Location: Brussels, Belgium", (2018).

[67] Schulman, J., F. Wolski, P. Dhariwal, A. Radford and O. Klimov, "Proximal policy optimization algorithms", arXiv preprint arXiv:1707.06347 (2017).

[68] Shi, Y., B. Xu, D. Wang and B. Zhang, "Using battery storage for peak shaving and frequency regulation: Joint optimization for superlinear gains", IEEE Transactions on Power Systems **33**, 3, 2882–2894 (2018).

[69] Smart Electric Power Alliance (SEPA), "2019 utility energy storage market snapshot", URL `https://sepapower.org/resource/2019-utility-energy-storage-market-snapshot` (2019).

[70] Subramanya, R., S. Sierla and V. Vyatkin, "Exploiting battery storages with reinforcement learning: a review for energy professionals", IEEE Access (2022).

[71] Sutton, R. S. and A. G. Barto, *Reinforcement learning: An introduction* (MIT press, 2018).

[72] Tang, Q., H. Guo and Q. Chen, "Bidding strategy evolution analysis based on multi-task inverse reinforcement learning", Electric Power Systems Research **212**, 108286 (2022).

[73] Tang, Q., H. Guo and Q. Chen, "Multi-market bidding behavior analysis of energy storage system based on inverse reinforcement learning", IEEE Transactions on Power Systems **37**, 6, 4819–4831 (2022).

[74] U.S. Department of Energy (DOE), "The spotlight: Solving challenges in energy storage", URL `https://www.energy.gov/sites/prod/files/2019/07/f64/2018-OTT-Energy-Storage-Spotlight.pdf` (2019).

[75] Vatandoust, B., A. Ahmadian, M. A. Golkar, A. Elkamel, A. Almansoori and M. Ghaljehei, "Risk-averse optimal bidding of electric vehicles and energy storage aggregator in day-ahead frequency regulation market", IEEE Transactions on Power systems (2018).

[76] Vázquez-Canteli, J. R. and Z. Nagy, "Reinforcement learning for demand response: A review of algorithms and modeling techniques", Applied energy **235**, 1072–1089 (2019).

[77] Vetter, J., P. Novák, M. R. Wagner, C. Veit, K.-C. Möller, J. Besenhard, M. Winter, M. Wohlfahrt-Mehrens, C. Vogler and A. Hammouche, "Ageing mechanisms in lithium-ion batteries", Journal of power sources **147**, 1-2, 269–281 (2005).

[78] Weng, L., "A (long) peek into reinforcement learning", lilianweng.github.io URL `https://lilianweng.github.io/posts/2018-02-19-rl-overview/` (2018).

[79] Weng, L., "Policy gradient algorithms", lilianweng.github.io/lil-log URL `https://lilianweng.github.io/lil-log/2018/04/08/policy-gradient-algorithms.html` (2018).

[80] Xu, B., Y. Dvorkin, D. S. Kirschen, C. A. Silva-Monroy and J.-P. Watson, "A comparison of policies on the participation of storage in us frequency regulation markets", in "2016 IEEE Power and Energy Society General Meeting (PESGM)", pp. 1–5 (IEEE, 2016).

[81] Xu, B., A. Oudalov, A. Ulbig, G. Andersson and D. S. Kirschen, "Modeling of lithium-ion battery degradation for cell life assessment", IEEE Transactions on Smart Grid **9**, 2, 1131–1140 (2016).

[82] Xu, B., J. Zhao, T. Zheng, E. Litvinov and D. S. Kirschen, "Factoring the cycle aging cost of batteries participating in electricity markets", IEEE Transactions on Power Systems **33**, 2, 2248–2259 (2017).

[83] Xu, H., X. Li, X. Zhang and J. Zhang, "Arbitrage of energy storage in electricity markets with deep reinforcement learning", arXiv preprint arXiv:1904.12232 (2019).

[84] Yao, D. L., S. S. Choi, K. J. Tseng and T. T. Lie, "A statistical approach to the design of a dispatchable wind power-battery energy storage system", IEEE Transactions on Energy Conversion **24**, 4, 916–925 (2009).

[85] Zhao, H., J. Zhao, J. Qiu, G. Liang, F. Wen, Y. Xue and Z. Y. Dong, "Data-driven risk preference analysis in day-ahead electricity market", IEEE Transactions on Smart Grid **12**, 3, 2508–2517 (2020).

[86] Zidar, M., P. S. Georgilakis, N. D. Hatziargyriou, T. Capuder and D. Škrlec, "Review of energy storage allocation in power distribution networks: applications, methods and future research", IET Generation, Transmission Distribution **10**, 3, 645–652 (2016).

[87] Ziebart, B. D., A. L. Maas, J. A. Bagnell, A. K. Dey *et al.*, "Maximum entropy inverse reinforcement learning.", in "Aaai", vol. 8, pp. 1433–1438 (Chicago, IL, USA, 2008).

[88] Zou, P., Q. Chen, Q. Xia, G. He and C. Kang, "Evaluating the contribution of energy storages to support large-scale renewable generation in joint energy and ancillary service markets", IEEE Transactions on Sustainable Energy **7**, 2, 808–818 (2015).

APPENDIX A

CONVERSION OF THE DETAILED FRAMEWORK TO MILP

This section explains the whole procedure of converting the detailed model, presented in Chapter 3, to a MILP. The model formulation is re-written below. The ULP equations are indexed with U and, L is used for the LLP equations.

Upper-level Problem:

$$\text{Max} \sum_{t\in\mathcal{T}}\sum_{i\in\mathcal{B}}\Big\{\Big[\pi^{E}_{i,t}P^{B,E}_{i,t}+\pi^{Rs}_{t}P^{B,Rs}_{i,t}+\pi^{RgC}_{t}P^{B,RgC}_{i,t}+\pi^{RgM}_{t}P^{B,RgM}_{i,t}\Big]\Delta t- \sum_{z\in\mathcal{Z}}\sum_{k\in\mathcal{K}}C^{Deg}_{i,k}P^{Dis}_{i,t,z,k}\Delta z\Big\} \tag{U.1}$$

Subject to:

$$-P^{Rate}_{i}\leq O^{E}_{i,t}\leq P^{Rate}_{i} \qquad \forall i\in\mathcal{B},\forall t\in\mathcal{T} \tag{U.2}$$

$$0\leq O^{Rs}_{i,t}\leq P^{Rate}_{i} \qquad \forall i\in\mathcal{B},\forall t\in\mathcal{T} \tag{U.3}$$

$$0\leq O^{RgC}_{i,t}\leq P^{Rate}_{i} \qquad \forall i\in\mathcal{B},\forall t\in\mathcal{T} \tag{U.4}$$

$$-P^{Rate}_{i}+P^{B,RgC}_{i,t}\leq P^{B,E}_{i,t}\leq P^{Rate}_{i}-P^{B,RgC}_{i,t}-P^{B,Rs}_{i,t} \qquad \forall i\in\mathcal{B},\forall t\in\mathcal{T} \tag{U.5}$$

$$PF_{i,t}=\frac{P^{B,RgM}_{i,t}}{R^{RgM}_{t}} \qquad \forall i\in\mathcal{B},\forall t\in\mathcal{T} \tag{U.6}$$

$$\sum_{i\in\mathcal{B}}PF_{i,t}\leq 1 \qquad \forall t\in\mathcal{T} \tag{U.7}$$

$$P^{B,E}_{i,t}+PF_{i,t}AGC_{t,z}=P^{TDis}_{i,t,z}-P^{TCh}_{i,t,z} \qquad \forall i\in\mathcal{B},\forall t\in\mathcal{T},\forall z\in\mathcal{Z} \tag{U.8}$$

$$0\leq P^{TDis}_{i,t,z}\leq v_{i,t,z}P^{Rate}_{i} \qquad \forall i\in\mathcal{B},\forall t\in\mathcal{T},\forall z\in\mathcal{Z} \tag{U.9}$$

$$0\leq P^{TCh}_{i,t,z}\leq (1-v_{i,t,z})P^{Rate}_{i} \qquad \forall i\in\mathcal{B},\forall t\in\mathcal{T},\forall z\in\mathcal{Z} \tag{U.10}$$

$$P^{TDis}_{i,t,z}(\frac{1}{\eta_i})=\sum_{k\in\mathcal{K}}P^{Dis}_{i,t,z,k} \qquad \forall i\in\mathcal{B},\forall t\in\mathcal{T},\forall z\in\mathcal{Z} \tag{U.11}$$

$$P^{TCh}_{i,t,z}\eta_i=\sum_{k\in\mathcal{K}}P^{Ch}_{i,t,z,k} \qquad \forall i\in\mathcal{B},\forall t\in\mathcal{T},\forall z\in\mathcal{Z} \tag{U.12}$$

$$P^{Ch}_{i,t,z,k},P^{Dis}_{i,t,z,k}\geq 0 \qquad \forall i\in\mathcal{B},\forall t\in\mathcal{T},\forall z\in\mathcal{Z},\forall k\in\mathcal{K} \tag{U.13}$$

$$e_{i,t,z,k}-e_{i,t,z-1,k}=(P^{Ch}_{i,t,z,k}-P^{Dis}_{i,t,z,k})\Delta z \qquad \forall i\in\mathcal{B},\forall t\in\mathcal{T},\forall z\neq 1\in\mathcal{Z},\forall k\in\mathcal{K} \tag{U.14}$$

$$e_{i,t,z,k}-e_{i,t-1,\bar{z},k}=(P^{Ch}_{i,t,z,k}-P^{Dis}_{i,t,z,k})\Delta z \qquad \forall i\in\mathcal{B},\forall t\in\mathcal{T},\tau=1,\forall k\in\mathcal{K} \tag{U.15}$$

$$0 \leq e_{i,t,z,k} \leq e_{i,k}^{Max} \qquad \forall i \in \mathcal{B}, \forall t \in \mathcal{T}, \forall z \in \mathcal{Z}, \forall k \in \mathcal{K} \text{ (U.16)}$$

$$SOC_i^{Min} + (P_{i,t}^{B,Rs} \Delta t) \leq \sum_{k \in \mathcal{K}} e_{i,t,z,k} \leq SOC_i^{Max} \qquad \forall i \in \mathcal{B}, \forall t \in \mathcal{T}, \forall z \in \mathcal{Z} \text{ (U.17)}$$

$$\sum_{k \in \mathcal{K}} e_{i,t,z,k} = SOC_i^{Init} \qquad \forall i \in \mathcal{B}, t = 0 \,\&\, z = \bar{z}, t = \bar{t} \,\&\, z = \bar{z} \text{ (U.18)}$$

$$v_{i,t,z} \in \{0,1\} \qquad \forall i \in \mathcal{B}, \forall t \in \mathcal{T}, \forall z \in \mathcal{Z} \text{ (U.19)}$$

Lower-level Problem:

$$\text{Min} \sum_{t \in \mathcal{T}} \Big[\sum_{j \in \mathcal{G}} \big(\alpha_{j,t}^{E} P_{j,t}^{G,E} + \alpha_{j,t}^{Rs} P_{j,t}^{G,Rs} + \alpha_{j,t}^{RgC} P_{j,t}^{G,RgC} + \alpha_{j,t}^{RgM} P_{j,t}^{G,RgM} \big) + \sum_{i \in \mathcal{B}} \big(\beta_{i,t}^{E} P_{i,t}^{B,E} + \beta_{i,t}^{Rs} P_{i,t}^{B,Rs} + \beta_{i,t}^{RgC} P_{i,t}^{B,RgC} + \beta_{i,t}^{RgM} P_{i,t}^{B,RgM} \big) \Big] \Delta t \text{ (L.1)}$$

Subject to:

$$P_j^{Min} + P_{j,t}^{G,RgC} \leq P_{j,t}^{G,E} \leq P_j^{Max} - P_{j,t}^{G,Rs} - P_{j,t}^{G,RgC} : [\delta_{j,t}^{min}, \delta_{j,t}^{max}] \qquad \forall j \in \mathcal{G}, \forall t \in \mathcal{T} \text{ (L.2)}$$

$$0 \leq P_{j,t}^{G,Rs} \leq P_j^{Rs,ramp} : [\epsilon_{j,t}^{min}, \epsilon_{j,t}^{max}] \qquad \forall j \in \mathcal{G}, \forall t \in \mathcal{T} \text{ (L.3)}$$

$$0 \leq P_{j,t}^{G,RgC} \leq P_j^{Rg,ramp} : [\varphi_{j,t}^{min}, \varphi_{j,t}^{max}] \qquad \forall j \in \mathcal{G}, \forall t \in \mathcal{T} \text{ (L.4)}$$

$$P_{j,t}^{G,RgC} \leq P_{j,t}^{G,RgM} \leq m_{j,t} P_{j,t}^{G,RgC} : [\gamma_{j,t}^{min}, \gamma_{j,t}^{max}] \qquad \forall j \in \mathcal{G}, \forall t \in \mathcal{T} \text{ (L.5)}$$

$$-O_{i,t}^{E} \leq P_{i,t}^{B,E} \leq O_{i,t}^{E} : [\xi_{i,t}^{min}, \xi_{i,t}^{max}] \qquad \forall i \in \mathcal{B}, \forall t \in \mathcal{T} \text{ (L.6)}$$

$$0 \leq P_{i,t}^{B,Rs} \leq O_{i,t}^{Rs} : [\rho_{i,t}^{min}, \rho_{i,t}^{max}] \qquad \forall i \in \mathcal{B}, \forall t \in \mathcal{T} \text{ (L.7)}$$

$$0 \leq P_{i,t}^{B,RgC} \leq O_{i,t}^{RgC} : [\lambda_{i,t}^{min}, \lambda_{i,t}^{max}] \qquad \forall i \in \mathcal{B}, \forall t \in \mathcal{T} \text{ (L.8)}$$

$$P_{i,t}^{B,RgC} \leq P_{i,t}^{B,RgM} \leq m_{i,t} P_{i,t}^{B,RgC} : [\mu_{i,t}^{min}, \mu_{i,t}^{max}] \qquad \forall i \in \mathcal{B}, \forall t \in \mathcal{T} \text{ (L.9)}$$

$$\sum_{j \in \mathcal{G}} P_{j,t}^{G,Rs} + \sum_{i \in \mathcal{B}} P_{i,t}^{B,Rs} \geq R_t^{Rs} : [\pi_t^{Rs}] \qquad \forall t \in \mathcal{T} \text{ (L.10)}$$

$$\sum_{j \in \mathcal{G}} P_{j,t}^{G,RgC} + \sum_{i \in \mathcal{B}} P_{i,t}^{B,RgC} \geq R_t^{RgC} : [\pi_t^{RgC}] \qquad \forall t \in \mathcal{T} \text{ (L.11)}$$

$$\sum_{j \in \mathcal{G}} P_{j,t}^{G,RgM} + \sum_{i \in \mathcal{B}} P_{i,t}^{B,RgM} \geq R_t^{RgM} : [\pi_t^{RgM}] \qquad \forall t \in \mathcal{T} \text{ (L.12)}$$

$$\sum_{j\in\mathcal{G}|j=n} P^{G,E}_{j,t} + \sum_{i\in\mathcal{B}|i=n} P^{B,E}_{i,t} = P^{Load}_{n,t} + \sum_{w\in\mathcal{N}} H_{nw}(\theta_{n,t} - \theta_{w,t}) : [\pi^{E}_{n,t}]$$

$$\forall n \in \mathcal{N}, \forall t \in \mathcal{T} \text{ (L.13)}$$

$$-TL_{nw} \leq H_{nw}(\theta_{n,t} - \theta_{w,t}) \leq TL_{nw} : [\omega^{min}_{nw,t}, \omega^{max}_{nw,t}] \qquad \forall (n,w) \in \mathcal{L}, \forall t \in \mathcal{T} \text{ (L.14)}$$

The LLP is a linear optimization as the bids of BESS are not variables for this problem. So, the KKT conditions of the LLP are necessary and sufficient to ensure its optimality. Hence, by including KKT conditions of the LLP as constraints for the ULP, it is possible to convert this problem into a single-level optimization. The associated dual variable of each LLP's constraint is written in front of the constraint in a bracket. It can be observed that most of the constraints have two dual variables with *min* and *max* superscripts as each of these constraints consists of two inequality conditions. The *min* superscripts are used for the inequality conditions corresponding to the lower limits, and similarly *max* superscripts are used for the upper limits. The KKT conditions of the LLP are as follows, note that the n subscript of the energy market price (π^E) is changed to i or j when it is applicable to represent the price at the bus of the BESS unit or other market participants' buses.

Primal Feasibility:

(L.2) - (L.14)

Stationary:

$$\alpha^{E}_{j,t} - \delta^{min}_{j,t} + \delta^{max}_{j,t} - \pi^{E}_{j,t} = 0 \qquad \forall j \in \mathcal{G}, \forall t \in \mathcal{T} \text{ (A.1)}$$

$$\alpha^{Rs}_{j,t} + \delta^{max}_{j,t} - \epsilon^{min}_{j,t} + \epsilon^{max}_{j,t} - \pi^{Rs}_{t} = 0 \qquad \forall j \in \mathcal{G}, \forall t \in \mathcal{T} \text{ (A.2)}$$

$$\alpha^{RgC}_{j,t} + \delta^{min}_{j,t} + \delta^{max}_{j,t} - \varphi^{min}_{j,t} + \varphi^{max}_{j,t} + \gamma^{min}_{j,t} -$$
$$m_{j,t}\gamma^{max}_{j,t} - \pi^{RgC}_{t} = 0 \qquad \forall j \in \mathcal{G}, \forall t \in \mathcal{T} \text{ (A.3)}$$

$$\alpha^{RgM}_{j,t} - \gamma^{min}_{j,t} + \gamma^{max}_{j,t} - \pi^{RgM}_{t} = 0 \qquad \forall j \in \mathcal{G}, \forall t \in \mathcal{T} \text{ (A.4)}$$

$$\beta_{i,t}^{E} - \xi_{i,t}^{min} + \xi_{i,t}^{max} - \pi_{i,t}^{E} = 0 \qquad \forall i \in \mathcal{B}, \forall t \in \mathcal{T} \quad \text{(A.5)}$$

$$\beta_{i,t}^{Rs} - \rho_{i,t}^{min} + \rho_{i,t}^{max} - \pi_{i,t}^{Rs} = 0 \qquad \forall i \in \mathcal{B}, \forall t \in \mathcal{T} \quad \text{(A.6)}$$

$$\beta_{i,t}^{RgC} - \lambda_{i,t}^{min} + \lambda_{i,t}^{max} + \mu_{i,t}^{min} - m_{i,t}\mu_{i,t}^{max} - \pi_{t}^{RgC} = 0 \qquad \forall i \in \mathcal{B}, \forall t \in \mathcal{T} \quad \text{(A.7)}$$

$$\beta_{i,t}^{RgM} - \mu_{i,t}^{min} + \mu_{i,t}^{max} - \pi_{t}^{RgM} = 0 \qquad \forall i \in \mathcal{B}, \forall t \in \mathcal{T} \quad \text{(A.8)}$$

$$\sum_{n \neq w} H_{nw}\pi_{n,t}^{E} - \sum_{n \neq w} H_{wn}\pi_{n,t}^{E} - \sum_{w > n} H_{nw}(\omega_{nw,t}^{min} - \omega_{nw,t}^{max}) +$$

$$\sum_{w < n} H_{wn}(\omega_{nw,t}^{min} - \omega_{nw,t}^{max}) = 0 \qquad \forall n \in \mathcal{N}, \forall t \in \mathcal{T} \quad \text{(A.9)}$$

Complementary Slackness:

$$\delta_{j,t}^{min}(P_{j}^{Min} + P_{j,t}^{G,RgC} - P_{j,t}^{G,E}) = 0 \qquad \forall j \in \mathcal{G}, \forall t \in \mathcal{T} \quad \text{(A.10)}$$

$$\delta_{j,t}^{max}(P_{j,t}^{G,E} - P_{j}^{Max} + P_{j,t}^{G,Rs} + P_{j,t}^{G,RgC}) = 0 \qquad \forall j \in \mathcal{G}, \forall t \in \mathcal{T} \quad \text{(A.11)}$$

$$\epsilon_{j,t}^{min}(P_{j,t}^{G,Rs}) = 0 \qquad \forall j \in \mathcal{G}, \forall t \in \mathcal{T} \quad \text{(A.12)}$$

$$\epsilon_{j,t}^{max}(P_{j,t}^{G,Rs} - P_{j}^{Rs,ramp}) = 0 \qquad \forall j \in \mathcal{G}, \forall t \in \mathcal{T} \quad \text{(A.13)}$$

$$\varphi_{j,t}^{min}(P_{j,t}^{G,RgC}) = 0 \qquad \forall j \in \mathcal{G}, \forall t \in \mathcal{T} \quad \text{(A.14)}$$

$$\varphi_{j,t}^{max}(P_{j,t}^{G,RgC} - P_{j}^{Rg,ramp}) = 0 \qquad \forall j \in \mathcal{G}, \forall t \in \mathcal{T} \quad \text{(A.15)}$$

$$\gamma_{j,t}^{min}(P_{j,t}^{G,RgC} - P_{j,t}^{G,RgM}) = 0 \qquad \forall j \in \mathcal{G}, \forall t \in \mathcal{T} \quad \text{(A.16)}$$

$$\gamma_{j,t}^{max}(P_{j,t}^{G,RgM} - m_{j,t}P_{j,t}^{G,RgC}) = 0 \qquad \forall j \in \mathcal{G}, \forall t \in \mathcal{T} \quad \text{(A.17)}$$

$$\xi_{i,t}^{min}(O_{i,t}^{E} + P_{i,t}^{B,E}) = 0 \qquad \forall i \in \mathcal{B}, \forall t \in \mathcal{T} \quad \text{(A.18)}$$

$$\xi_{i,t}^{max}(P_{i,t}^{B,E} - O_{i,t}^{E}) = 0 \qquad \forall i \in \mathcal{B}, \forall t \in \mathcal{T} \quad \text{(A.19)}$$

$$\rho_{i,t}^{min}(P_{i,t}^{B,Rs}) = 0 \qquad \forall i \in \mathcal{B}, \forall t \in \mathcal{T} \quad \text{(A.20)}$$

$$\rho_{i,t}^{max}(P_{i,t}^{B,Rs} - O_{i,t}^{Rs}) = 0 \qquad \forall i \in \mathcal{B}, \forall t \in \mathcal{T} \quad \text{(A.21)}$$

$$\lambda_{i,t}^{min}(P_{i,t}^{B,RgC}) = 0 \qquad \forall i \in \mathcal{B}, \forall t \in \mathcal{T} \quad \text{(A.22)}$$

$$\lambda_{i,t}^{max}(P_{i,t}^{B,RgC} - O_{i,t}^{RgC}) = 0 \qquad \forall i \in \mathcal{B}, \forall t \in \mathcal{T} \quad \text{(A.23)}$$

$$\mu_{i,t}^{min}(P_{i,t}^{B,RgC} - P_{i,t}^{B,RgM}) = 0 \qquad \forall i \in \mathcal{B}, \forall t \in \mathcal{T} \quad \text{(A.24)}$$

$$\mu_{i,t}^{max}(P_{i,t}^{B,RgM} - m_{i,t}P_{i,t}^{B,RgC}) = 0 \qquad \forall i \in \mathcal{B}, \forall t \in \mathcal{T} \quad \text{(A.25)}$$

$$\pi_t^{Rs}(R_t^{Rs} - \sum_{j\in\mathcal{G}} P_{j,t}^{G,Rs} - \sum_{i\in\mathcal{B}} P_{i,t}^{B,Rs}) = 0 \qquad \forall t \in \mathcal{T} \quad \text{(A.26)}$$

$$\pi_t^{RgC}(R_t^{RgC} - \sum_{j\in\mathcal{G}} P_{j,t}^{G,RgC} - \sum_{i\in\mathcal{B}} P_{i,t}^{B,RgC}) = 0 \qquad \forall t \in \mathcal{T} \quad \text{(A.27)}$$

$$\pi_t^{RgM}(R_t^{RgM} - \sum_{j\in\mathcal{G}} P_{j,t}^{G,RgM} - \sum_{i\in\mathcal{B}} P_{i,t}^{B,RgM}) = 0 \qquad \forall t \in \mathcal{T} \quad \text{(A.28)}$$

$$\omega_{nw,t}^{min}(TL_{nw} + H_{nw}(\theta_{n,t} - \theta_{w,t})) = 0 \qquad \forall (n,w) \in \mathcal{L}, \forall t \in \mathcal{T} \quad \text{(A.29)}$$

$$\omega_{nw,t}^{max}(H_{nw}(\theta_{n,t} - \theta_{w,t}) - TL_{nw}) = 0 \qquad \forall (n,w) \in \mathcal{L}, \forall t \in \mathcal{T} \quad \text{(A.30)}$$

Dual Feasibility:

$$\delta_{j,t}^{min} \geq 0, \delta_{j,t}^{max} \geq 0, \epsilon_{j,t}^{min} \geq 0, \epsilon_{j,t}^{max} \geq 0 \qquad \forall j \in \mathcal{G}, \forall t \in \mathcal{T} \quad \text{(A.31)}$$

$$\varphi_{j,t}^{min} \geq 0, \varphi_{j,t}^{max} \geq 0, \gamma_{j,t}^{min} \geq 0, \gamma_{j,t}^{max} \geq 0 \qquad \forall j \in \mathcal{G}, \forall t \in \mathcal{T} \quad \text{(A.32)}$$

$$\xi_{i,t}^{min} \geq 0, \xi_{i,t}^{max} \geq 0, \rho_{i,t}^{min} \geq 0, \rho_{i,t}^{max} \geq 0 \qquad \forall i \in \mathcal{B}, \forall t \in \mathcal{T} \quad \text{(A.33)}$$

$$\lambda_{i,t}^{min} \geq 0, \lambda_{i,t}^{max} \geq 0, \mu_{i,t}^{min} \geq 0, \mu_{i,t}^{max} \geq 0 \qquad \forall i \in \mathcal{B}, \forall t \in \mathcal{T} \quad \text{(A.34)}$$

$$\pi_{n,t}^{E} \geq 0, \pi_t^{Rs} \geq 0, \pi_t^{RgC} \geq 0, \pi_t^{RgM} \geq 0 \qquad \forall n \in \mathcal{N}, \forall t \in \mathcal{T} \quad \text{(A.35)}$$

$$\omega_{nw,t}^{min} \geq 0, \omega_{nw,t}^{max} \geq 0 \qquad \forall (n,w) \in \mathcal{L}, \forall t \in \mathcal{T} \quad \text{(A.36)}$$

Using the provided KKT conditions for LLP, we can solve the following single-level optimization problem instead of the presented bi-level model.

Max (U.1)

Subject to:

(U.2) – (U.19)

(L.2) – (L.14)

(A.1) – (A.36)

The objective function and complementary slackness constraints ((A.10) to (A.30)) of the above-mentioned optimization problem are non-linear. Big-M method is used for handling non-linearity in the complementary slackness constraints. For example, (A.10) can be replaced with following equations where $r_{j,t}^{\delta^{min}}$ is a binary variable and M is a sufficiently large number.

$$\delta_{j,t}^{min} \leq (1 - r_{j,t}^{\delta^{min}})M \qquad \forall j \in \mathcal{G}, \forall t \in \mathcal{T} \quad \text{(A.37)}$$

$$P_{j,t}^{G,E} - P_{j}^{Min} - P_{j,t}^{G,RgC} \leq r_{j,t}^{\delta^{min}} M \qquad \forall j \in \mathcal{G}, \forall t \in \mathcal{T} \quad \text{(A.38)}$$

Based on (A.38), if $P_j^{Min} + P_{j,t}^{G,RgC} = P_{j,t}^{G,E}$ (lower-limit of constraint (L.2) binding), then $r_{j,t}^{\delta^{min}} = 0$; and based on (A.37), $\delta_{j,t}^{min}$ can have any value between zero and M. But if lower-limit of (L.2) is not binding ($P_j^{Min} + P_{j,t}^{G,RgC} < P_{j,t}^{G,E}$), $r_{j,t}^{\delta^{min}}$ must be one; and due to (A.37), $\delta_{j,t}^{min} = 0$. Therefore, the combination of (A.37) and (A.38) is equivalent to complimentary constraint (A.10) when M is chosen wisely. Similarly, (A.11) to (A.30) are replaced with following equations.

$$\delta_{j,t}^{max} \leq (1 - r_{j,t}^{\delta^{max}})M \qquad \forall j \in \mathcal{G}, \forall t \in \mathcal{T} \quad \text{(A.39)}$$

$$P_{j}^{Max} - P_{j,t}^{G,E} - P_{j,t}^{G,Rs} - P_{j,t}^{G,RgC} \leq r_{j,t}^{\delta^{max}} M \qquad \forall j \in \mathcal{G}, \forall t \in \mathcal{T} \quad \text{(A.40)}$$

$$\epsilon_{j,t}^{min} \leq (1 - r_{j,t}^{\epsilon^{min}})M \qquad \forall j \in \mathcal{G}, \forall t \in \mathcal{T} \quad \text{(A.41)}$$

$$P_{j,t}^{G,Rs} \leq r_{j,t}^{\epsilon^{min}} M \qquad \forall j \in \mathcal{G}, \forall t \in \mathcal{T} \quad \text{(A.42)}$$

$$\epsilon_{j,t}^{max} \leq (1 - r_{j,t}^{\epsilon^{max}})M \qquad \forall j \in \mathcal{G}, \forall t \in \mathcal{T} \quad \text{(A.43)}$$

$$P_{j}^{Rs,ramp} - P_{j,t}^{G,Rs} \leq r_{j,t}^{\epsilon^{max}} M \qquad \forall j \in \mathcal{G}, \forall t \in \mathcal{T} \quad \text{(A.44)}$$

$$\varphi_{j,t}^{min} \leq (1 - r_{j,t}^{\varphi^{min}})M \qquad \forall j \in \mathcal{G}, \forall t \in \mathcal{T} \quad \text{(A.45)}$$

$$P_{j,t}^{G,RgC} \leq r_{j,t}^{\varphi^{min}} M \qquad \forall j \in \mathcal{G}, \forall t \in \mathcal{T} \quad \text{(A.46)}$$

$$\varphi_{j,t}^{max} \leq (1 - r_{j,t}^{\varphi^{max}})M \qquad \forall j \in \mathcal{G}, \forall t \in \mathcal{T} \quad \text{(A.47)}$$

$$P_{j}^{Rg,ramp} - P_{j,t}^{G,RgC} \leq r_{j,t}^{\varphi^{max}} M \qquad \forall j \in \mathcal{G}, \forall t \in \mathcal{T} \quad \text{(A.48)}$$

$$\gamma_{j,t}^{min} \leq (1 - r_{j,t}^{\gamma^{min}})M \qquad \forall j \in \mathcal{G}, \forall t \in \mathcal{T} \quad \text{(A.49)}$$

$$P_{j,t}^{G,RgM} - P_{j,t}^{G,RgC} \leq r_{j,t}^{\gamma^{min}} M \qquad \forall j \in \mathcal{G}, \forall t \in \mathcal{T} \quad \text{(A.50)}$$

$$\gamma_{j,t}^{max} \leq (1 - r_{j,t}^{\gamma^{max}}) M \qquad \forall j \in \mathcal{G}, \forall t \in \mathcal{T} \quad \text{(A.51)}$$

$$m_{j,t} P_{j,t}^{G,RgC} - P_{j,t}^{G,RgM} \leq r_{j,t}^{\gamma^{max}} M \qquad \forall j \in \mathcal{G}, \forall t \in \mathcal{T} \quad \text{(A.52)}$$

$$\xi_{i,t}^{min} \leq (1 - r_{i,t}^{\xi^{min}}) M \qquad \forall i \in \mathcal{B}, \forall t \in \mathcal{T} \quad \text{(A.53)}$$

$$O_{i,t}^{E} + P_{i,t}^{B,E} \leq r_{i,t}^{\xi^{min}} M \qquad \forall i \in \mathcal{B}, \forall t \in \mathcal{T} \quad \text{(A.54)}$$

$$\xi_{i,t}^{max} \leq (1 - r_{i,t}^{\xi^{max}}) M \qquad \forall i \in \mathcal{B}, \forall t \in \mathcal{T} \quad \text{(A.55)}$$

$$O_{i,t}^{E} - P_{i,t}^{B,E} \leq r_{i,t}^{\xi^{max}} M \qquad \forall i \in \mathcal{B}, \forall t \in \mathcal{T} \quad \text{(A.56)}$$

$$\rho_{i,t}^{min} \leq (1 - r_{i,t}^{\rho^{min}}) M \qquad \forall i \in \mathcal{B}, \forall t \in \mathcal{T} \quad \text{(A.57)}$$

$$P_{i,t}^{B,Rs} \leq r_{i,t}^{\rho^{min}} M \qquad \forall i \in \mathcal{B}, \forall t \in \mathcal{T} \quad \text{(A.58)}$$

$$\rho_{i,t}^{max} \leq (1 - r_{i,t}^{\rho^{max}}) M \qquad \forall i \in \mathcal{B}, \forall t \in \mathcal{T} \quad \text{(A.59)}$$

$$O_{i,t}^{Rs} - P_{i,t}^{B,Rs} \leq r_{i,t}^{\rho^{max}} M \qquad \forall i \in \mathcal{B}, \forall t \in \mathcal{T} \quad \text{(A.60)}$$

$$\lambda_{i,t}^{min} \leq (1 - r_{i,t}^{\lambda^{min}}) M \qquad \forall i \in \mathcal{B}, \forall t \in \mathcal{T} \quad \text{(A.61)}$$

$$P_{i,t}^{B,RgC} \leq r_{i,t}^{\lambda^{min}} M \qquad \forall i \in \mathcal{B}, \forall t \in \mathcal{T} \quad \text{(A.62)}$$

$$\lambda_{i,t}^{max} \leq (1 - r_{i,t}^{\lambda^{max}}) M \qquad \forall i \in \mathcal{B}, \forall t \in \mathcal{T} \quad \text{(A.63)}$$

$$O_{i,t}^{RgC} - P_{i,t}^{B,RgC} \leq r_{i,t}^{\lambda^{max}} M \qquad \forall i \in \mathcal{B}, \forall t \in \mathcal{T} \quad \text{(A.64)}$$

$$\mu_{i,t}^{min} \leq (1 - r_{i,t}^{\mu^{min}}) M \qquad \forall i \in \mathcal{B}, \forall t \in \mathcal{T} \quad \text{(A.65)}$$

$$P_{i,t}^{B,RgM} - P_{i,t}^{B,RgC} \leq r_{i,t}^{\mu^{min}} M \qquad \forall i \in \mathcal{B}, \forall t \in \mathcal{T} \quad \text{(A.66)}$$

$$\mu_{i,t}^{max} \leq (1 - r_{i,t}^{\mu^{max}}) M \qquad \forall i \in \mathcal{B}, \forall t \in \mathcal{T} \quad \text{(A.67)}$$

$$m_{i,t} P_{i,t}^{B,RgC} - P_{i,t}^{B,RgM} \leq r_{i,t}^{\mu^{max}} M \qquad \forall i \in \mathcal{B}, \forall t \in \mathcal{T} \quad \text{(A.68)}$$

$$\pi_{t}^{Rs} \leq (1 - r_{i,t}^{\pi^{Rs}}) M \qquad \forall t \in \mathcal{T} \quad \text{(A.69)}$$

$$\sum_{j \in \mathcal{G}} P_{j,t}^{G,Rs} + \sum_{i \in \mathcal{B}} P_{i,t}^{B,Rs} - R_{t}^{Rs} \leq r_{i,t}^{\pi^{Rs}} M \qquad \forall t \in \mathcal{T} \quad \text{(A.70)}$$

$$\pi_{t}^{RgC} \leq (1 - r_{i,t}^{\pi^{RgC}}) M \qquad \forall t \in \mathcal{T} \quad \text{(A.71)}$$

$$\sum_{j\in\mathcal{G}} P_{j,t}^{G,RgC} + \sum_{i\in\mathcal{B}} P_{i,t}^{B,RgC} - R_t^{RgC} \le r_{i,t}^{\pi^{RgC}} M \qquad \forall t \in \mathcal{T} \quad \text{(A.72)}$$

$$\pi_t^{RgM} \le (1 - r_{i,t}^{\pi^{RgM}}) M \qquad \forall t \in \mathcal{T} \quad \text{(A.73)}$$

$$\sum_{j\in\mathcal{G}} P_{j,t}^{G,RgM} + \sum_{i\in\mathcal{B}} P_{i,t}^{B,RgM} - R_t^{RgM} \le r_{i,t}^{\pi^{RgM}} M \qquad \forall t \in \mathcal{T} \quad \text{(A.74)}$$

$$\omega_{nw,t}^{min} \le (1 - r_{i,t}^{\omega^{min}}) M \qquad \forall (n,w) \in \mathcal{L}, \forall t \in \mathcal{T} \quad \text{(A.75)}$$

$$TL_{nw} + H_{nw}(\theta_{n,t} - \theta_{w,t}) \le r_{i,t}^{\omega^{min}} M \qquad \forall (n,w) \in \mathcal{L}, \forall t \in \mathcal{T} \quad \text{(A.76)}$$

$$\omega_{nw,t}^{max} \le (1 - r_{i,t}^{\omega^{max}}) M \qquad \forall (n,w) \in \mathcal{L}, \forall t \in \mathcal{T} \quad \text{(A.77)}$$

$$TL_{nw} - H_{nw}(\theta_{n,t} - \theta_{w,t}) \le r_{i,t}^{\omega^{max}} M \qquad \forall (n,w) \in \mathcal{L}, \forall t \in \mathcal{T} \quad \text{(A.78)}$$

An equivalent linear equation is derived below to replace (U.1). Based on the strong duality, the objective function of LLP (L.1) is equal to the following equation.

$$\begin{aligned}
&\sum_{t\in\mathcal{T}} \Big[\sum_{j\in\mathcal{G}} \big(\alpha_{j,t}^{E} P_{j,t}^{G,E} + \alpha_{j,t}^{Rs} P_{j,t}^{G,Rs} + \alpha_{j,t}^{RgC} P_{j,t}^{G,RgC} + \alpha_{j,t}^{RgM} P_{j,t}^{G,RgM}\big) + \\
&\sum_{i\in\mathcal{B}} \big(\beta_{i,t}^{E} P_{i,t}^{B,E} + \beta_{i,t}^{Rs} P_{i,t}^{B,Rs} + \beta_{i,t}^{RgC} P_{i,t}^{B,RgC} + \beta_{i,t}^{RgM} P_{i,t}^{B,RgM}\big) \Big] \Delta t = \\
&\sum_{t\in\mathcal{T}} \Big[\sum_{j\in\mathcal{G}} \big(\delta_{j,t}^{min} P_j^{Min} - \delta_{j,t}^{max} P_j^{Max} - \epsilon_{j,t}^{max} P_j^{Rs,Ramp} - \varphi_{j,t}^{max} P_j^{Rg,Ramp}\big) - \\
&\sum_{i\in\mathcal{B}} \big(\xi_{i,t}^{min} O_{i,t}^{E} + \xi_{i,t}^{max} O_{i,t}^{E} + \rho_{i,t}^{max} O_{i,t}^{Rs} + \lambda_{i,t}^{max} O_{i,t}^{RgC}\big) - \sum_{n\in\mathcal{N}} P_{n,t}^{Load} \pi_{n,t}^{E} - \\
&\sum_{nw\in\mathcal{L}} \big(\omega_{nw,t}^{min} TL_{nw} + \omega_{nw,t}^{max} TL_{nw}\big) + \pi_t^{Rs} R_t^{Rs} + \pi_t^{RgC} R_t^{RgC} + \pi_t^{RgM} R_t^{RgM} \Big] \Delta t
\end{aligned} \qquad \text{(A.79)}$$

Additionally, By multiplying both sides of (A.5) to $P_{i,t}^{B,E}$, we will have

$$\beta_{i,t}^{E} P_{i,t}^{B,E} - \xi_{i,t}^{min} P_{i,t}^{B,E} + \xi_{i,t}^{max} P_{i,t}^{B,E} - \pi_{i,t}^{E} P_{i,t}^{B,E} = 0 \qquad \text{(A.80)}$$

Substituting (A.18) and (A.19) in (A.80) and summing over all storage units ($\sum_{i\in\mathcal{B}}$) will result in

$$\sum_{i\in\mathcal{B}} \big(\xi_{i,t}^{min} O_{i,t}^{E} + \xi_{i,t}^{max} O_{i,t}^{E}\big) = \sum_{i\in\mathcal{B}} \big(\pi_{i,t}^{E} P_{i,t}^{B,E} - \beta_{i,t}^{E} P_{i,t}^{B,E}\big) \qquad \text{(A.81)}$$

Similarly, by multiplying $P_{i,t}^{B,E}$ to (A.6), then substituting (A.20) and (A.21) in it and summing over all storage units ($\sum_{i\in\mathcal{B}}$), we can write

$$\sum_{i\in\mathcal{B}} \rho_{i,t}^{max} O_{i,t}^{Rs} = \sum_{i\in\mathcal{B}} \left(\pi_t^{Rs} P_{i,t}^{B,Rs} - \beta_{i,t}^{Rs} P_{i,t}^{B,Rs}\right) \tag{A.82}$$

Multiplying $P_{i,t}^{B,RgC}$ to (A.7), then substituting (A.22),(A.23) and (A.25) in it will result in

$$\beta_{i,t}^{RgC} P_{i,t}^{B,RgC} + \lambda_{i,t}^{max} O_{i,t}^{RgC} + \mu_{i,t}^{min} P_{i,t}^{B,RgC} - \mu_{i,t}^{max} P_{i,t}^{B,RgM} - \pi_t^{RgC} P_{i,t}^{B,RgC} = 0 \tag{A.83}$$

Additionally, by multiplying $P_{i,t}^{B,RgM}$ to (A.8), and substituting (A.24) in it, we will have

$$\beta_{i,t}^{RgM} P_{i,t}^{B,RgM} - \mu_{i,t}^{max} P_{i,t}^{B,RgC} + \mu_{i,t}^{max} P_{i,t}^{B,RgM} - \pi_t^{RgM} P_{i,t}^{B,RgM} = 0 \tag{A.84}$$

Merging (A.83) and (A.84) and summing over all storage units ($\sum_{i\in\mathcal{B}}$) will results in

$$\sum_{i\in\mathcal{B}} \lambda_{i,t}^{max} O_{i,t}^{RgC} = \sum_{i\in\mathcal{B}} \left(\pi_t^{RgC} P_{i,t}^{B,RgC} + \pi_t^{RgM} P_{i,t}^{B,RgM} - \beta_{i,t}^{RgC} P_{i,t}^{B,RgC} - \beta_{i,t}^{RgM} P_{i,t}^{B,RgM}\right) \tag{A.85}$$

Then, by substituting (A.81), (A.82) and (A.85) in (A.79), we will have

$$\begin{aligned}
&\sum_{t\in\mathcal{T}} \Big[\sum_{i\in\mathcal{B}} \left(\pi_{i,t}^{E} P_{i,t}^{B,E} + \pi_t^{Rs} P_{i,t}^{B,Rs} + \pi_t^{RgC} P_{i,t}^{B,RgC} + \pi_t^{RgM} P_{i,t}^{B,RgM}\right) \Big] \Delta t = \\
&\sum_{t\in\mathcal{T}} \Big[\sum_{j\in\mathcal{G}} \left(\delta_{j,t}^{min} P_j^{Min} - \delta_{j,t}^{max} P_j^{Max} - \epsilon_{j,t}^{max} P_j^{Rs,Ramp} - \varphi_{j,t}^{max} P_j^{Rg,Ramp} - \right. \\
&\left. \alpha_{j,t}^{E} P_{j,t}^{G,E} - \alpha_{j,t}^{Rs} P_{j,t}^{G,Rs} - \alpha_{j,t}^{RgC} P_{j,t}^{G,RgC} - \alpha_{j,t}^{RgM} P_{j,t}^{G,RgM}\right) - \sum_{n\in\mathcal{N}} P_{n,t}^{Load} \pi_{n,t}^{E} - \\
&\sum_{nw\in\mathcal{L}} \left(\omega_{nw,t}^{min} TL_{nw} + \omega_{nw,t}^{max} TL_{nw}\right) + \pi_t^{Rs} R_t^{Rs} + \pi_t^{RgC} R_t^{RgC} + \pi_t^{RgM} R_t^{RgM} \Big] \Delta t
\end{aligned} \tag{A.86}$$

It is obvious that (A.86) is linear and equal to nonlinear part of ULP's objective function (U.1). Hence, it is possible to substitute it in objective function to tackle

non-linearity. As a result, the following optimization is the conversion of original bi-level problem to a MILP.

$$\text{Max} \sum_{t\in\mathcal{T}} \Big\{ \Big[\sum_{j\in\mathcal{G}} \big(\delta_{j,t}^{min} P_j^{Min} - \delta_{j,t}^{max} P_j^{Max} - \epsilon_{j,t}^{max} P_j^{Rs,Ramp} - \varphi_{j,t}^{max} P_j^{Rg,Ramp} -$$
$$\alpha_{j,t}^{E} P_{j,t}^{G,E} - \alpha_{j,t}^{Rs} P_{j,t}^{G,Rs} - \alpha_{j,t}^{RgC} P_{j,t}^{G,RgC} - \alpha_{j,t}^{RgM} P_{j,t}^{G,RgM}\big) - \sum_{n\in\mathcal{N}} P_{n,t}^{Load} \pi_{n,t}^{E} -$$
$$\sum_{nw\in\mathcal{L}} \big(\omega_{nw,t}^{min} TL_{nw} + \omega_{nw,t}^{max} TL_{nw}\big) + \pi_t^{Rs} R_t^{Rs} + \pi_t^{RgC} R_t^{RgC} + \pi_t^{RgM} R_t^{RgM} \Big] \Delta t -$$
$$\sum_{i\in\mathcal{B}} \sum_{z\in\mathcal{Z}} \sum_{k\in\mathcal{K}} C_{i,k}^{Deg} P_{i,t,z,k}^{Dis} \Delta z \Big\}$$

Subject to:

(U.2) – (U.19)

(L.2) – (L.14)

(A.1) – (A.9)

(A.31) – (A.78)

APPENDIX B

TEST CASE SYSTEM INFORMATION

Table B.1: Information of the Test Case System's Generators

Bus Number	P^{Min} (MW)	P^{Max} (MW)	$P^{Rs,ramp}$ (MW)	$P^{Rg,ramp}$ (MW)	α^{E} ($\frac{\$}{\text{MWh}}$)	α^{Rs} ($\frac{\$}{\text{MWh}}$)	α^{RgC} ($\frac{\$}{\text{MWh}}$)	α^{RgM} ($\frac{\$}{\text{MWh}}$)
1	8	20	30	15	97.4	14.6	39	6.8
1	8	20	30	15	97.4	14.6	39	6.8
1	22	55	37	18.5	33.8	5.1	13.5	2.4
1	22	55	37	18.5	33.8	5.1	13.5	2.4
2	8	20	30	15	97.4	14.6	39	6.8
2	8	20	30	15	97.4	14.6	39	6.8
2	22	55	37	18.5	36.9	5.5	14.8	2.6
2	22	55	37	18.5	36.9	5.5	14.8	2.6
7	22	55	37	18.5	30.9	4.6	12.3	2.2
7	22	55	37	18.5	30.9	4.6	12.3	2.2
13	170	355	41.4	20.7	25.4	3.8	10.2	1.8
15	5	12	10	5	100	15	40	7
15	5	12	10	5	100	15	40	7
15	5	12	10	5	100	15	40	7
15	5	12	10	5	100	15	40	7
15	5	12	10	5	100	15	40	7
15	22	55	37	18.5	28.4	4.3	11.4	2
15	22	55	37	18.5	28.4	4.3	11.4	2
15	22	55	37	18.5	28.4	4.3	11.4	2
16	62	155	30	15	23.2	3.5	9.3	1.6
18	170	355	41.4	20.7	28.6	4.3	11.4	2
21	170	355	41.4	20.7	27.5	4.1	11	1.9
22	22	55	37	18.5	25.9	3.9	10.4	1.8
22	22	55	37	18.5	25.9	3.9	10.4	1.8
23	170	355	41.4	20.7	29.5	4.4	11.8	2.1
23	170	355	41.4	20.7	29.5	4.4	11.8	2.1

Table B.2: Transmission Lines Information

From Bus	To Bus	Reactance (p.u.)	Thermal Limit
1	2	0.014	175
1	3	0.211	175
1	5	0.085	175
2	4	0.127	175
2	6	0.192	175
3	9	0.119	175
3	24	0.084	400
4	9	0.104	175
5	10	0.088	175
6	10	0.061	175
7	8	0.061	175
8	9	0.165	175
8	10	0.165	175
9	11	0.084	400
9	12	0.084	400
10	11	0.084	400
10	12	0.084	400
11	13	0.048	500
11	14	0.042	500
12	13	0.048	500
12	23	0.097	500
13	23	0.087	500
14	16	0.059	500
15	16	0.017	500
15	21	0.049	500
15	21	0.049	500
15	24	0.052	500
16	17	0.026	500
16	19	0.023	500
17	18	0.014	500
17	22	0.105	500
18	21	0.026	500
18	21	0.026	500
19	20	0.04	500
19	20	0.04	500
20	23	0.022	500
20	23	0.022	500
21	22	0.068	500